SIMULATION OF THE DYNAMICALLY COUPLED KC-135 TANKER AND REFUELING BOOM

THESIS

Jeremy J. Smith, Captain, USAF

AFIT/GAE/ENY/07-M21

DEPARTMENT OF THE AIR FORCE
AIR UNIVERSITY

AIR FORCE INSTITUTE OF TECHNOLOGY

Wright-Patterson Air Force Base, Ohio

AFIT/GAE/ENY/07-M21

SIMULATION OF THE DYNAMICALLY COUPLED KC-135 TANKER AND REFUELING BOOM

THESIS

Presented to the Faculty

Department of Aeronautics and Astronautics

Graduate School of Engineering and Management

Air Force Institute of Technology

Air University

Air Education and Training Command

In Partial Fulfillment of the Requirements for the

Degree of Master of Science in Aeronautical Engineering

Jeremy J. Smith, BSAE

Captain, USAF

March 2007

AFIT/GAE/ENY/07-M21

SIMULATION OF THE DYNAMICALLY COUPLED KC-135 TANKER AND REFUELING BOOM

Jeremy J. Smith, BSAE
Captain, USAF

Approved:

Dr. Donald L. Kunz (Chairman)	date
Major Eric Swenson (Member)	date
Major Paul Blue (Member)	date

AFIT/GAE/ENY/07M-21

Abstract

Future Air Force requirements for the use of unmanned aircraft will require Automated Aerial Refueling (AAR). Current AAR research requires a precision model to simulate the refueling process of a KC-135 tanker and a UAV. There are existing high fidelity models of the tanker aircraft, refueling boom and proposed receiver aircraft. However, none of the models are coupled. Since boom orientation and motion is known to change the trim of the tanker aircraft, which in turn influences all other aspects of the refueling process, a new model is needed.

The new model was created by integrating an existing KC-135 tanker and refueling boom model. The tanker boom equations of motion were coupled using joint coordinates and the velocity transformation. Assessment of the new model investigated boom and tanker motion in comparison with other established models. Ultimately, behavior of the new model was validated by a comparison of simulation results to flight test data.

The research culminated with the successful validation of the new model. Boom and tanker behavior of the new model matched that of both the established tanker and boom models as well as the flight test data. Even though the KC-135 has been flying for nearly 50 years, this is the first model that captures the dynamic interactions of the aircraft and its aerial refueling boom.

ACKNOWLEDGEMENTS

I would like to express my extreme gratitude to my thesis advisor, Dr. Donald Kunz for his guidance throughout the course of this research. In addition to the faculty here at AFIT, I would like to thank my elemetary and high school teachers for giving me the foundation that has enabled me to reach this point. Finally, and most importantly, I would like to thank my family back home, who have been and always will be the best teachers anyone could ask for.

Table of Contents

List of Figures

Page

List of Tables

List of Symbols

a	acceleration vector
A_X,A_Y,A_Z	tanker velocity components
B	velocity transformation matrix
C	direction cosine matrix
F	force vector, or block matrix for a floating joint
$\mathbf{I}$	3x3 Identity matrix
I	Inertia matrix for a component
M	moment vector, or Mach number
m	mass
n	unit vector defining principal motion axis
P	block matrix for a prismatic joint
P,Q,R	tanker roll, pitch, and yaw rates
Q	generalized force
r	position vector
U	block matrix for a universal joint
u_E	extended length of the boom extension
V_X,V_Y,V_Z	tanker velocity components

Greek symbols

η	joint velocity or acceleration vector
$_B$	tanker pitch angle
$_F$	fixed boom pitch angle
$_B$	tanker roll angle
$_B$	tanker yaw angle
$_F$	fixed boom yaw angle
	angular velocity vector

Superscripts and subscripts

B	tanker
E	boom extension
F	fixed boom
I	inertial reference frame
S	overall system

Reference Frames	
B.....................	tanker reference frame
E.....................	boom extension reference frame
F.....................	fixed boom reference frame
I	inertial reference frame
W	ruddevator reference frame
Operators	
$(\cdot)$	time derivative
$(\sim)$	skew symmetric matrix defined such that $\tilde{A}^T = -\tilde{A}$

SIMULATION OF THE DYNAMICALLY COUPLED KC-135 TANKER AND REFULEING BOOM

I. Introduction

Background

Unmanned Aerial Vehicles (UAVs) are becoming more and more of an important component of the modern battlespace. The Predator and Global Hawk are predominantly intelligence gathering aircraft designed to loiter above and turn their vast array of sensors down on the battlefield for extended periods of time. Since Predator's inception in 1995, it has been equipped with hellfire missiles in order to interdict time sensitive targets on the ground. A greatly upgraded, hunter-killer version of the Predator, the MQ-9 Reaper, is now in System Design and Development with a full rate production decision expected in 2009. The advancements include a 3000lb payload capacity to include the capability of delivering 500lb Joint Direct Attack Munitions.

When this current generation of UAVs deploys to a theater of operations, they must be broken down at their home station, boxed up, flown to their new base, reassembled and then test flown. This disassembly-reassembly process must be accomplished before the aircraft can actually take part in a mission. This is a somewhat satisfactory arrangement given the mission and relative complexity of the aircraft involved. However, expanded roles and aircraft are already being developed for the second generation UAVs. The Unmanned Combat Aerial Vehicle (UCAV) technology demonstrator was originally intended as a small, relatively short range aircraft for use in Suppression of Enemy Air Defense (SEAD) missions. The aircraft has since been expanded to a vehicle about the size of an F-35 with same variety of missions including formation flight, multi aircraft attack and aerial refueling. Refueling a UAV in flight introduces issues not experienced during manned refueling operations. In order to address these issues and to train personnel involved in the refueling process, advanced, high-fidelity models and simulations are necessary.

Currently, high-fidelity models of the KC-135 tanker, the refueling boom, and the UAVs exist separately, but no existing single system models the dynamic interactions among them. In order for second generation UAVs to deploy from stateside home stations to overseas theaters without going through the disassembly-reassembly process, UAVs must be capable of Automated Aerial Refueling (AAR). A high fidelity model integrating the behavior of the tanker, boom, and UAV must be developed in order to facilitate this. This thesis will serve as the first step in generating this fully integrated model for AAR simulations by developing a coupled, high fidelity model of the KC-135 tanker and refueling boom.

System Description

The USAF KC-135 family of tanker aircraft are derivatives of the Boeing 707, America's first transport plane powered by turbojet engines (see Figure 1). Originally designed and built in the 1950's, more than 500 KC-135's remain in the USAF inventory today. The aircraft is 136.25' long, has a wingspan of 130.83' and is capable of carrying a transferable fuel load of 200,000 lbs. Fuel is transferred from tanker to receiver via a flying boom.

During refueling, the receiver aircraft basically flies in formation with the tanker and a boom operator flies the boom into contact with the receiver's receptacle. The boom operator lies prone in a control station facing aft in the bulbous section of the aft fuselage directly below USAF aircraft identifying marker.

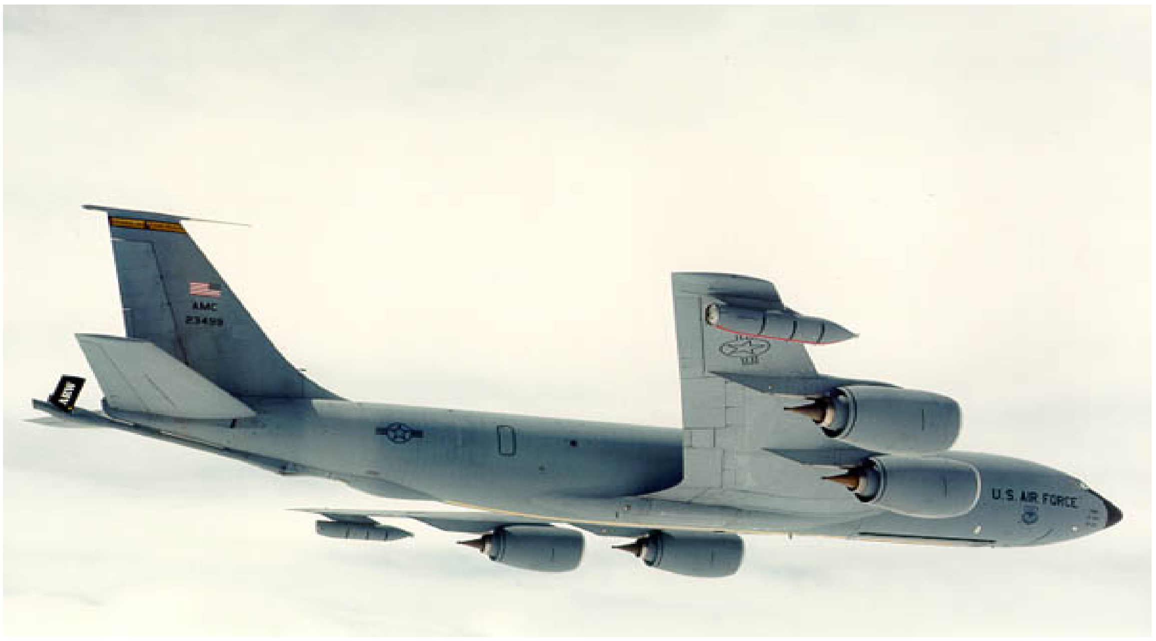

Figure 1. USAF KC-135 Stratotanker with Flying Boom in the Stowed Position (3).

The flying boom itself consists of two distinct pieces. The fixed boom is the portion that can be seen in Figure 1 and consists of 27.75' long tube-like fairing with an elliptical cross section. The fixed boom travels aft from the boom attachment point, past the fairing that houses the boom's control surfaces and ends at the tip as seen above in Figure 1. The boom extension can be seen in Figure 2. It is a 27' foot long cylinder with a fuel transfer nozzle at the tip. While in the stowed position, the boom extension is retracted completely inside the fixed boom. The extension can extend out of the fixed boom to a maximum extension position of 20 feet outside the fixed boom.

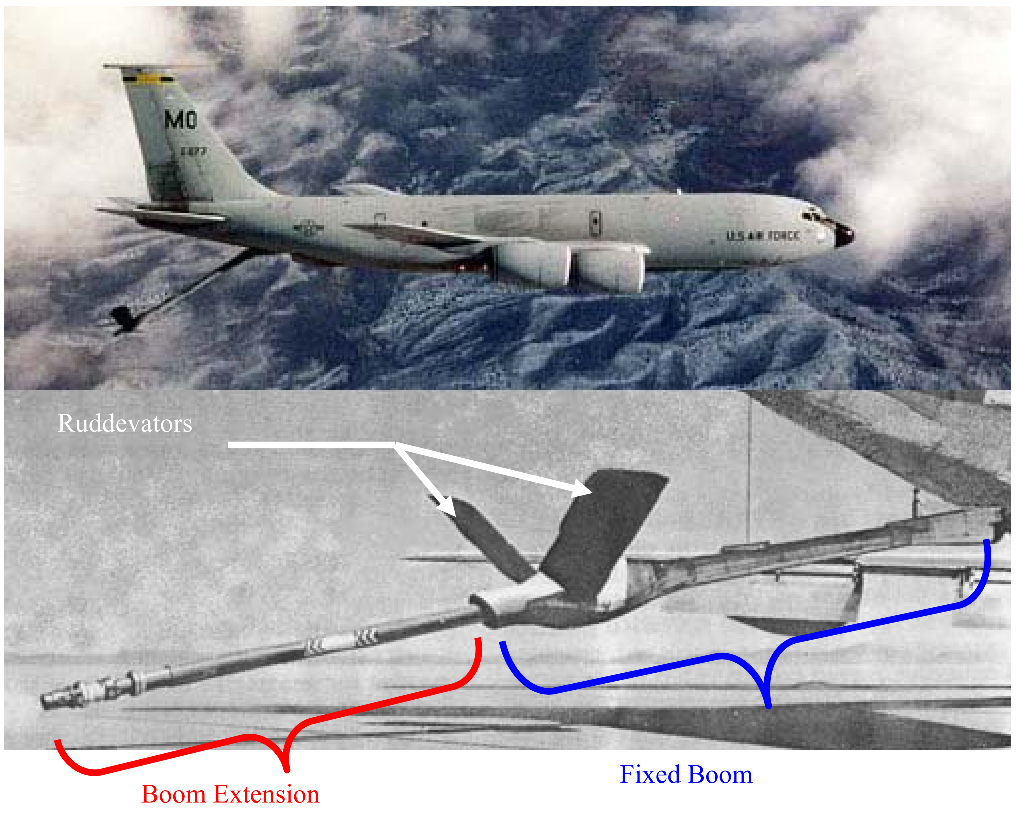

Figure 2. KC-135 with Refueling Boom Pitched Down (top) Refueling Boom (bottom) (11: 2).

The KC-135 aerial refueling boom is attached to the aircraft at the boom pivot by a vertical pin and a yoke and trunnion assembly a combination known as the boom fork. The boom fork is shown in Figure 3. The vertical pin allows the boom to yaw while the yoke and trunnion allows pitching movement.

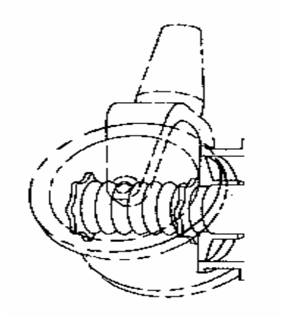

Figure 3. Boom Fork (12).

The boom's control surfaces, shown in Figure 5, are known as ruddevators. These surfaces are what allow the boom operator to manually fly the boom to the receiver aircraft's receptacle. They consist of a NACA 65-012 airfoil section (Figure 4) with a 2.583' chord length. The ruddevators are mounted at a 42^{o} dihedral angle on the fixed boom and have a 5.083' span from root to tip. In addition to the manual controls afforded the boom operator, an automatic system controls the ruddevators during flight while connected with a receiver aircraft. The purpose of the automatic system is to manage the position of the ruddevators in order to control aerodynamic loads on the boom during connected flight.

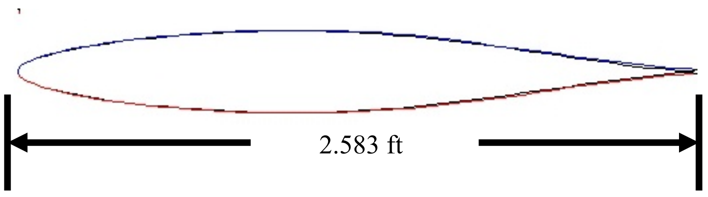

Figure 4. Naca 65-012 Airfoil Showing Ruddevator Chord (13)

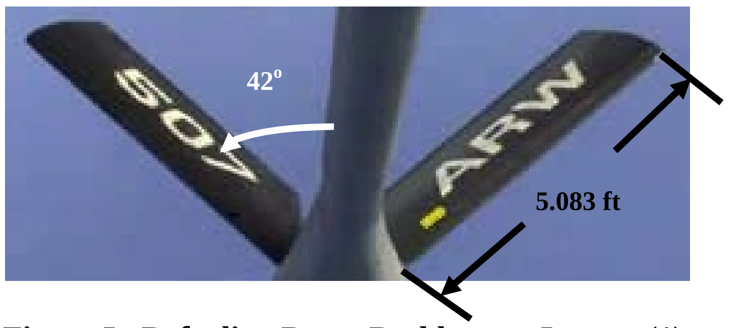

Figure 5. Refueling Boom Ruddevator Layout (1).

Existing Models

Currently, there are high fidelity models of both the KC-135 and its refueling boom, but in no existing model are the dynamic interactions between the tanker and boom taken into account.

The high fidelity KC-135 tanker model was developed for the Air Force Research Laboratory (AFRL). The model was written in Simulink and aircraft states, such as mass, orientation, speed, and altitude, can be initialized from two separate Matlab script files. The model has the ability to operate on autopilot mode for both straight and level and typical race-track type refueling patterns or to take manually commanded pilot inputs. The boom pivot location is attached and tracked, though again, there are no interactions between the tanker and boom.

The model basically consists of a few major systems broken down into numerous sub and other minor systems. The major systems include the autopilot, control system and the actual vehicle model. The *Vehicle Model* system contains all the aerodynamic and moment of inertia calculations that are fed into the tanker's equations of motion (EOMs).

The tanker EOMs were developed with the typical aircraft coordinate system (origin located at the tanker's mass center, the x-axis going out the nose, the y-axis pointing to right and z axis pointing down). The EOMs are written in the following form:

$$\begin{bmatrix} m_B[\mathbf{I}] & [0] \\ [0] & [I] \end{bmatrix} \begin{Bmatrix} \{\dot{v}\} \\ \{\dot{\omega}\} \end{Bmatrix} = \begin{Bmatrix} \{F\} \\ \{M\} - [\tilde{\omega}][I]\{\omega\} \end{Bmatrix} \tag{1}$$

where the far left hand term is the 6x6 mass/inertia matrix, the second term on the left hand side is the 6x1 vector of linear and angular accelerations, and the right hand side is a 6x1 vector of aerodynamic and gravitational forces and moments acting on the tanker. This is the matrix-vector version of Newton's Second Law of Motion, F = ma or M = I$\ddot{\omega}$.

To solve Equation 1, the AFRL model calculates the force/moment vector on the right hand side from the aircraft states. The EOMs are solved for the acceleration vector by multiplying both sides of Equation 1 by the inverse of the mass/inertia matrix. The acceleration vector is then integrated twice to find velocity and position vectors for the tanker. Prior to the second integration, the angular rates must be transformed to aircraft attitude rates.

In this research, three models of the boom will be discussed. The first is the Boom Operator Part Task Trainer (BOPTT). This model is used in the training of boom operators and has been used in tandem with AFRL's tanker model to perform AAR simulations even though they do not model the dynamic interactions between the tanker and boom. Development of the EOMs for this model treated the boom as a stand alone rigid body attached to the tanker at the boom fork. The boom fork was assumed to translate through the air as though on an imaginary rigid rail. The boom itself was allowed to go through its normal motion, but neither model was affected by the other.

The second boom model was developed at the Air Force Institute of Technology (AFIT) by Campbell in 1989. Again, EOM development considered the boom as a standalone rigid body. This model was developed to research the possibility of expanding the boom's refueling envelope (7:1).

The third and most recent boom model was developed by Smith and Kunz (11). In a paper presented at the 2006 AIAA Modeling and Simulation Conference, they described a method of deriving the EOMs that would potentially couple the tanker and boom. They developed a Matlab model of the boom using those EOMs and compared its motion to that of the BOPTT and AFIT model. The test results indicated that they had developed another representative boom model.

Current AAR Research

Most current work in the AAR area is centered around different types of control/guidance systems that enable the UAV receiver aircraft to maneuver into and remain in a refueling position. Blake, et al designed a linear position tracking controller for the UAV (2). A collaboration between West Virginia University and Perugia University (Italy) has investigated a "control scheme based on a sensor fusion between GPS-based and Machine Vision-based measurements" with a probe and drogue type refueling system (5, 6). Other studies at AFRL have looked at developing an overall real time simulation environment with tanker, boom, and UAV operator stations to simulate the entire process (4, 8). None of these studies discuss the coupling effects of the tanker and boom. However, the Southwestern Research Institute has investigated developing an aerodynamic model of the coupled tanker and boom through computational fluid dynamics (15:9).

Problem Statement

While the AFRL tanker model and the three boom models are all valid training tools and offer insight into the behavior of the tanker and boom, no existing model can describe the behavior of the tanker and boom as a single system. For manned refueling missions, this is satisfactory because each person in the loop (tanker pilot, boom operator, receiver pilot) can make any necessary adjustments to ensure the refueling event is a success. This will not be the case during AAR because one of the decision makers, the receiver pilot, has been taken out of the loop. In order to accurately predict behaviors of the tanker boom system, a new model must be developed that couples the dynamic interactions between the KC-135 tanker and its refueling boom.

Research objectives:

The objective of this research is to develop and validate a dynamically coupled model of the KC-135 and its refueling boom that has the potential to be an effective research tool. AFRL's KC-135 Simulink model will serve as the baseline program to be modified. In order to leave the majority of this highly reliable model untouched, most modifications to this program will be made to the V*ehicle Model* system. Every effort will be made to ensure that the original inputs and outputs will remain as is, though some things will inevitably have to change. The EOMs and boom model developed by Kunz and Smith will serve as tools to help modify the AFRL tanker model and in turn develop the first dynamically coupled model of the KC-135 tanker and its refueling boom.

Validation of the new model will initially be accomplished by examining its simulation results against those obtained from AFRL's KC-135 model and the Kunz/Smith boom model. Evaluation of the model will include investigating motion of the boom and tanker as separate entities, and then as a coupled system.

Tanker response to the attached boom and commanded changes in boom motion will be examined, as will changes in boom motion due to it being dynamically attached to the tanker. There should be some visible effects from the coupling of the tanker and boom, but these changes should be rather small in nature. Final validation of the new model will come from comparing the coupled model's simulation results with existing flight test data. The data includes tanker and boom responses to commanded changes in boom position.

II Methodology

Overview

This chapter will discuss Kunz and Smith's development of the coupled EOMs for the tanker and boom, the AFRL Simulink model and its operation, and finally the method in which the two models were integrated to form the coupled model. An understanding of the EOMs and parts of the existing model is of obvious importance. The goal of this research is to combine the two and create a new model. This chapter will help explain why certain approaches were taken and how they were implemented.

Coupled Equations of Motion

As mentioned in Chapter 1, Kunz and Smith developed the EOMs that dynamically couple the KC-135 and its refueling boom. They did so using joint coordinates and the velocity transformation. "The velocity transformation…relates absolute Cartesian velocities to relative joint velocities" (11:1-2). This method allows individual derivation of the EOMs for any number of rigid bodies that are connected by mechanical joints. The final form of the coupled EOMs (Equation 2) slightly resemble those of Equation 1 in that they can be solved for acceleration as one would solve a set of linear algebraic equations.

$$B^T I_s B\ddot{\eta} = B^T (Q_s - I_s \dot{B}\dot{\eta}) \tag{2}$$

B and $\dot{B}$ in Equation 2 are the velocity and acceleration transformation matrices, respectively. I_s is the system's uncoupled mass-inertia matrix. Q_s is the uncoupled force/moment vector and is the same thing as the right hand side of Equation 1. $\dot{\eta}$ and $\ddot{\eta}$ are vectors of the joint velocities and accelerations, respectively.

To form Equation 2, each rigid body in the system has its own respective coordinate system from which a set of EOMs is developed. Concatenating the separate sets of EOMs into block-matrix form and adding the velocity and acceleration transformation matrices forms the uncoupled EOMs for the system.

The mechanical joints in the system generate constraints that couple the entire system. The number of constraints is determined by the motion the specific type of joint allows. Joint types, allowable motion and corresponding number of constraints are shown in Table 1.

Table 1. Mechanical Joints

Joint Type	Allowable Motion	# of Constraints
Revolute	Rotation in 1 direction	5
Prismatic	Translation in 1 direction	5
Cylindrical	Rotation in 1 direction and Translation in 1 direction	4
Universal	Rotation in 2 directions	4
Spherical	Rotation in 3 directions	3
Floating Body	Rotation and Translation in all directions	0

Finally, the velocity and acceleration transformation matrices are formed. These are a concatenation of several smaller block matrices that are dependent upon the connection arrangement and joint type. For example, consider the system in Figure 6.

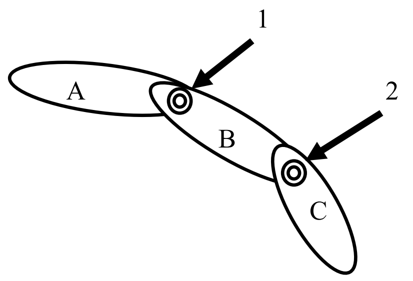

Figure 6. Rigid Bodies Connected by Mechanical Joints

In this system, there are three rigid bodies (A, B and C) connected by joints 1 and 2. This system would have three sets of EOMs, similar in form to Equation 1, with each set having been written in its own reference frame. Assembling these into block-matrix form would give the uncoupled EOMs for the system. Joints 1 and 2 would determine the constraints required for the velocity and acceleration transformation to couple the system and solution to the system of equations readily follows.

In developing coupled EOMs for the KC-135 and refueling boom, the tanker/boom system was modeled as three rigid bodies. The tanker was modeled as a rigid body connected to the inertial frame via a floating body joint (no constraints). The tanker’s coordinate frame is that of a typical aircraft coordinate system (x out the nose, y toward the right wing, z nominally down) with the origin located at the aircraft’s mass center. This defined the **B** (body) reference frame (see Figure 7).

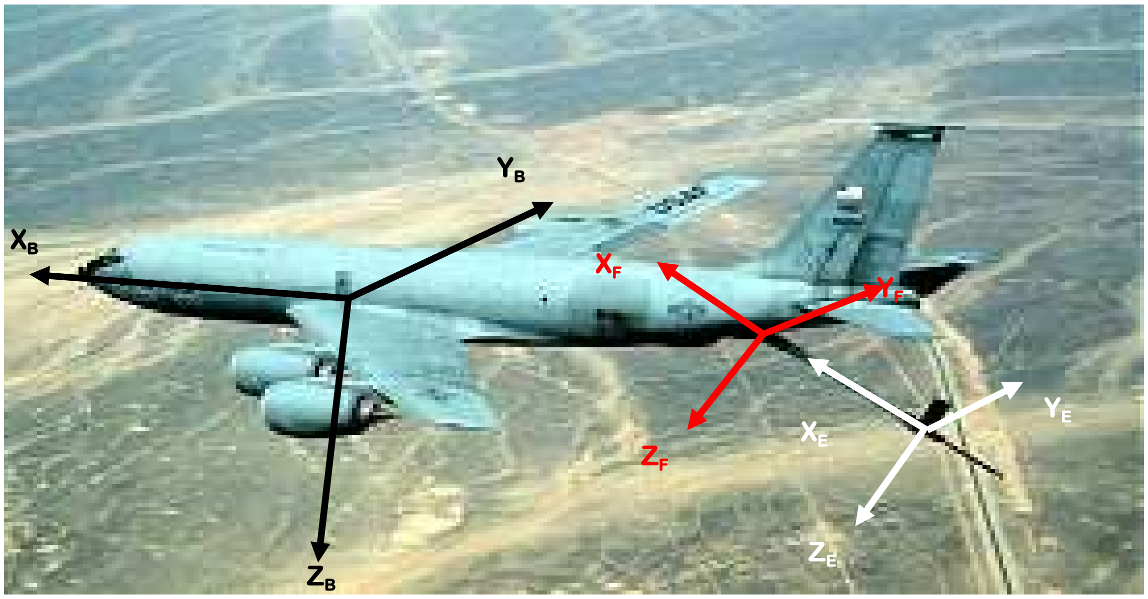

Figure 7. Origin of Coordinate Frames Used to Derive the Uncoupled EOMs (arrows are all pointing in the positive direction) (14).

The two parts of the boom, the fixed boom and boom extension, were modeled as seperate rigid bodies. Since the boom fork only allows the fixed boom to pitch and yaw, this connection was modeled as a universal joint and generates four motion constraints in the system. The fixed boom's coordinate system, the **F** (fixed) reference frame, originated at the boom pivot, and the axes "are defined such that when the boom yaw and pitch angles are zero, the [fixed] boom axes are aligned with the tanker axes" (11:4). This means that the boom would be stowed at a negative pitch angle. Also, with the origin at the boom pivot, the entire length of the fixed boom is in the negative x direction of the **F** frame.

The boom extension is only allowed to translate in and out of the fixed boom, so the joint connection between the two bodies is a prismatic joint. This introduces five more constraints for a total of nine. The **E** (extension) reference frame was originated at the tip of the fixed boom, and the axes were defined to always be aligned with the **F** frame. Note that the boom extension would extend in the negative x direction of the **E** frame. Figure 7 shows the layout of the three different coordinate frames.

This leaves three sets of six uncoupled EOMs for the tanker, fixed boom, and boom extension, respectively. Each set was written with respect to their own reference frame. Concatenating the three sets into block matrix form gives the system's uncoupled EOMs shown in Equation 3

$$\begin{bmatrix} m_B[\mathbf{I}] & 0 & 0 & 0 & 0 & 0 \\ 0 & [I_B] & 0 & 0 & 0 & 0 \\ 0 & 0 & m_F[\mathbf{I}] & -m_F[\tilde{r}_F] & 0 & 0 \\ 0 & 0 & m_F[\tilde{r}_F] & [I_F] & 0 & 0 \\ 0 & 0 & 0 & 0 & m_E[\mathbf{I}] & -m_E[\tilde{r}_E] \\ 0 & 0 & 0 & 0 & m_E[\tilde{r}_E] & [I_E] \end{bmatrix} \begin{Bmatrix} \{\dot{v}_B\} \\ \{\dot{\omega}_B\} \\ \{\dot{v}_F\} \\ \{\dot{\omega}_F\} \\ \{\dot{v}_E\} \\ \{\dot{\omega}_E\} \end{Bmatrix} = \begin{Bmatrix} \{F_B\} \\ \{M_B\}-[\tilde{\omega}_B][I_B]\{\omega_B\} \\ \{F_F\}-m_F[\tilde{\omega}_F][\tilde{\omega}_F]\{r_F\} \\ \{M_F\}-[\tilde{\omega}_F][I_F]\{\omega_F\} \\ \{F_E\}-m_E[\tilde{\omega}_E][\tilde{\omega}_E]\{r_E\} \\ \{M_E\}-[\tilde{\omega}_E][I_E]\{\omega_E\} \end{Bmatrix} \tag{3}$$

Or compactly written as

$$[I_s]\{a\}=\{Q_s\} \tag{4}$$

where I_s is the 18x18 mass/inertia matrix for the system, a is the 18x1 uncoupled acceleration vector for the three bodies, and Q_s is the 18x1 uncoupled force/moment vector. Both Q_s and I_s can be directly input into Equation 2.

Subtracting the total number of constraints from the total number of degrees of freedom in the uncoupled system will show how many degrees of freedom the coupled system will have. Equation 5 shows how to determine the number of degrees of freedom a coupled system of rigid bodies connected by joints will contain. This defines the size of the joint velocity and acceleration vectors, $\dot{\eta}$ and $\ddot{\eta}$. Since the three rigid bodies of the tanker/boom system have a total of nine degrees of freedom, $\dot{\eta}$ and $\ddot{\eta}$ are each 9x1 vectors.

$$\textit{Coupled System DOF = 6 x (\# of rigid bodies) – (number of constraints)} \qquad (5)$$

In the tanker/boom system, the KC-135 joint is a floating body. This adds no motion constraints to the overall system. The tanker's six degrees of freedom take up the first six states in $\ddot{\eta}$ (A_x, A_y, A_z, $\dot{P}$, $\dot{Q}$, $\dot{R}$). This accounts for the linear and angular accelerations of the tanker in all three axes. States seven and eight, $\ddot{\psi}_F$ and $\ddot{\theta}_F$, account for the allowable angular accelerations (pitch and yaw) of the fixed boom. The final state, $\ddot{u}_E$, is the linear acceleration of the boom extension as it telescopes in and out of the fixed boom. All together, $\dot{\eta}$ and $\ddot{\eta}$ are nine state vectors defined by the following:

$$\dot{\eta} = \begin{Bmatrix} V_x \\ V_y \\ V_z \\ P \\ Q \\ R \\ \dot{\psi}_F \\ \dot{\theta}_F \\ \dot{u}_E \end{Bmatrix} \qquad \ddot{\eta} = \begin{Bmatrix} A_x \\ A_y \\ A_z \\ \dot{P} \\ \dot{Q} \\ \dot{R} \\ \ddot{\psi}_F \\ \ddot{\theta}_F \\ \ddot{u}_E \end{Bmatrix} \qquad (6)$$

$\dot{\eta}$ will be input into Equation 2 first according to the initial condition of each state, and then will be updated at each time step throughout the simulation. $\ddot{\eta}$ is the vector that will be obtained by solving Equation 2.

The overall size of the velocity transformation matrix, *B*, is determined from the coupled tanker/boom system's degrees of freedom, and the total number of degrees of freedom in the uncoupled system. The coupled system's degrees of freedom defined above determines the total number of columns in the *B* matrix and corresponds to the length of the vectors in Equation 6. The number of rows in *B* can be found by examining the length of the acceleration vector *a* in Equation 4. This vector represents all directions of motion available in the uncoupled system. The coupled tanker/boom system has nine degrees of freedom and eighteen uncoupled degrees of freedom. Therefore, the velocity transformation matrix is an 18x9 matrix.

Each joint type has a corresponding block matrix that fits into the velocity transformation matrix, *B*. The size of that block is determined by the joint type. The rows of the block will always be determined by the six unconstrained degrees of freedom. The number of columns equals the allowable degrees of freedom defined by a particular joint type. The tanker as a floating body has no constraints, so it will be a 6x6 block. The fixed boom (universal joint) has two degrees of freedom and creates a 6x2 block. The boom extension a single degree of freedom and will be a 6x1 block.

"The position of these block matrices within the velocity transformation matrix is determined by the order in which the bodies are connected, and by the type of joint that connects the bodies" (11:7). For the tanker/boom system, the velocity transformation matrix will be in the form of Equation 7.

$$B = \begin{pmatrix} F_{BB} & 0 & 0 \\ F_{FB} & U_{FF} & 0 \\ F_{EB} & U_{EF} & P_{EE} \end{pmatrix} \tag{7}$$

where the F_{xx} (floating) blocks are 6x6, the U_{xx} (universal) blocks are 6x2 and the P_{xx} (prismatic) blocks are 6x1. The block's order of placement can be seen by looking from right to left at the bottom row of *B*, "the boom extension is connected to the fixed boom by a prismatic joint, the fixed boom is connected to the tanker by a universal joint, and the tanker is a floating body" (4:7). The contents of the respective blocks contain the required direction cosine matrices, position vectors, and rotation axes for going between the different reference frames. Equation 8 shows the block matrices for the bottom row of *B*.

$$F_{EB} = \begin{pmatrix} C^{EI} & -C^{EB}\tilde{r}^{B}_{E/B} \\ 0 & C^{EB} \end{pmatrix} \qquad U_{EF} = \begin{pmatrix} 0 & 0 \\ C^{EB}n^{B}_{\psi} & C^{EF}n^{F}_{\theta} \end{pmatrix} \qquad P_{EE} = \begin{pmatrix} n^{E}_{U} \\ 0 \end{pmatrix} \tag{8}$$

With all the blocks in place, Equation 7 can be directly input into Equation 2. The remaining unknown piece of Equation 2 is the acceleration transformation matrix, $\dot{B}$, which is the time derivative of the velocity transformation matrix, *B*.

As mentioned in Chapter 1, the Kunz/Smith boom model based on these EOMs was developed in Matlab. The EOMs were written in first order form to ensure compatibility with Matlab's differential equation solution functions. The model was validated for uncoupled boom motion against both the AFIT and BOPTT model.

The AFRL KC-135 Model

An overview of the major systems of AFRL's KC-135 Simulink model is shown in Figure 8. The function performed by each respective major system is also included in Figure 8. The model is initialized by running two separate Matlab script files: *sim_tanker_boom.m* and *init_AAR_tanker.m*. The first file requires input of an initial state of the tanker including position, velocity, engine settings, type of path to fly (i.e. straight and level, racetrack, etc.), and if control inputs are coming from the autopilot or manually. The second file sets up the mass profile and trim condition of the tanker. Gain schedules for the automatic control system, constants for the WGS-84 inertial frame system and the initial conditions on states to be integrated (such as $\dot{P}, \dot{Q}, \& \dot{R}$), in the simulation are also set. The majority of work performed by the model is done in the *Vehicle Model* system. A breakdown of this system, its subsystems and their inputs and outputs is shown in Figure 9.

There are a few things to note from Figure 9. First, though there is a *Boom Position* subsystem, it does not take into account any interactions that would occur between the tanker and boom. The boom position this function calculates appears to be the difference between the tanker and boom's center of gravity based on initial conditions. Secondly, the body forces and moments from the *Aero/Propulsion Model* and the inertia matrix from the *Mass Properties* block are fed directly into the *Rigid Body Motion* subsystem.

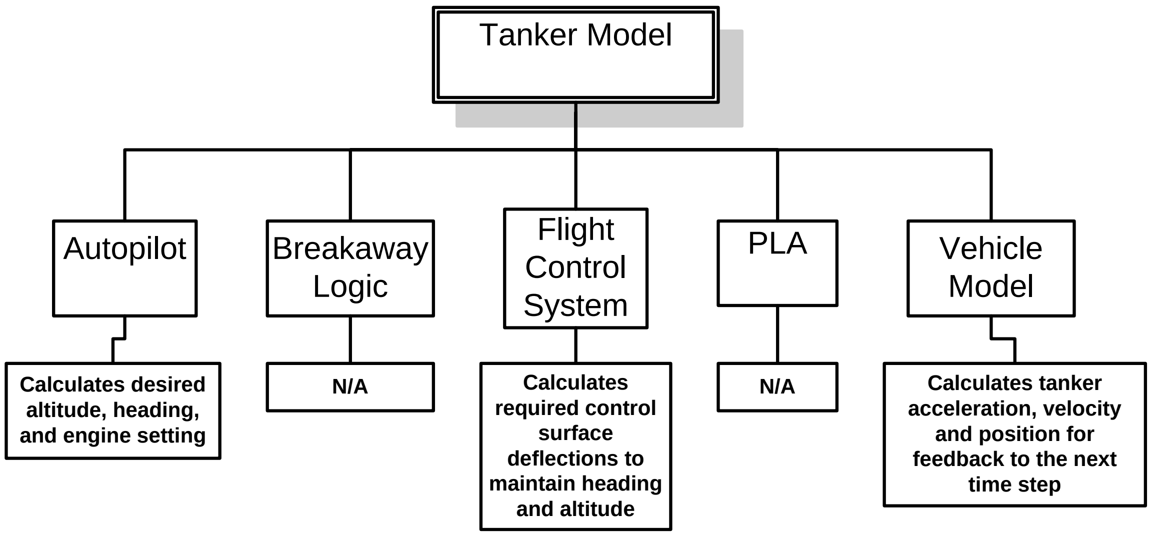
Tanker Model
Autopilot
Breakaway Logic
Flight Control System
PLA
Vehicle Model
Calculates desired altitude, heading, and engine setting
N/A
Calculates required control surface deflections to maintain heading and altitude
N/A
Calculates tanker acceleration, velocity and position for feedback to the next time step

Figure 8. Major Systems of the AFRL Tanker Model

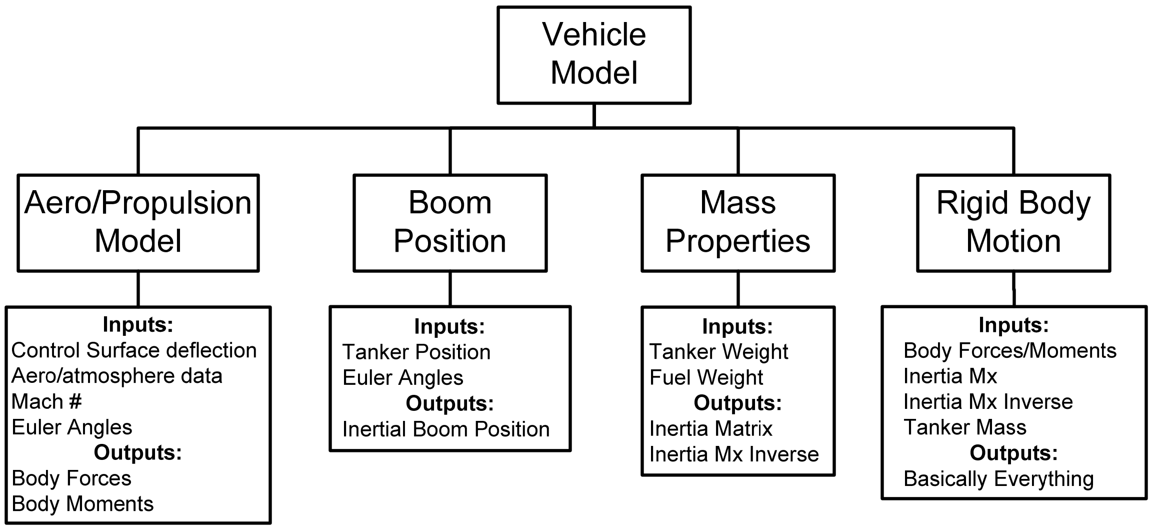
Vehicle Model
Aero/Propulsion Model
Boom Position
Mass Properties
Rigid Body Motion
Inputs: Control Surface deflection, Aero/atmosphere data, Mach #, Euler Angles
Outputs: Body Forces, Body Moments
Inputs: Tanker Position, Euler Angles
Outputs: Inertial Boom Position
Inputs: Tanker Weight, Fuel Weight
Outputs: Inertia Matrix, Inertia Mx Inverse
Inputs: Body Forces/Moments, Inertia Mx, Inertia Mx Inverse, Tanker Mass
Outputs: Basically Everything

Figure 9. The Vehicle Model System, Associated Subsystems, and Their Inputs and Outputs

The *Rigid Body Motion* module takes the inputs and solves Equation 1 for the tanker's acceleration vector. The linear accelerations are integrated twice to get velocity and position, respectively. The angular accelerations are integrated once to find the angular rates. These are fed back through the system. The tanker Euler angles, inertial position and velocity vectors are calculated from quaternions. Many other variations of these states are also calculated and set up for feedback through the system or output to a specified location, but are not discussed here because they are not important to the effort of creating a coupled model. An overview of *Rigid Body Motion's* subsystems can be seen in Figure 10.

There are some points to note in Figure 10 as well. The quaternion and angular velocity vector coming out of the *Equations of Motion* block are both fed back to the *Form Accelerations* block and fed forward to the *Alternate States* block. The acceleration vectors calculated from the *Form Accelerations* block are fed forward to the *Equations of Motion* subsystem. The *Equations of Motion* block is not exactly as it seems; its only function is to integrate the accelerations coming out of the *Form Accelerations* block. The EOMs are actually solved in the *Form Accelerations* module.

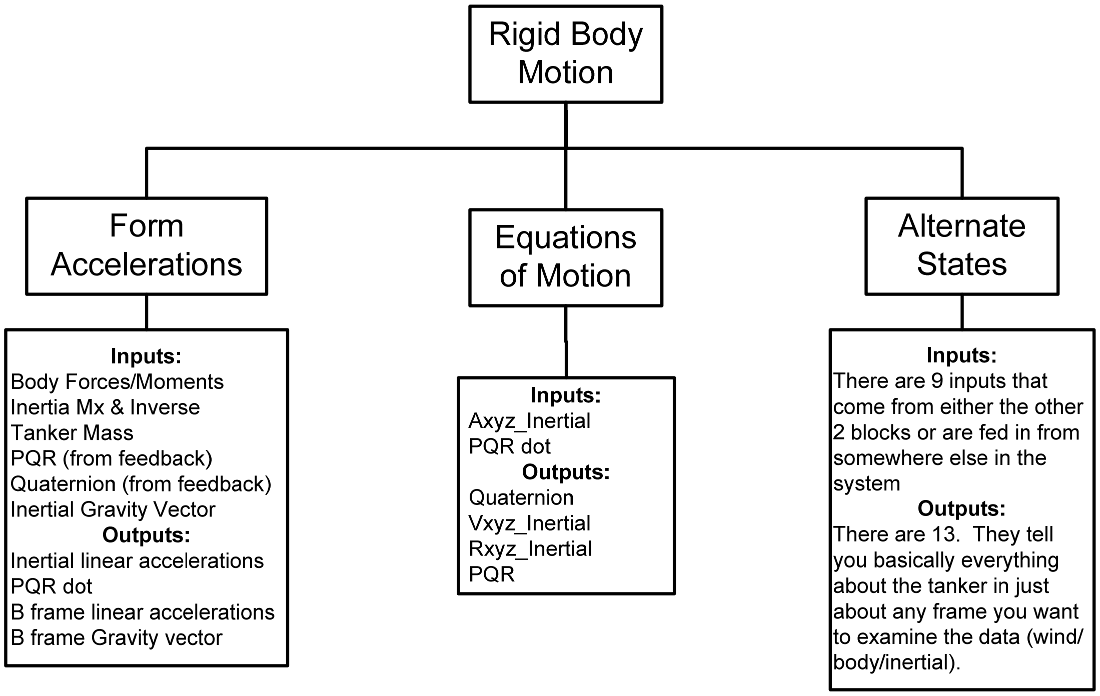
Rigid Body Motion
Form Accelerations
Equations of Motion
Alternate States
Inputs:
Body Forces/Moments
Inertia Mx & Inverse
Tanker Mass
PQR (from feedback)
Quaternion (from feedback)
Inertial Gravity Vector
Outputs:
Inertial linear accelerations
PQR dot
B frame linear accelerations
B frame Gravity vector
Inputs:
Axyz_Inertial
PQR dot
Outputs:
Quaternion
Vxyz_Inertial
Rxyz_Inertial
PQR
Inputs:
There are 9 inputs that come from either the other 2 blocks or are fed in from somewhere else in the system
Outputs:
There are 13. They tell you basically everything about the tanker in just about any frame you want to examine the data (wind/ body/inertial).

Figure 10: Subsystems of Rigid Body Motion Including Inputs and Outputs

Implementing the Coupled Equations of Motion in the AFRL Tanker Model

The first modification was to the initialization files. Init_AAR_tanker.m was modified to include the mass properties and dimensions of the fixed boom, ruddevators and boom extension. The initial state of the system was changed to include the addition of the fixed boom and boom extension. New inputs required were the initial pitch and yaw angles of the boom, the boom's angular rates, initial position of the ruddevators and the position of the boom extension.

The majority of modifications to the AFRL model took place in the *Rigid Body Motion* system generally, and the *Form Accelerations* subsystem specifically. A goal of modifying the AFRL model is to leave much of it untouched. Many required parameters for the coupled equations of motion are already calculated elsewhere in the AFRL model and in turn only have to be routed to the correct place. For example, the tanker's body forces and moments and the mass/inertia matrix as calculated by the AFRL model were left alone. Those values are needed to complete the coupled EOMs, but there was no need to build an entirely new function to compute them. Instead, they were just rerouted and concatenated into the coupled EOMs. Other parameters that are created by the coupled EOMs, such as the nine state joint velocity and position vectors, must be fed back during each time step.

The primary means of modification was placing embedded Matlab functions in the *Form Accelerations* subsystem. Embedded Matlab functions are basically standalone Simulink blocks written in the Matlab language. There is a limited availability of Matlab tools usable in embedded function. For example, dynamically sizing an array inside a loop is not allowed. The size of the variable must be defined first, and once that size is assigned, it cannot change. The functions can take in and output any number of one or two dimensional arrays defined by the user. Table 2 shows the embedded functions added to the AFRL model, and a short discussion of each will follow. Code for the embedded functions can be seen in Appendix C.

Table 2. List of Embedded Functions and their purpose

Function	**Purpose**
TankerMass	Generate the 6x6 Mass/Inertia Matrix of the Tanker Generate rhs of Tanker's 6x1 Force/Moment Vector
FixedBoom	Generate the 6x6 Mass/Inertia Matrix of the Fixed Boom Generate rhs of Fixed Boom's 6x1 Force/Moment Vector
BoomExt	Generate the 6x6 Mass/Inertia Matrix of the Boom Extension Generate rhs of Boom Extension's 6x1 Force/Moment Vector
Uncoupled18x18	Concatenate the 3 6x6 Mass/Inertia matrices into the 18x18 system Mass/Inertia Matrix Is
FixedBoomDrag_Gravity	Calculate the aerodynamic and gravitational force and moment contribution of the Fixed Boom
LeftRuddevator	Calculate the aerodynamic and gravitational force and moment contribution of the Left Ruddevator
RightRuddevator	Calculate the aerodynamic and gravitational force and moment contribution of the Right Ruddevator
BoomExtension_Drag_Gravity	Calculate the aerodynamic and gravitational force and moment contribution of the Boom Extension
VelocityTransformation	Calculate the Velocity Transformation Matrix, B
AccelerationTransformations	Calculate the Acceleration Transformation Matrix, B_dot
Combined	Concatenate all the body and gravitational forces/moments to form the system's 18x1 Force/Moment vector
RHS_I_Bdot_eta	performs [Is]*[Bdot]*[ηdot]
etadoubledot	solves the coupled EOMs for the 9 state joint acceleration vector

A total of 13 embedded functions were added to the *Form Accelerations* subsystem. Since most of the embedded functions share a majority of required inputs, a single vector was created to serve as their input. This helped clean up the appearance of the new *Form Accelerations* block and made signal routing much easier. .

TankerMass: Inputs to this function were the tanker's mass and inertia matrix as calculated by the original model. Basically, this took Simulink's version the tanker's inertia matrix, which was a six component vector containing the mass moment of inertia for each principal direction, and formed the 6x6 mass/inertia matrix of the tanker. Also the $[\tilde{\omega}_B][I_B]\{\omega_B\}$ portion of the tanker's section of Q_s in Equation 4 was calculated and output.

FixedBoom: Inputs were the tanker's angular velocity and the pitch/yaw position and rate of the boom. It calculated the fixed boom's mass/inertia matrix, along with the $m_F[\tilde{\omega}_F][\tilde{\omega}_F]\{r_F\}$ and $[\tilde{\omega}_F][I_F]\{\omega_F\}$ portions of Q_s corresponding to the fixed boom.

BoomExt: Inputs were the boom extension's position, the tanker's angular velocity and the pitch/yaw position and rate of the boom. It calculated the boom extension's mass/inertia matrix, along with the $m_E[\tilde{\omega}_E][\tilde{\omega}_E]\{r_E\}$ and $[\tilde{\omega}_E][I_E]\{\omega_E\}$ portions of Q_s corresponding to the boom extension.

Uncoupled18x18: Took in the three 6x6 mass/inertia matrices and the three 6x1 right portions of Q_s. Assembled the 18x18 mass/inertia matrix for the system and the 18x1 right side of Q_s.

FixedBoomDragGravity: Inputs to this system include the tanker's inertial velocity vector and Euler angles, as well as the fixed boom's pitch/yaw attitude and rates. The incremental aerodynamic forces on the fixed boom were calculated using the drag relationship and integrated from the boom tip to the boom pivot. The fixed boom was modeled as a cylinder of varying diameter and the drag coefficient was found from the cylinder's relationship to the local Reynold's number. This function's output was the 6x1 aerodynamic and gravitational force/moment vectors of the fixed boom.

LeftRuddevator: Inputs here were the translational and angular velocities and Euler angles of the tanker and the fixed boom's pitch/yaw attitude and rates. Aerodynamic forces were calculated using general aerodynamic strip theory as would be used on any wing or control surface. An additional coordinate system was needed for this calculation, and it originated where the ruddevator would intersect the fixed boom centerline. All three axes initially aligned with those of the F frame. This coordinate system was then rotated 42^o about the x axis to account for the ruddevator dihedral angle. This rotation puts the left ruddevator on the negative y axis and defines the $\mathbf{W}_L$ frame. The local velocity was calculated and the angle of attack was corrected for yawed flow. With this corrected angle of attack, lift and drag coefficients were calculated and the incremental forces and moments were calculated across the ruddevator span. The incremental forces were then integrated from the ruddevator tip inboard. Once the force and moment contribution of left ruddevator had been calculated in the $\mathbf{W}_L$ frame, they were transformed to act at the boom pivot, which is also the origin of the **F** frame.

RightRuddevator: Same inputs and calculations performed as in the LeftRuddevator function, but this time the coordinate system was rotated -42^o about the x axis to form the W_R frame. In turn, the positive y direction went from the origin outboard to the right ruddevator tip, and the incremental forces and moments were integrated from inboard to outboard. The ruddevator reference frames are shown in Figure 11.

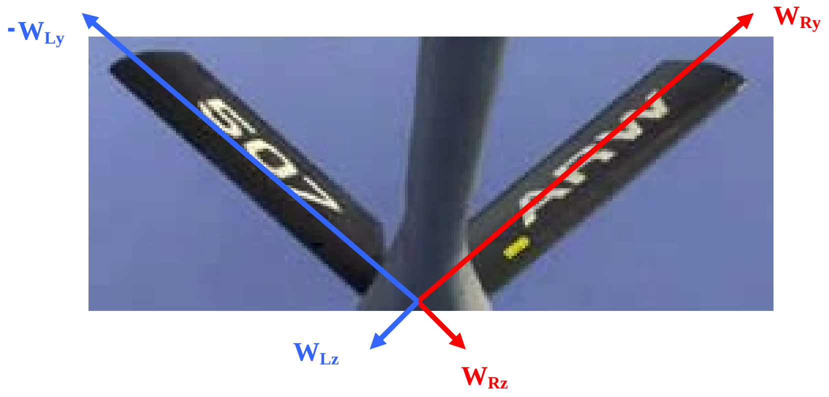

Figure 11. Ruddevator Coordinate Frames (1)

BoomExtension_Drag_Gravity: Aerodynamic forces and moments for the boom extension were calculated in the same manner as the elliptical portion of the fixed boom, with the exception that the boom extension has a fixed diameter. Obviously, if the boom extension is completely inside the fixed boom, it adds no drag to the system. If the boom extension has telescoped out of the fixed boom, the incremental drag forces are calculated and then integrated from the boom extension's tip to the tip of the fixed boom.

VelocityTransformation: Takes in the tanker and fixed boom position angles and the boom extension's position. Computes the floating, universal and prismatic blocks of Equation 7 and then assembles them into the 18x9 velocity transformation matrix *B*.

AccelerationTransformation: Takes in the tanker and fixed boom attitudes and the pitch/yaw rate of the fixed boom. Computes the derivative of the velocity transformation matrix, which is the acceleration transformation matrix $\dot{B}$.

Combined: Takes in the tanker body forces and moments originally calculated by the AFRL model, and all the aerodynamic and gravitational forces/moments for the fixed boom, ruddevators and boom extension. Recall that the Left/Right Ruddevator function transformed their forces and moments to act at the boom pivot, which is the origin of the **F** reference frame. Here, both ruddevator forces and moments are added to the forces and moments for the fixed boom. Once that was done, everything was concatenated into an 18x1 force vector, which is the left portion of Q_s from Equation 4.

RHS_I_Bdot_eta: Takes in I_s from the Uncoupled18x18 function, $\dot{B}$ from the AccelerationTransformation function, the joint velocity vector, $\dot{\eta}$ that was fed back from the *Equations of Motion* system from the AFRL model, and the tanker's inertial velocity vector. Computes the $I_s \dot{B} \dot{\eta}$ portion of Equation 2.

etadoubledot: Takes in I_s from the Uncoupled18x18 function, the fully assembled 18x1 Q_s vector, and the velocity transformation matrix, B from the VelocityTransformation function. Computes the joint acceleration vector, $\ddot{\eta}$, of the coupled tanker/boom system. This is the final solution to Equation 2, the EOMs that were derived to couple the tanker and boom, at a particular time step.

After coming out of the *etadoubledot* function, the joint acceleration vector is then fed forward to the *Equations of Motion* system. Originally, there were two Simulink integration block systems in the *Equations of Motion* system; one for the linear and another for the angular accelerations of the tanker. Prior to entering the Equations of Motion system, the tanker's linear accelerations were converted to the inertial frame. In order to keep the original model going with all its calculations involving the various forms of the basic data, the linear and angular accelerations of the tanker (the first 6 states of $\ddot{\eta}$) were extracted from $\ddot{\eta}$. The tanker's linear accelerations were converted to the inertial frame and then they along with the tanker's angular accelerations were sent through the AFRL model's two original integration block systems. Inside the *Equations of Motion* system, a third Simulink integration block system was added and set up to receive $\ddot{\eta}$, integrate it twice and extract the joint velocity and position vectors that were required for feedback through the *Form Accelerations* system. The modified portions of the AFRL Simulink model can be seen in Appendix A

III Data Analysis

Overview

Data collection and analysis for this thesis basically involved performing simulations of the new model, and comparing those results to similar simulations performed using the Kunz/Smith boom model and the AFRL tanker model. Of particular interest was investigating the motion of the boom and tanker, and taking note to see if the newly developed equations of motion did exhibit any coupling tendencies between the tanker and boom. For final validation, simulation results were compared to data recorded during a flight test.

The first evaluation of the new coupled Simulink model was to run the simulation with the tanker limited to unaccelerated, straight and level flight. This effectively puts the tanker back on the assumed rigid rail of the original AFRL model because the tanker will not be able to respond to any boom motion. Everything in the tanker's acceleration and velocity vector, except the tanker's initial velocity, must be forced to zero in order to accomplish this. These conditions replicate the comparison of the Kunz/Smith boom to the BOPTT and AFIT boom models. Comparisons between the new model and the Kunz/Smith model were used for initial validation of boom motion in the new model. Boom response to symmetric and asymmetric ruddevator step deflections will be investigated. In both cases, boom motion should be very similar in this series of simulations. Since the Kunz/Smith model has already been validated as an effective representation of boom behavior, this test will serve to validate the behavior of the new model's boom.

The second step in model validation will study the effect of coupling the boom and tanker. If the two bodies have in fact been effectively coupled, there should be small, but noticeable changes in the behavior of the tanker and boom. A comparison of tanker motion between the AFRL tanker model and the coupled model will show any effects the boom has on the tanker. The two models were compared in straight and level flight, and no control inputs were commanded to the boom in the coupled simulation. To investigate the effect of the tanker on boom motion, the coupled model simulation will be performed twice; once with the tanker constrained to straight and level flight, and then with no motion constraints placed on the tanker. This test will show the tanker's coupling effect on the boom. There should be no large differences in response for any of these test cases. There should be a settling period involved with the coupled model in all attitudes, but tanker and boom motion should generally follow that of the existing models.

To investigate the tanker effects on controlled boom motion, the six degree symmetric and asymmetric ruddevator deflection tests will be repeated with the steady level flight constraint removed. These results will then be compared to the previous results of the same simulation performed with the steady flight constraint in place.

To study the effects of commanded boom motion on the tanker, a ten degree symmetric and asymmetric ruddevator deflection will be commanded in the fully coupled model. A comparison will be made between this simulation, and simulation performed by the AFRL and coupled model with no control inputs.

Final validation will come from comparison of the coupled model to existing flight test data recorded during a series of flight tests. The test cases to be examined will compare tanker and boom response to a schedule of ruddevator deflections. If simulations from the new model behave with consistency and can resemble the responses of the available data, then the new coupled model can be validated as a reasonable tool with which to study the motion of the tanker/boom system.

Test Scenario Setup

The basic conditions for the test cases in this research were centered on a nominal configuration of the KC-135 tanker and aerial refueling boom. The tanker was assumed to be in trim at the initial conditions shown in Table 3. The only other manual inputs to the system were the position angles of the ruddevators. Everything else required to determine the initial state of the tanker and boom was calculated by the two Matlab initialization files. There are no structural, aerodynamic, position or rate limits placed on the boom. The ruddevator's automatic control system is not included. However, as long as the system is placed in a realistic initial setting, such as the nominal case described in Table 3, and no grossly exaggerated inputs are used, the system stays inside its envelope.

Table 3. Nominal States for an Assumed Trimmed Tanker/Boom System

Velocity	670 fps
Altitude	25000 ft (std Atm)
Boom Pitch	30 deg
Boom Yaw	0 deg
Boom Extension	12.2 ft
Ruddevator Position	-22.68 deg

Boom Motion with the Tanker in Unaccelerated, Straight and Level Flight

The first examination of the new model will look at boom behavior only, which is accomplished by limiting the tanker to unaccelerated, straight and level flight. This motion constraint effectively uncouples the system and will allow direct comparison of new model's boom motion to that of the Kunz/Smith model. The EOMs in Kunz/Smith and the new coupled model are the same, but are implemented with different numerical techniques, so there should be very little difference in the behavior of both models. Differences could also arise because the two models compute the trim state of the tanker differently. The coupled model includes engine dynamics as part of its trim and subsequent force calculations, whereas the Kunz/Smith model is purely aerodynamic. At the initial conditions in Table 3, the coupled model's tanker was trimmed at a 1.46^o pitch angle. The tanker in the Kunz/Smith model was trimmed at 0^o pitch. Figure 12 shows the boom's pitch response to a symmetric, six degree step input to the ruddevators.

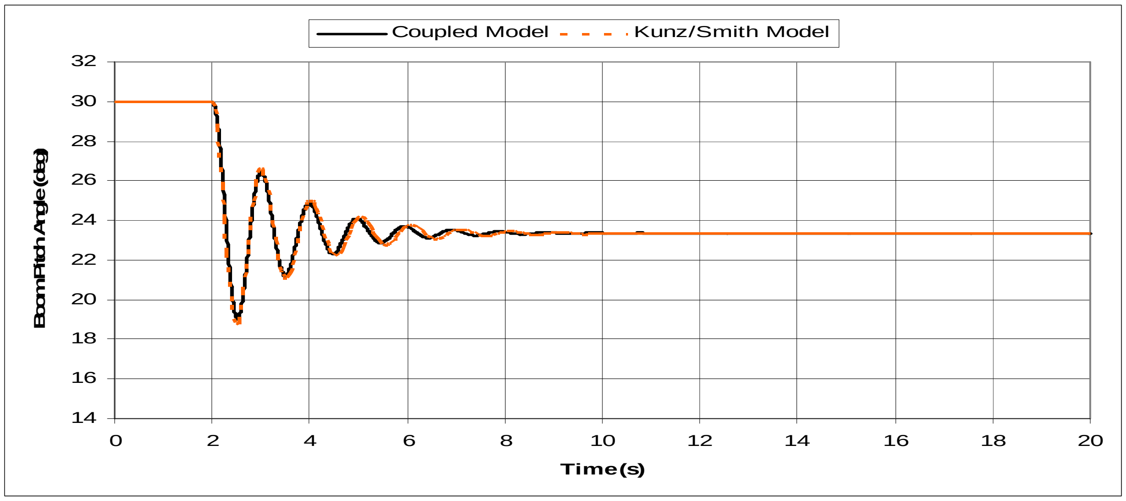

Figure 12. Boom Pitch Response to a Six Degree Symmetric Ruddevator Deflection.

The step was commanded at two seconds. As expected, the Kunz/Smith and coupled models basically mirror each other. The coupled model tracks the motion of the Kunz/Smith model, but has slightly higher frequency and damping. This can be explained by the differences in numerical techniques used. To accomplish the required integration of incremental forces and moments on the fixed boom, ruddevators and boom extension, Kunz and Smith used the Matlab function *quadv*, which is based on the adaptive Simpson's rule for quadrature. The new Simulink model uses an integration routine based on the trapezoidal rule to perform the same operations.

In addition, when determining the incremental lift and drag coefficients on the ruddevators, Kunz and Smith use a two-dimensional table lookup and interpolation based on local the angle of attack and Mach number along the span of the ruddevators. Due to limitations involved with using embedded Matlab functions in a Simulink model, this was reduced to a one dimensional interpolation in the coupled model. Ruddevator lift and drag coefficient data was available in tabular form at Mach numbers of 0, 0.2, 0.3, 0.4, 0.5, 0.6, 0.8, and 1. The new model calculates the local Mach number and angle of attack along the ruddevator span, selects the closest Mach number table available, and then the coefficients are determined by a linear interpolation based on the local angle of attack. Therefore, the ruddevators in the coupled model generated slightly different forces than the Kunz/Smith model.

The forces generated by the ruddevators in the coupled model were about 7-8% larger than those of Kunz/Smith, and in turn the new model's ruddevators have more control authority than those of the Kunz/Smith model. Boom yaw response is not examined in this case because the maximum yaw motion is on the order of 10^{-6} degrees.

Next, a six degree asymmetric step deflection was commanded to the ruddevators. For the case in Figure 13, the left ruddevator deflection was a negative six degrees (from nominal to -28.68^o), and the right was positive (from nominal to -16.68^o). Again, the coupled model has a higher frequency and damping, but in this case, the initial response is of larger amplitude and the boom eventually converges to a slightly higher pitch angle than that of the Kunz/Smith model. This is where the different initial trim states of the models can be seen. In the boom pitch angle plot of Figure 13, the coupled model's boom starts in its nominal 30^o pitch down state and initially starts to climb in an effort to find its true trim state. Kunz and Smith note that in the coupled system, the ruddevators help force the boom down when it is in a yawed state (4:9). This occurs during the initial response to the ruddevator deflection where the coupled model's more authoritative controls force the boom further down.

Simulation results for boom behavior in the new model match that of the Kunz/Smith. There are slight, but acceptable, differences in motion due to the different numerical techniques used. This proves that the new model adequately produces uncoupled boom motion similar to the existing and previously verified models.

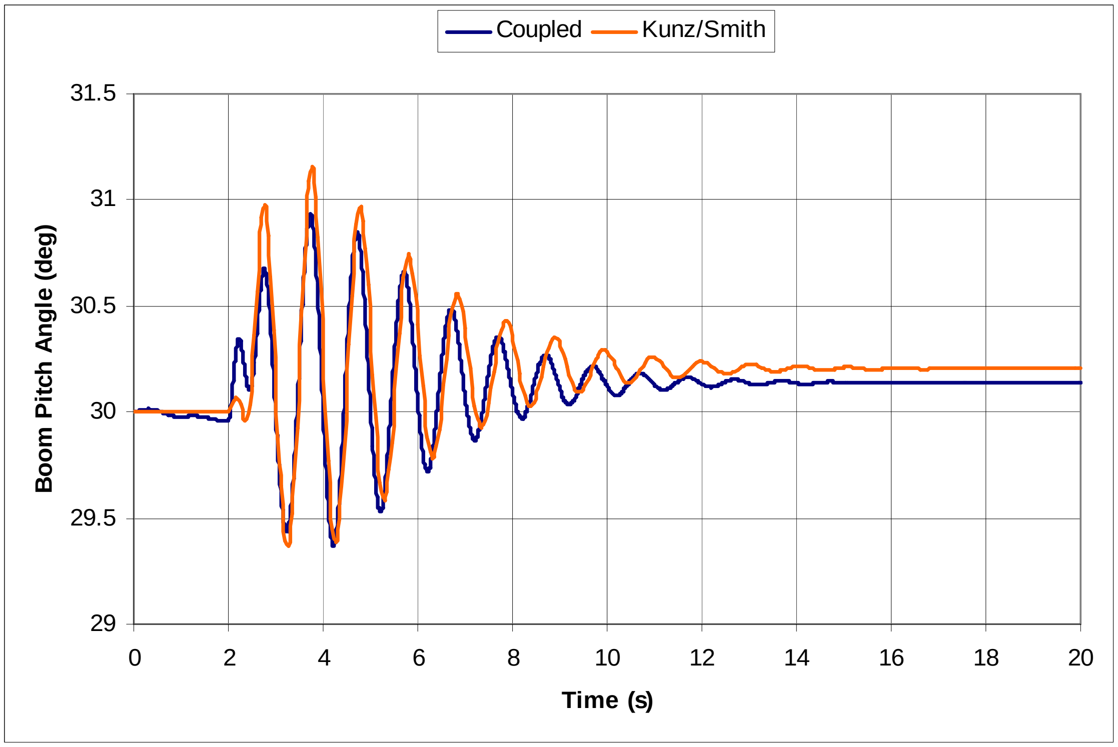

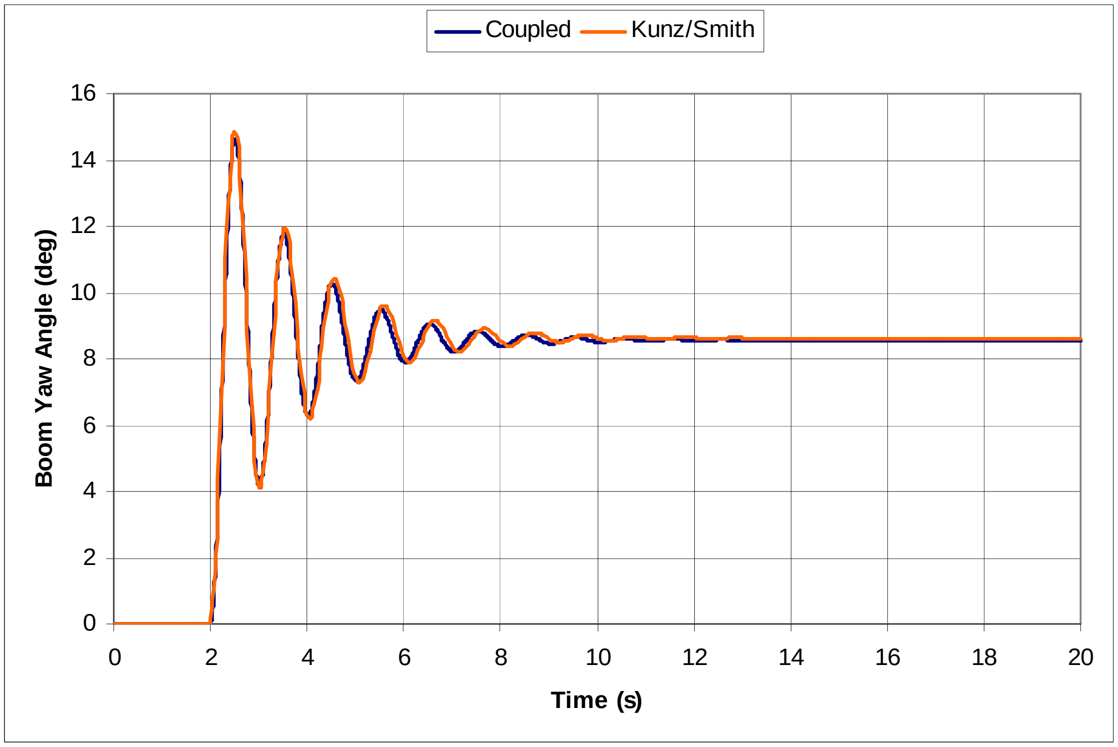

Figure 13. Boom Yaw and Pitch Response to a Six Degree Asymmetric Ruddevator Deflection.

The Effect of Coupling the Tanker and Boom

To investigate the effect of coupling the boom to the tanker, the tanker in the coupled model must be removed from the unaccelerated, steady flight constraint. With that restriction gone, a simulation was performed using no ruddevator control inputs to look at the changes in both boom and tanker behavior. To study the effect on the tanker, these results were compared to a simulation performed using the AFRL tanker model. To study the coupling effect on the boom, the results from this simulation were compared to those of the coupled model with the steady flight restriction still on the tanker.

The coupling effect of the boom and tanker can be seen in Figure 14 and Figure 15. Boom effects on the tanker are easily noticeable. First is the initial transient of the coupled model as the tanker adjusts to the boom. It quickly settles into a slightly more nose up attitude. Afterwards, the coupled tanker continues to remain in a more nose up attitude. This is because the nose down moment caused by the drag force on the boom is overcome by the nose up moment generated by its weight. The difference in the tanker pitch angle is not significant, but the fact that there is a difference shows that coupling between the boom and tanker is taking place in the new model and that this change conforms to the expected physics of the situation.

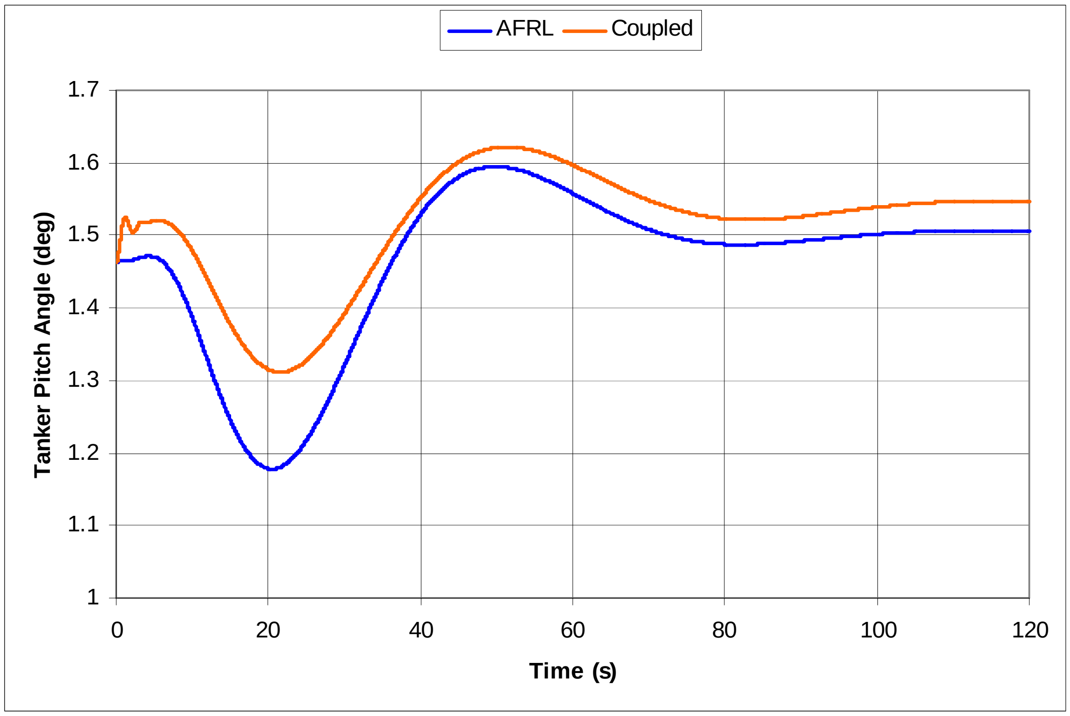

Figure 14. Tanker Pitch Angle Comparison from the Coupled and AFRL Model

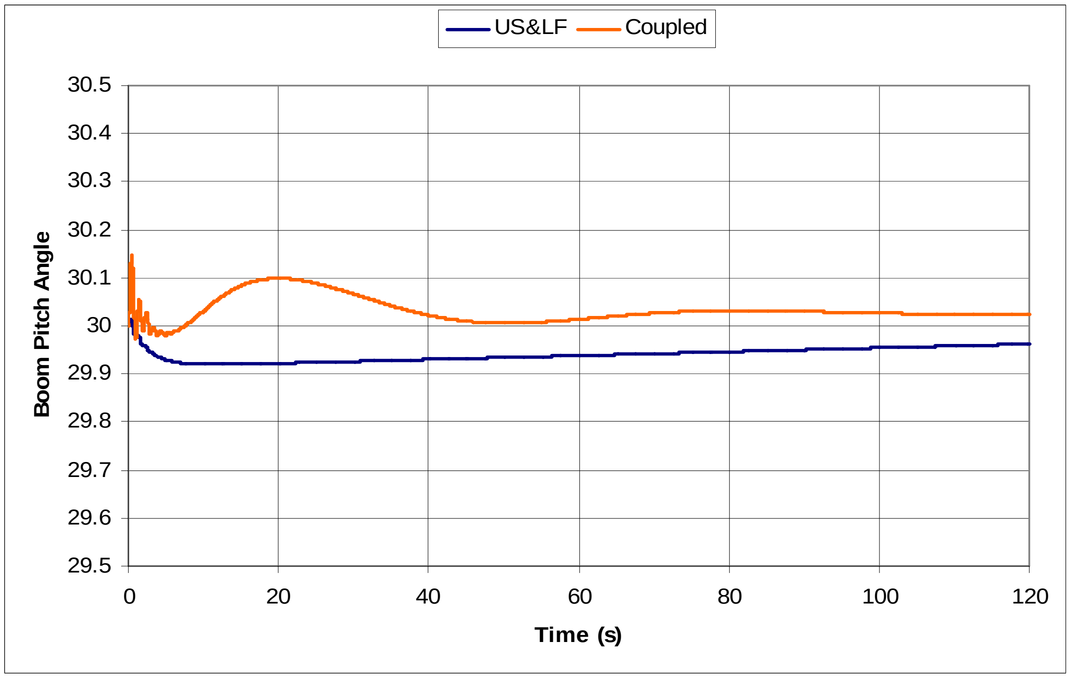

Figure 15. Boom Pitch Angle Comparison: Coupled and Steady, Level Flight Constrained

Figure 15 shows the effect of the tanker on the boom. The tanker appears to have very little impact on the boom. Again, there is the initial transient followed by the boom settling in a slightly more pitch down attitude. Also of note is the pitch motion of the boom is measured with respect to the tanker centerline. As expected, the simulation with the steady level flight constraint showed no reaction to changes in tanker attitude. For the coupled model, recall that positive boom pitch is measured in degrees down from the aircraft centerline. After the initial transient (t = 0-8 sec), the tanker pitch attitude noses down and the boom pitches up. Some of this increase in boom pitch is likely related to the fact the reference frame for the measurement moved upwards, but the value of the tanker pitch and boom pitch changes are not the same. At the maximum change, tanker pitch decreased by ~0.2^{o} while boom pitch only increased ~0.1^{o}. This indicates that the ruddevators are pushing the boom in the opposite direction. This trend continues in both directions as the tanker pitch settles out. The change in trim is rather small, but again, the fact that there was any change shows that the dynamics of the tanker and boom are in indeed interacting.

The results of this test are another good sign for the viability of the new model. They showed that there were in fact dynamic interactions taking place between the tanker and boom. Behavior changes were small but noticeable, and in agreement with the expected physics of the situation.

Tanker Effects on Boom Motion with Boom Control Inputs

To find out what effects the tanker has on boom motion, the first two simulations (six degree symmetric and asymmetric ruddevator step inputs) were repeated with the unaccelerated, steady flight constraint removed.

Figure 16 shows that the tanker has a negligible effect on boom motion when a symmetric ruddevator deflection is commanded. The coupled boom also shows the same initial transient as the boom and tanker begin to settle. Eventually, the boom settles out to a more increased pitch down angle than US&LF, but not enough to have any real effect on the boom motion.

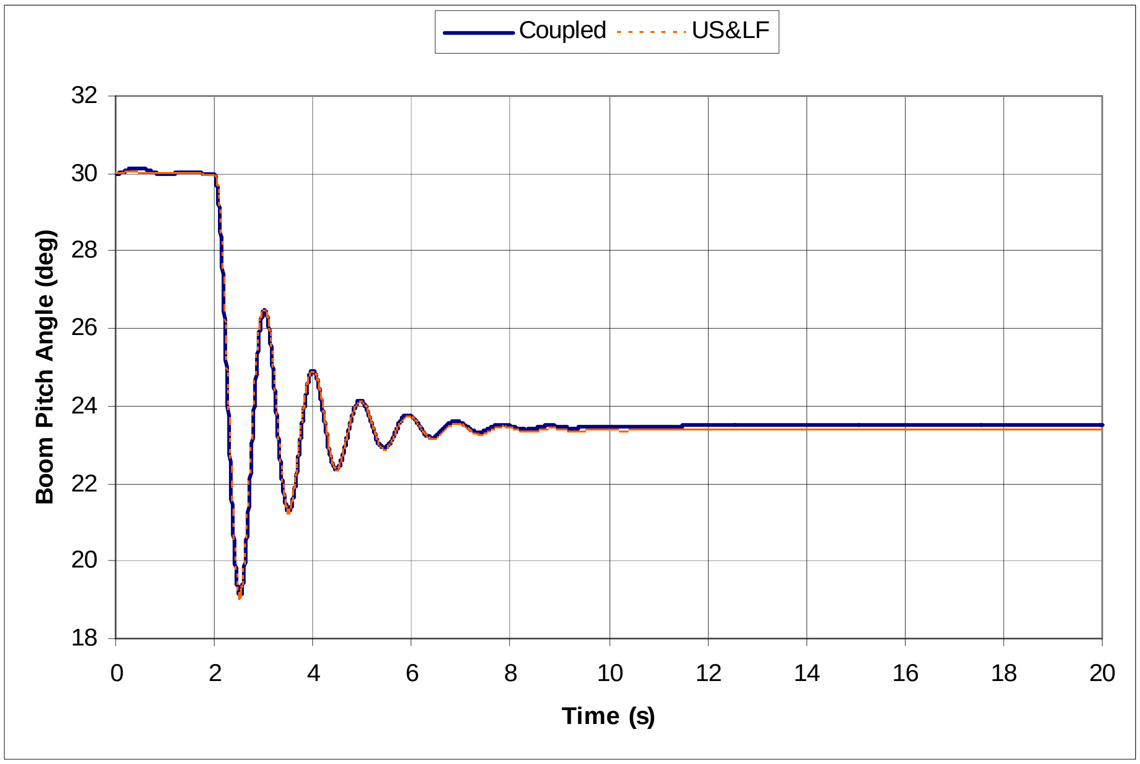

Figure 16. Comparison of Boom Pitch Response to a Six Degree Symmetric Ruddevator Deflection.

Coupled boom response to a six degree asymmetric control input can be seen in Figure 17. Again, the tanker does not make any significant difference in the yaw motion of the boom. The initial effect of coupling the tanker and boom can again be seen in the boom's pitch transient during the two seconds before the ruddevator input is commanded. The coupled boom's pitch trims out about 0.25^o more pitch down than the US&LF case.

These results are also promising. The tanker is exhibiting an influence, however small, on the motion of the boom. Of note is that the no matter the input, the boom trimmed out to a slightly increased pitch angle. This is expected based on the results shown in Figure 15.

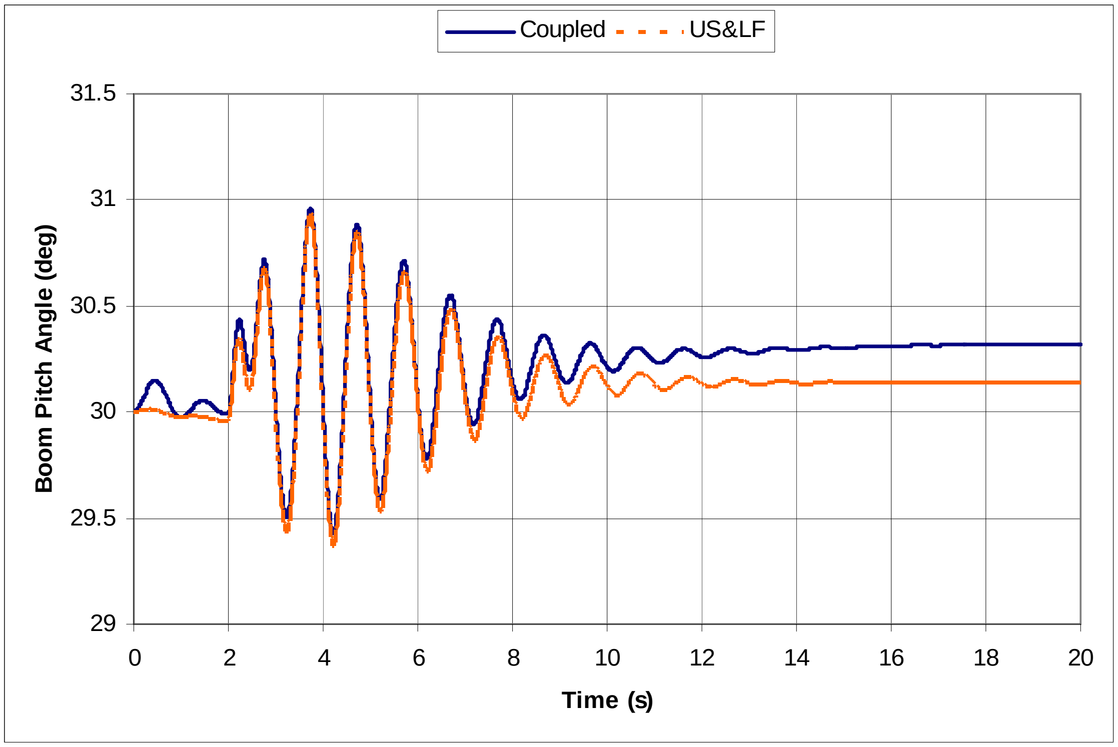

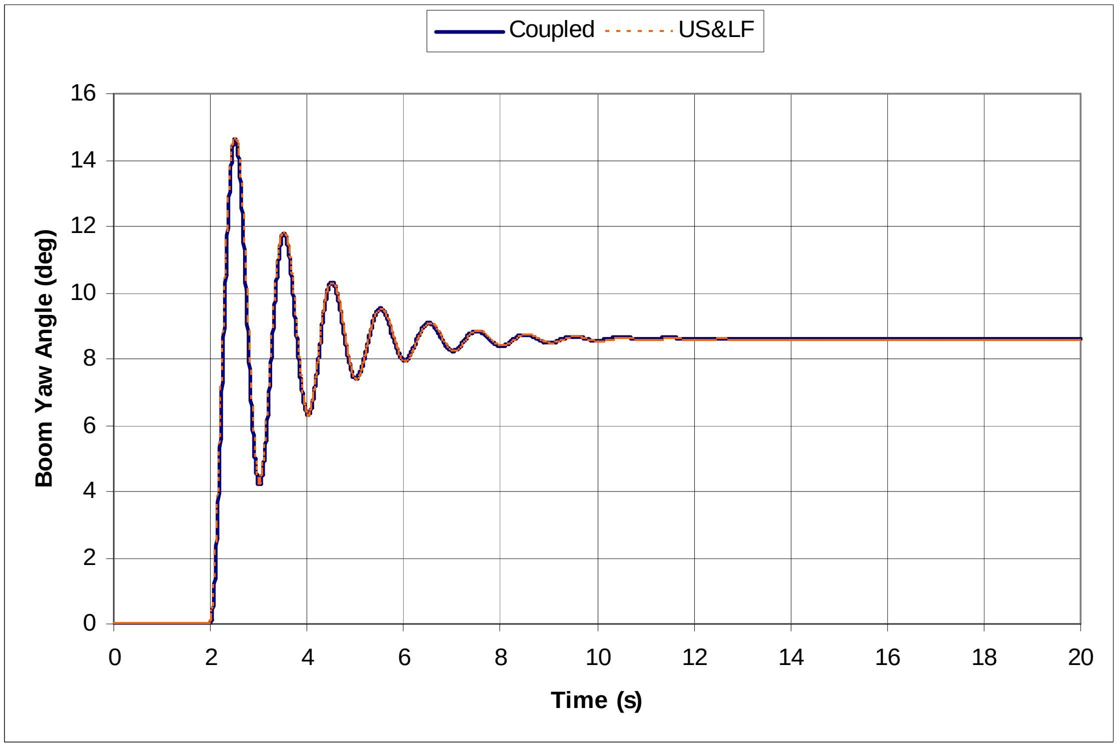

Figure 17. Comparison of Boom Pitch and Yaw Response to a Six Degree Symmetric Ruddevator Deflection.

Boom Effects on Tanker Motion with Boom Control Inputs

The next step in validating the new coupled model involved comparing changes in tanker attitude as a result of commanded boom motion. The coupled (w/ no control inputs) and AFRL models were compared to the results of coupled model simulations performed with ten degree symmetric and asymmetric ruddevator inputs. The deflections were commanded to take place at the 30 second point in the simulation.

Figure 18 shows the results of the simulation where the symmetric ruddevator deflection was input. As noticed before, symmetric ruddevators deflection will only cause the boom to pitch. The tanker's response is not really affected by the pitching motion of the boom. There is a noticeable transient at 30 seconds when the ruddevator deflection is commanded, and the tanker settles into a slightly lower pitch attitude than does the coupled model when no ruddevator deflection was commanded. The boom itself settles from 30^o to about 19^o pitch down.

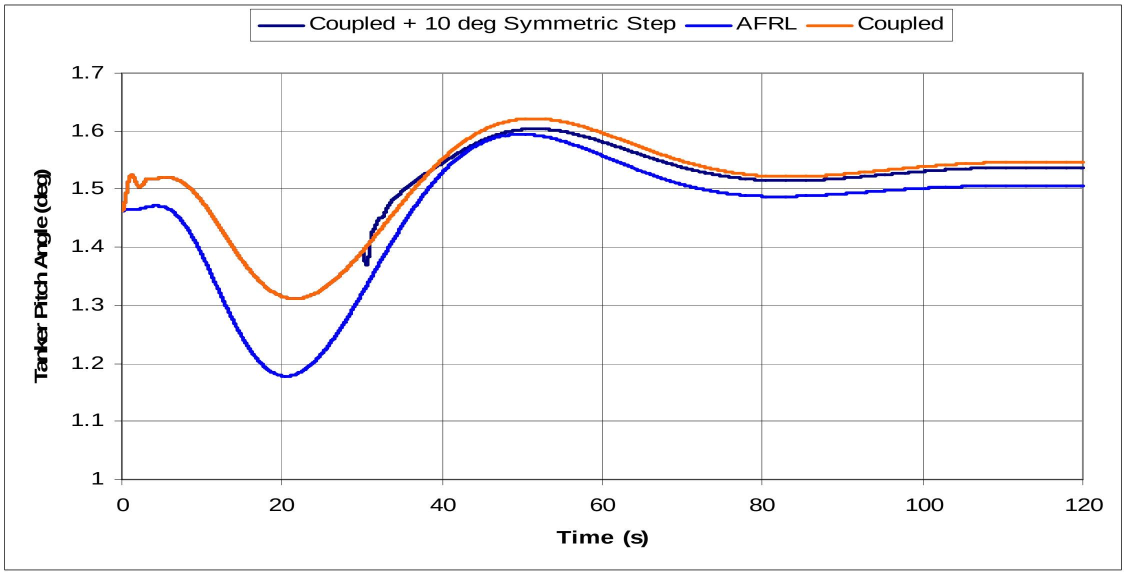

Figure 18. Tanker Pitch Response to a Ten Degree Symmetric Ruddevator Deflection

Next was a comparison of simulations performed with an asymmetric ruddevator deflection. For this particular simulation, it is important to clearly understand the final state of the tanker/boom system at the end of the simulation. The boom moved from the 30^o pitch and 0^o yaw position to 19^o pitch and 15^o yaw. This places the boom in a higher pitch attitude in the freestream on the left side of the aircraft. The tanker's pitch attitude behaves almost exactly the same as in previous tests, but here is where we see the first changes to the tanker's yaw and roll attitude due to the boom. The tanker ended up with a slight negative (right wing up) roll attitude and a steadily increasing negative yaw (nose left) attitude. These results are shown in Figure 19.

The tanker's pitch response remains virtually unchanged from the symmetric input case, but did go up a miniscule amount settling a little closer to the final value of the coupled model with no inputs. The change in the roll and yaw angles is due to the final placement of the boom in this test case.

As mentioned previously, the boom trims out under the left side of the aircraft. This adds an extra mass component to the left of the tanker's center of gravity which in turn generates a moment that forces the left wing down (a negative roll attitude). In similar fashion, the drag component of the boom generates a negative yawing moment (nose left).

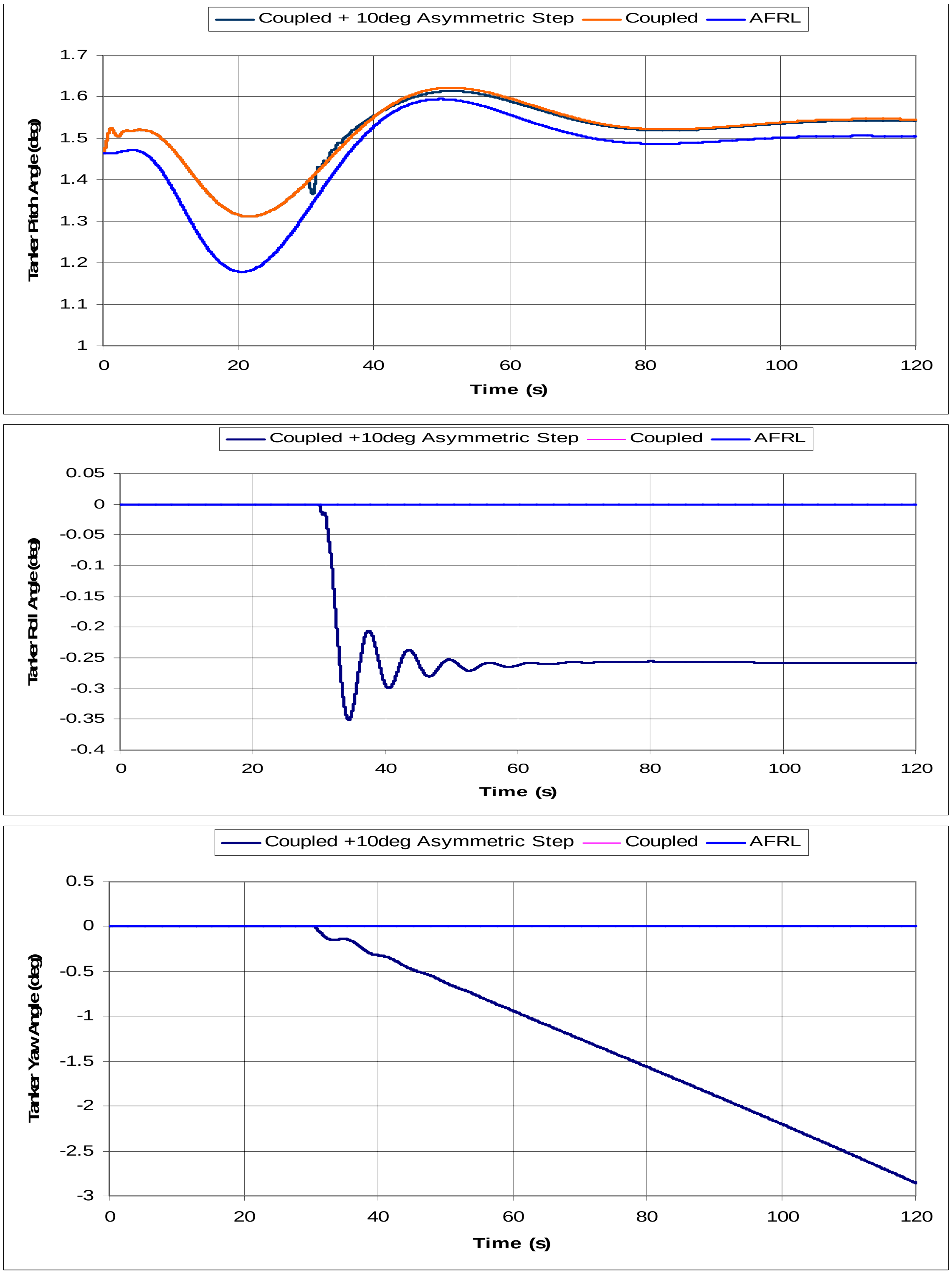

Figure 19. Tanker Pitch, Roll and Yaw Response to a Ten Degree Asymmetric Ruddevator Deflection

These results correspond to what should be expected to happen for the tanker/boom system in this particular configuration. However, the yaw attitude of the tanker does not settle into a new trim condition, but instead the tanker trims into a steady level turn to the left.

These tests have shown that the tanker responds to the boom as would be expected. The changes are not large, but those that occur agree with the physics of the problem.

Comparison to Flight Test Data

The final validation for the newly developed model will attempt to compare results obtained from the simulation to flight test data collected for the Air Force in 1998 (3). The data itself is very limited as a comparative tool. No numeric data was available, only pictures of the time histories for each test are available. Some scales used for the flight tests do not lend to easy interpretation. For example, the pitch rates generated by the simulation ranged from -0.1^{o}/s up to 0.1^{o}/s. The scale of the pitch rate time history ran from -4^{o}/s up to 4^{o}/s. Accordingly, the flight test data hung around zero but could not be interpreted to make a direct comparison to the simulation results useful. For comparisons such as that one, a generalization could be made indicating that the simulation was not generating completely false data, but there was nothing to corroborate its results. Also, tanker attitude comparisons may be of little use.

In the test scenarios examined, the tanker was being flown manually, whereas the simulation completely relies on the model of the autopilot for tanker control inputs. That being said, where the flight test data could be interpreted and an effective comparison made between it and the simulation, it was performed and will be discussed. Otherwise, items such as the attitude rates of the tanker will not.

The entire scenario of the flight test was not recreated in the simulation. The scope of the research was only interested in validating the general behavior of this approach to coupling the tanker and refueling boom. The initial trim condition of the tanker and boom for the flight test was different from the configuration run in the simulation. The altitude (~21000 ft) and speed (~622 fps) of the tanker was slightly lower than that of the nominal case. The tanker's pitch attitude (2.5^o) and weight (240k lbf) was higher, and the initial position of the boom was a little different from nominal as well.

For the simulation runs, the tanker/boom system was left in the nominal case of Table 3. Data from the flight test time histories was manually read and placed into a file so that comparisons could be made on a single graph. When the simulation data had been collected and plotted, the flight test data was shifted up or down so that its initial value would match that of the simulation. From this point, the comparisons of the boom and tanker behavior trends could be examined.

The two flight test cases to be examined were both quite similar. The tanker and refueling boom were both initially flying straight and level in a trim configuration. A series of ruddevator deflections was commanded, and the data acquisition system measured and recorded time histories for numerous aircraft and boom parameters. Each test case lasted about 80 seconds. The first deflection schedule commanded a series of symmetric inputs to examine the boom's pitch behavior. The second was a series of asymmetric deflections to investigate the boom's yaw behavior.

The series of ruddevator commands changed the ruddevator control input method for the simulation. In each of the earlier simulations, the ruddevator position was set before the simulation started. If necessary, a single step change to this initial position was made at a desired point in time. Ruddevator deflections from the flight test data were part of the time histories returned by the data acquisition system. For use in the simulation, the complete time history of ruddevator position was modeled as a series of straight lines with respect to time. Distinct points of interest, basically where the ruddevator position changed slope, were used to generate both a time and position vector of ruddevator position. These vectors were placed into the embedded functions for the left and right ruddevator, and transitions between the distinct points were approximated by a linear interpolation.

The results of the first simulation (symmetric ruddevator deflection) can be seen in Figure 20. The first chart shows the ruddevator deflection schedule that was commanded in this test. This delfection schedule was designed to investigate the pitch response of the boom. The model's boom pitch motion generally followed the flight test data. The model moved to greater extremes when the ruddevators were held in place after a linear deflection. Otherwise, the boom's pitch changed or leveled out every time the ruddevators did the same. Here, the differences are not large, and considering the manual interpretation and shifting of the test data, the general trend of the simulation is consistent with the flight test. This is not the case with the yaw attitude of the boom.

There appears to be very little agreement between the flight test data and the simulation results. The simulation does not actually exhibit any yaw response. This is not unexpected because in no prior simulation did the boom have a significant yaw response to a symmetric ruddevator input.

Recall that the flight test scenario was not completely recreated, and that the purpose of this particular test was to study the pitch response of the boom. Also, the simulations were run under ideal conditions where there are no wind gusts, changes in wind direction, boom interactions with the tanker wake, or many other things that happen in the real world. All prior simulations reveal that a symmetric ruddevator deflection will induce no change in the yaw of the boom, but will cause boom pitch to exhibit a certain type of behavior. Correspondingly, in this test with symmetric ruddevator deflections, the pitch behavior of the flight test boom has been matched by the simulation. In comparison to the flight test data, there is no agreement with the yaw behavior of the boom, and this is where real world effects are seen. The ideal environment generates no change in yaw, whereas the real world does.

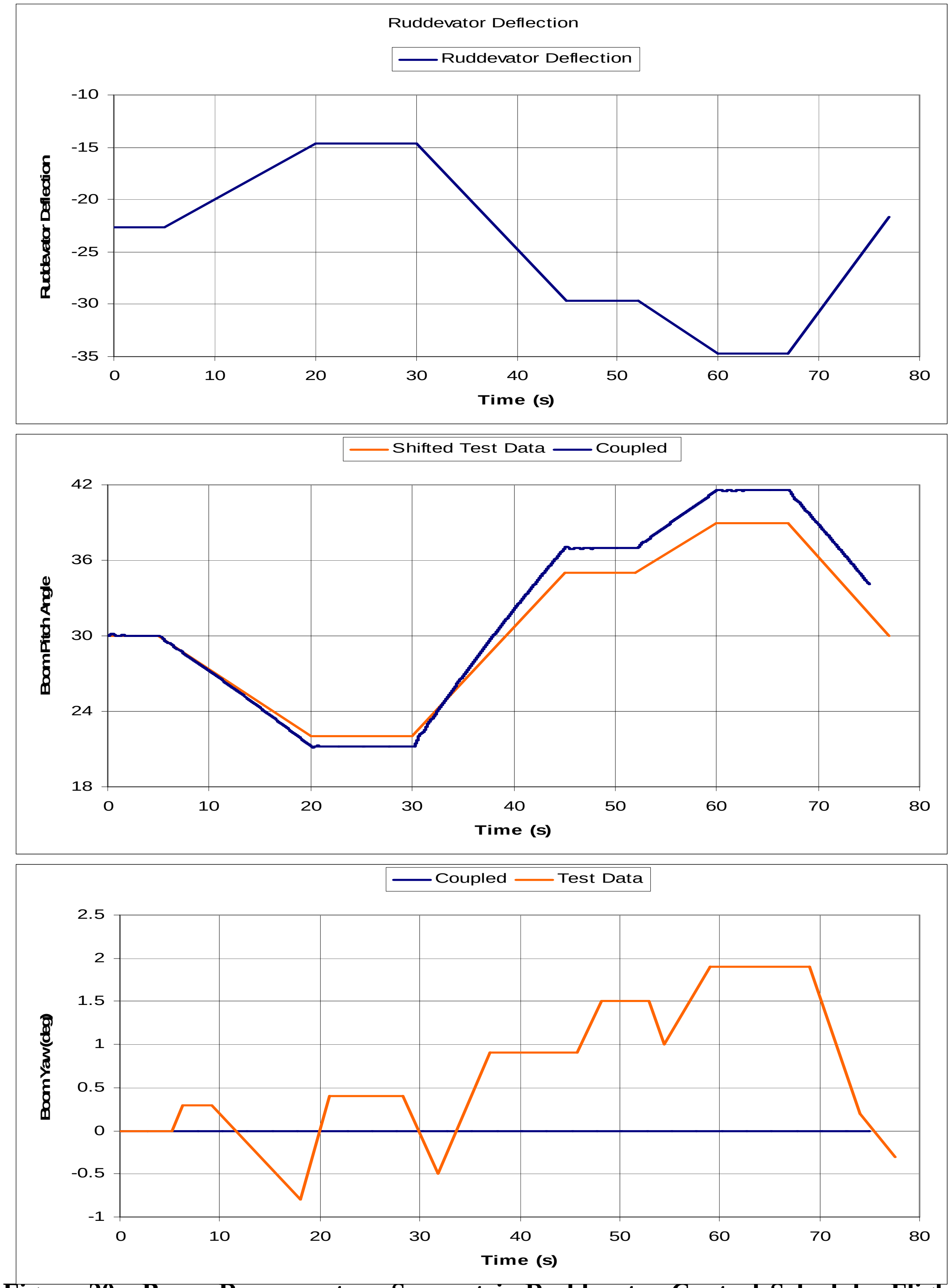

Figure 20. Boom Response to a Symmetric Ruddevator Control Schedule: Flight Test Data –vs- Simulation

Figure 21 shows the results of the second simulation. Again, the first chart shows the ruddevator deflection schedule. This test commanded a series of asymmetric ruddevator deflections intended to investigate boom yaw response to the commanded inputs. Just as in the symmetric test case, the off-axis test, which in this case was boom pitch response, does not correspond very well to the flight test data. On the other hand, the yaw motion of the boom matched almost perfectly. Again, the extremes of the motion were a little larger for the simulation than in the flight test data and can be explained by the manual interpretation and shifting of the test data. Looking closely at the two specific flight tests, it is apparent that each ruddevator control schedule was designed to investigate boom behavior for a specific axis and real world interactions caused the differences in the off-axis behavior.

The overall results of the combined research presented in this chapter corroborate this. In all previous cases where a symmetric ruddevator deflection was commanded, there was no effect on the boom's yaw position. With this information, of the lack of agreement in boom yaw position in Figure 20 and boom pitch position in figure 21 lessens in importance. What is significant is that the simulation performance did exhibit the same behaviors as the boom in the flight test when compared to the defined purpose of the test.

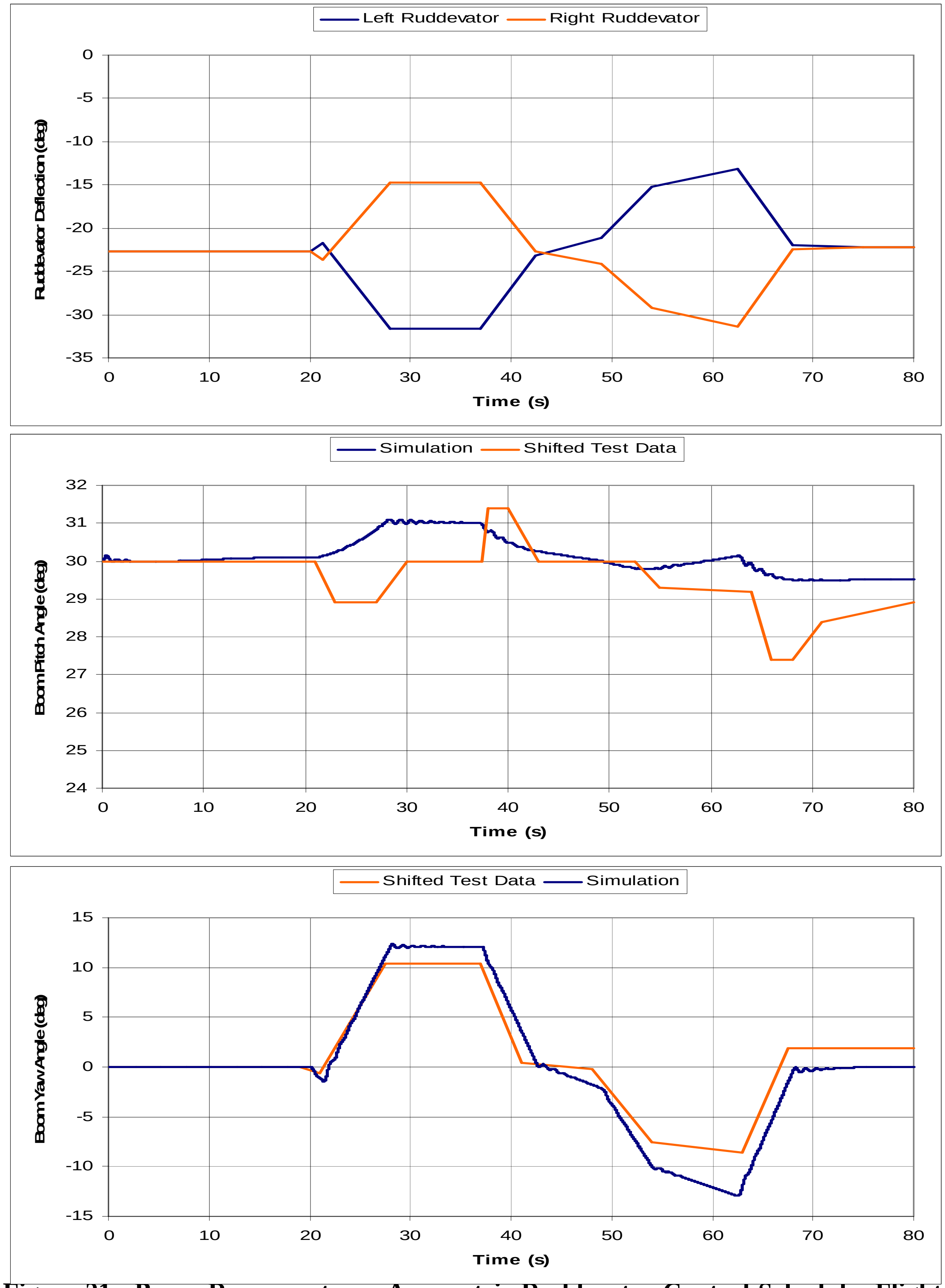

Figure 21. Boom Response to an Aymmetric Ruddevator Control Schedule: Flight Test Data –vs- Simulation

IV. Conclusions and Recommendations

Conclusions

In the KC-135's nearly 50 years of flight, no simulation has been developed to model the dynamic interactions of the tanker aircraft and its aerial refueling boom. This thesis has filled that knowledge gap. Using the EOMs developed by Kunz and Smith in tandem with AFRL's model of the KC-135 tanker, the first model to reasonably simulate the behavior of the tanker and boom as a single, dynamically coupled system has been developed

After all the simulations have been examined, it is safe to say that this model is a viable tool to further extend research in the area of AAR. Results obtained from this model were consistent with those obtained from the established AFRL tanker model and the Kunz/Smith boom model. The slight behavior differences between the simulations can mostly be explained by the numerics used to solve the problem.

In the two simulations that were compared to flight test data, it is important to note that each flight test event was performed to measure either the boom's pitch or yaw performance. Symmetric ruddevator deflections tested the pitch motion of the boom, and the results of the simulation matched the trends of the test data when comparing that mode of motion. Asymmetric ruddevator deflections tested the yaw behavior of the boom, and once again, the simulation matched the trends of the test data when comparing the yaw motion of the boom.

The goals for the focus and scope of this research have been reached. There are certainly improvements that could be made to the model and further testing and refinement could expand the model's viability beyond that of a basic research tool. This study was undertaken to develop and validate a model that coupled the dynamic interactions between the KC-135 tanker aircraft and its refueling boom, and this goal has been accomplished.

Suggestions for further Study

Several things could be done to make this model a more valuable tool for AAR research. The tests run in this thesis centered around a nominal configuration of the tanker and boom system, so the test envelope should be expanded. Refinements could be made to improve the accuracy of the simulation and the computational efficiency of the model could also be improved. Finally a full blown AAR simulation could be developed by the addition of a receiver aircraft to this model.

Before the model can be considered completely viable, it needs to be thoroughly examined in conditions other than the nominal case. Racetrack patterns, different tanker mass and attitude configurations, and different boom attitudes and extension positions should be studied. If possible, some further tests should be compared to raw flight test data. Comparisons between the available flight test data and tanker behavior (attitude and body rates) proved to be virtually non-existent due to limitations of the available data. Also, any real world position, rate, and aerodynamic limits, along with the ruddevator control system, should be added to the boom portion of the model.

Refinements to the model could also improve its accuracy. For example, Kunz/Smith table lookup and interpolation to find the lift and drag coefficients would more accurately represent the true forces generated by the ruddevators. A different numerical integration scheme might also be useful and might be able to add to the efficiency of the model as well.

If the model is intended for use in real time simulations involving pilots and boom operators, this particular model will not be useful. The efficiency of the model could be improved greatly. The best case scenario would be for the entire model to be converted into Simulink blocks. If the embedded Matlab functions are to be kept in place, the inputs to those blocks could be reworked to remove repetitive declarations and calculations therein. Improving the efficiency of the model would be especially important when the next few steps of AAR research are carried out

A model should be developed that incorporates a receiver aircraft connected to the tanker in an aerial refueling situation to investigate the interaction of the three bodies together. Just as the in development of this model, a new set of EOMs must be developed in a manner that will allow for integration with this model or an improvement on it. The joint coordinate and velocity transformation methods could possibly be adapted to include the receiver aircraft so that only one new set of equations would have to be derived. This would allow investigation into the behavior of the three bodies dynamically interacting together as they would during refueling operations when the receiver aircraft is connected to the boom and tanker.

Appendix A

Vehicle Model

Generalized Airframe Model Structure

INPORT 1:
Surf Commands In:
delPF_d
delElevonL_d
delElevonR_d
delClamL_d
delClamR_d

INPORT 2:
PLA In:
PLA_deg

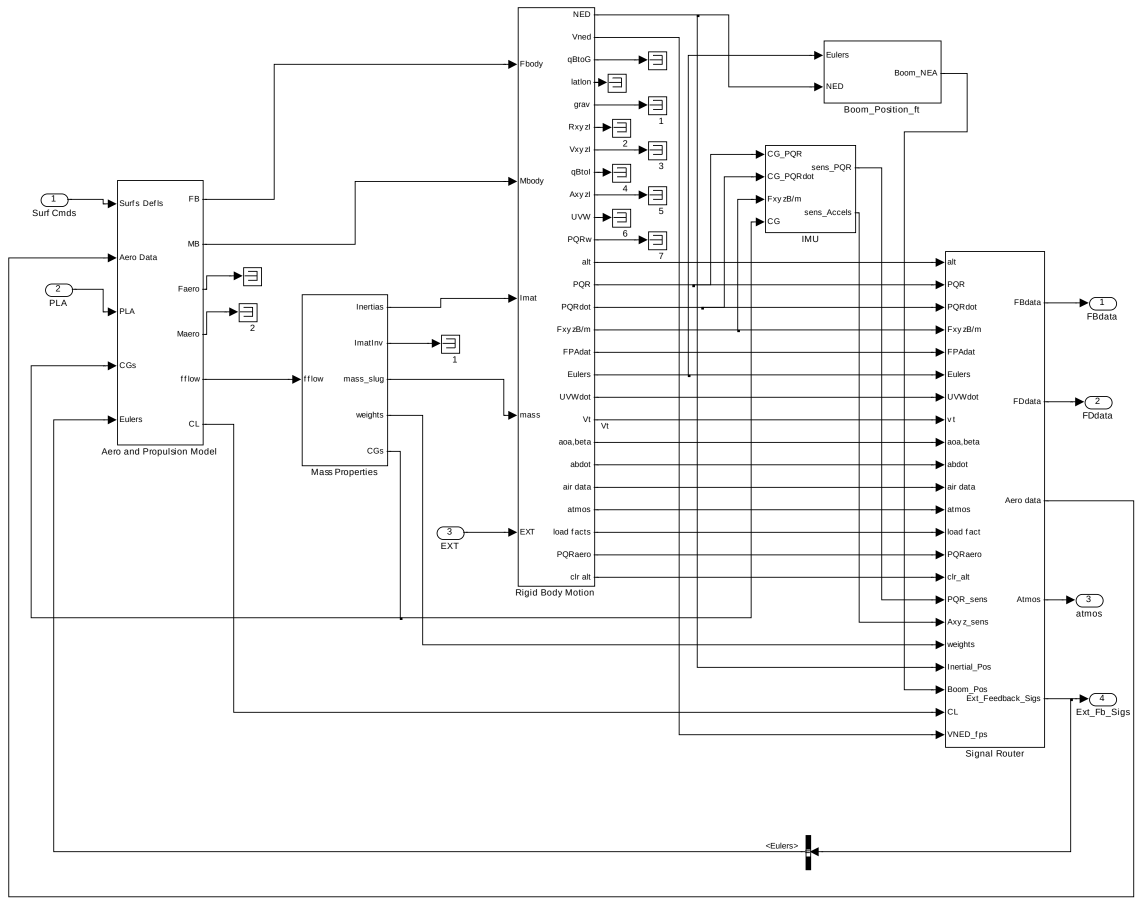

OUTPORT 1:
DATA TO FB FILTERS
Mach
Altitude_ft
Alpha_deg
Beta_deg
Roll_deg
Pitch_deg
Yaw_deg
Psens_dps
Qsens_dps
Rsens_dps
AXsens_fps2
AYsens_fps2
AZsens_fps2
Airspeed_fps
qbar_psf
Ptotal_psf
Pstatic_psf
wt_fuel_lb
wt_stores_lb

OUTPORT 2:
MISC FLT DYN DATA
Pdot_dps2
Qdot_dps2
Rdot_dps2
Udot_fps2
Vdot_fps2
Wdot_fps2
NL_g
Gamma_v_rad
Alpha_dot_rps
P_rps
Q_rps
R_rps
Clr_altitude_ft

OUTPORT 3:
TSPI Data
North_ft
East_ft
Down_ft

OUTPORT 4:
ATMOSPHERE
Tair_degR
rho_slpft3

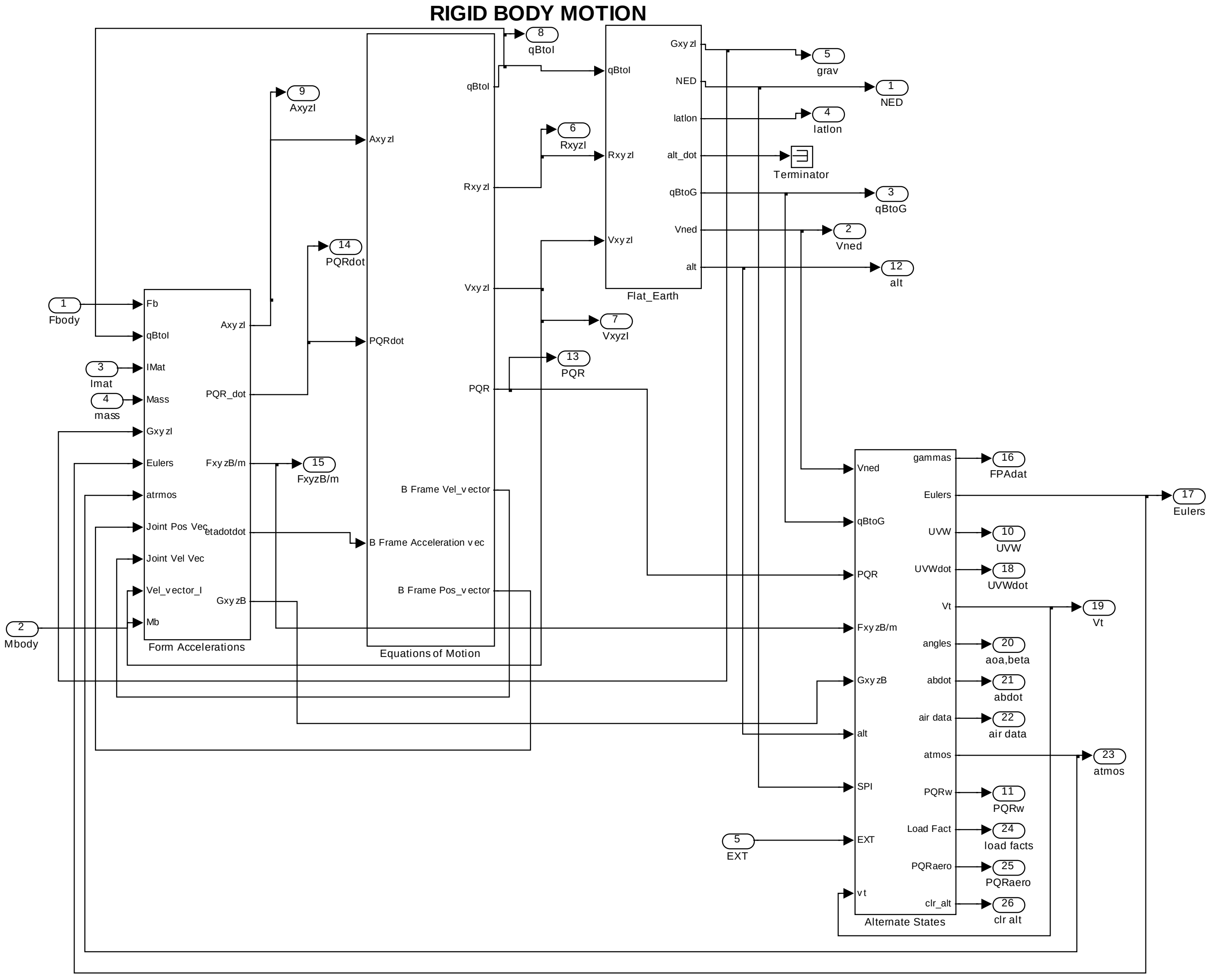
RIGID BODY MOTION
Fbody
qBtoI
Imat
mass
Fb
IMat
Mass
GxyzI
Eulers
atrmos
Joint Pos Vec
Joint Vel Vec
Vel_vector_I
Mb
AxyzI
PQR_dot
FxyzB/m
etadotdot
GxyzB
Form Accelerations
Mbody
AxyzI
PQRdot
FxyzB/m
qBtoI
RxyzI
VxyzI
PQR
B Frame Vel_vector
B Frame Acceleration vec
B Frame Pos_vector
Equations of Motion
qBtoI
RxyzI
VxyzI
PQR
Flat_Earth
NED
latlon
alt_dot
qBtoG
Vned
alt
Terminator
grav
NED
latlon
qBtoG
Vned
alt
Vned
qBtoG
PQR
FxyzB/m
GxyzB
alt
SPI
EXT
vt
Alternate States
gammas
Eulers
UVW
UVWdot
Vt
angles
abdot
air data
atmos
PQRw
Load Fact
PQRaero
clr_alt
FPAdat
Eulers
UVW
UVWdot
Vt
aoa,beta
abdot
air data
atmos
PQRw
load facts
PQRaero
clr alt
EXT

FORM ACCELERATIONS

Calculate body axis acceleration components

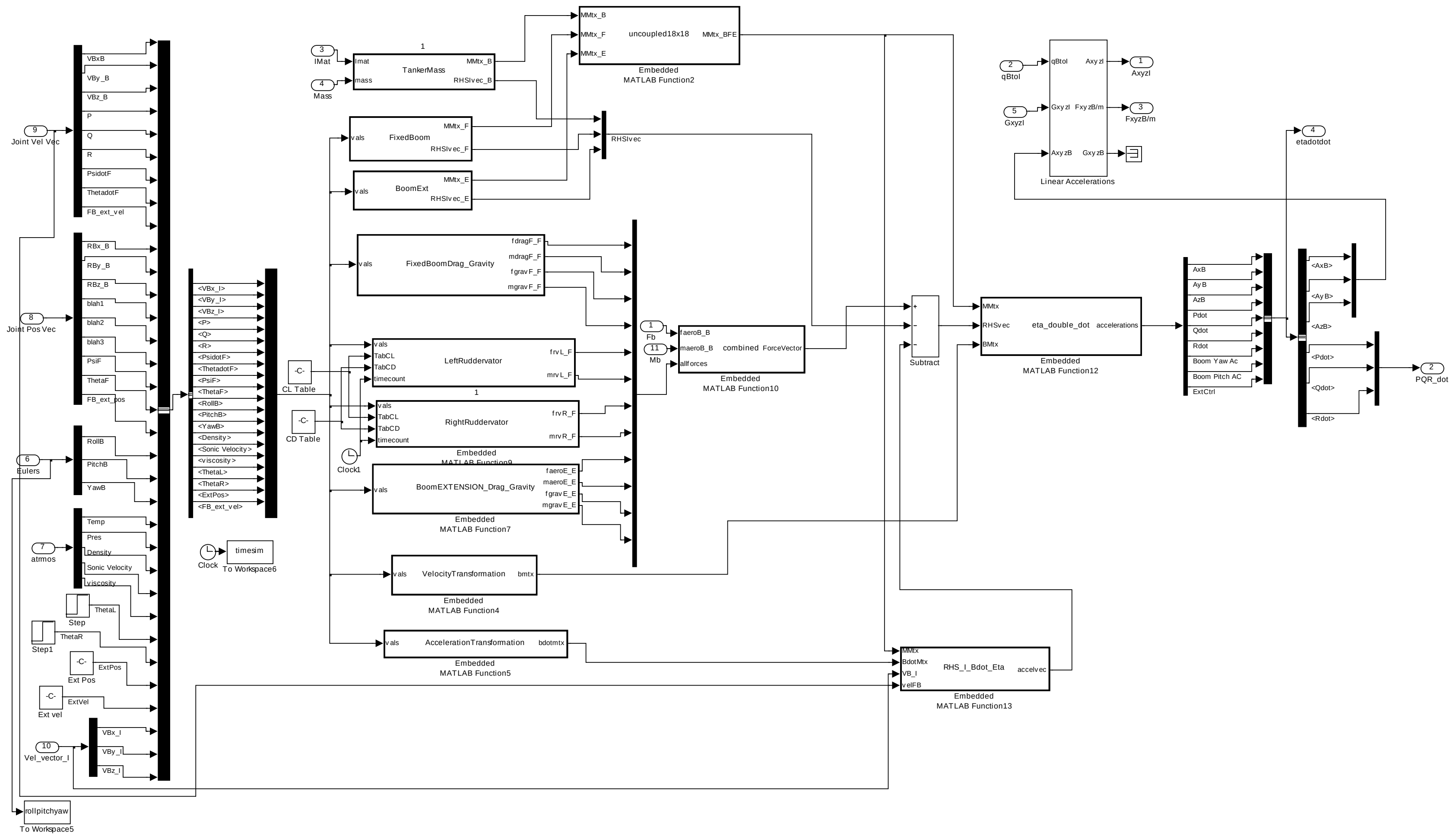

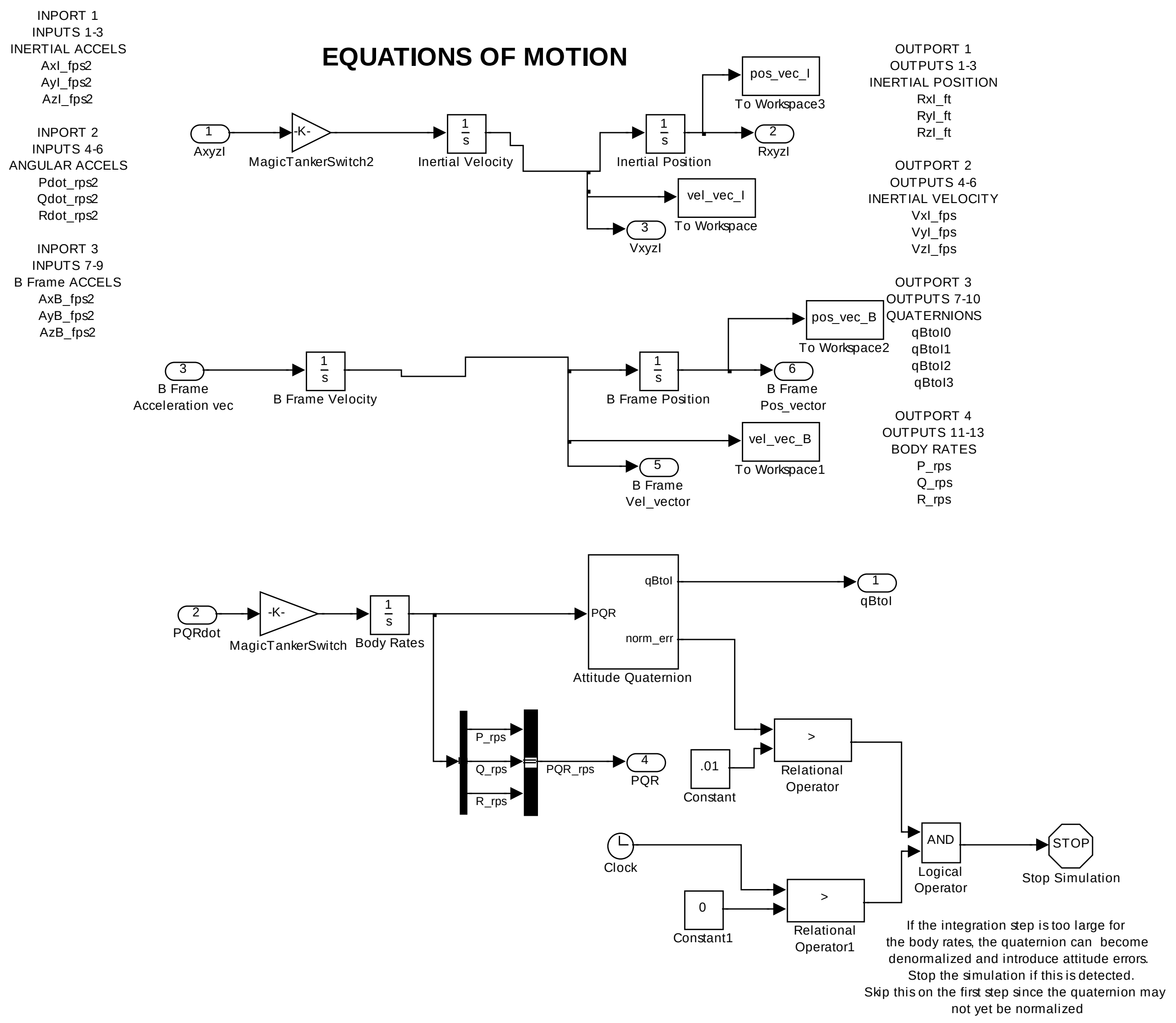

INPORT 1
INPUTS 1-3
INERTIAL ACCELS
AxI_fps2
AyI_fps2
AzI_fps2

INPORT 2
INPUTS 4-6
ANGULAR ACCELS
Pdot_rps2
Qdot_rps2
Rdot_rps2

INPORT 3
INPUTS 7-9
B Frame ACCELS
AxB_fps2
AyB_fps2
AzB_fps2

OUTPORT 1
OUTPUTS 1-3
INERTIAL POSITION
RxI_ft
RyI_ft
RzI_ft

OUTPORT 2
OUTPUTS 4-6
INERTIAL VELOCITY
VxI_fps
VyI_fps
VzI_fps

OUTPORT 3
OUTPUTS 7-10
QUATERNIONS
qBtoI0
qBtoI1
qBtoI2
qBtoI3

OUTPORT 4
OUTPUTS 11-13
BODY RATES
P_rps
Q_rps
R_rps

If the integration step is too large for
the body rates, the quaternion can become
denormalized and introduce attitude errors.
Stop the simulation if this is detected.
Skip this on the first step since the quaternion may
not yet be normalized

T35

BOOM OPERATOR CONTROL CHARACTERISTICS
ELEVATION
TNKR (070042) MID

KSR R98-271 KC-135R VOL II

EVENT NUMBER:	8.B.1.b.t	PROJECT NAME:	KC-135 AR Data Collection
ICP WINDOW:	0.00 -> 1.50 SEC	AIRCRAFT NAME:	Boeing KC-135R
TEST:	070	SERIAL NUMBER:	61-0320
RUN:	042		

Configuration and Trim

CALIBRATED ALT (FT)	= 20881.	KCAS (KT)	= 272.0	TRUE ALPHA (DEG)	= 2.9
AMBIENT AIR TEMP (C)	= -10.7	MACH NUMBER	= 0.603	TRUE BETA (DEG)	= -0.5
GEAR POSITION	= UP	YAW DAMPER	= ON	RUDDER BOOST	= ON
FLAP DEF (DEG)	= 0.0	EFAS	= OFF		
AX CORRECTED (G)	= 0.049	PITCH RATE (DEG/SEC)	= 0.0	PITCH ATTITUDE (DEG)	= 2.9
AY CORRECTED (G)	= 0.011	ROLL RATE (DEG/SEC)	= 0.0	ROLL ATTITUDE (DEG)	= -0.9
AZ CORRECTED (G)	= -0.997	YAW RATE (DEG/SEC)	= 0.0	HEADING (DEG)	= 291.1
STABILIZER DEF (DEG)	= -2.6			ELEVATOR TAB (DEG)	= 1.2
LT AILERON TAB (DEG)	= -0.7	RT AILERON TAB (DEG)	= -0.9	RUDDER TAB (DEG)	= 0.7
LT OTBD AIL (DEG)	= 0.0	LT OTBD SPLR (DEG)	= 0.4	ELEVATOR (DEG)	= -0.4
LT INBD AIL (DEG)	= -0.6	LT INBD SPLR (DEG)	= 0.1	RUDDER DEF (DEG)	= -0.4
RT INBD AIL (DEG)	= 0.6	RT INBD SPLR (DEG)	= 0.4	AUTOPILOT	= OFF
RT OTBD AIL (DEG)	= 0.0	RT OTBD SPLR (DEG)	= 0.4		

Weight And Balance

AIRCRAFT WEIGHT (LB)	= 245683.	CG LONG (%MAC)	= 30.73	IXX (SLUG-SQ FT)	= 3797251.
		CG LONG (FT)	= -71.71	IYY (SLUG-SQ FT)	= 3576204.
FUEL WEIGHT (LB)	= 122894.	CG LATERAL (FT)	= 0.16	IZZ (SLUG-SQ FT)	= 7210255.
FUEL TEMP (DEG C)	= 14.4	CG VERTICAL (FT)	= -16.25	IXZ (SLUG-SQ FT)	= 234547.

Engine Parameters

Engine 1		Engine 2		Engine 3		Engine 4	
N1 (%)	= 75.6	N1 (%)	= 74.8	N1 (%)	= 75.2	N1 (%)	= 74.9
EGT (DEG C)	= 593.	EGT (DEG C)	= 610.	EGT (DEG C)	= 588.	EGT (DEG C)	= 593.
N2 (%)	= 90.7	N2 (%)	= 90.2	N2 (%)	= 90.7	N2 (%)	= 90.4
FF (LB/HR)	= 2536.	FF (LB/HR)	= 2549.	FF (LB/HR)	= 2471.	FF (LB/HR)	= 2516.
THRUST POS (IN)	= 2.8	THRUST POS (IN)	= 2.9	THRUST POS (IN)	= 2.9	THRUST POS (IN)	= 2.8

Boom Parameters

AR CONNECT	= NO	AR DISCONNECT	= NO	AR READY	= YES
BOOM TELESCOPE (FT)	= 15.8	BOOM AZIMUTH (DEG)	= 1.7	BOOM ELEVATION (DEG)	= 27.2

DRAWN 22:53:01 03sep98
POST 13apr98
CONV 13apr98

KOHLMAN SYSTEMS RESEARCH

CHG 1
T8.B.1.019

PREPARED BY KSR

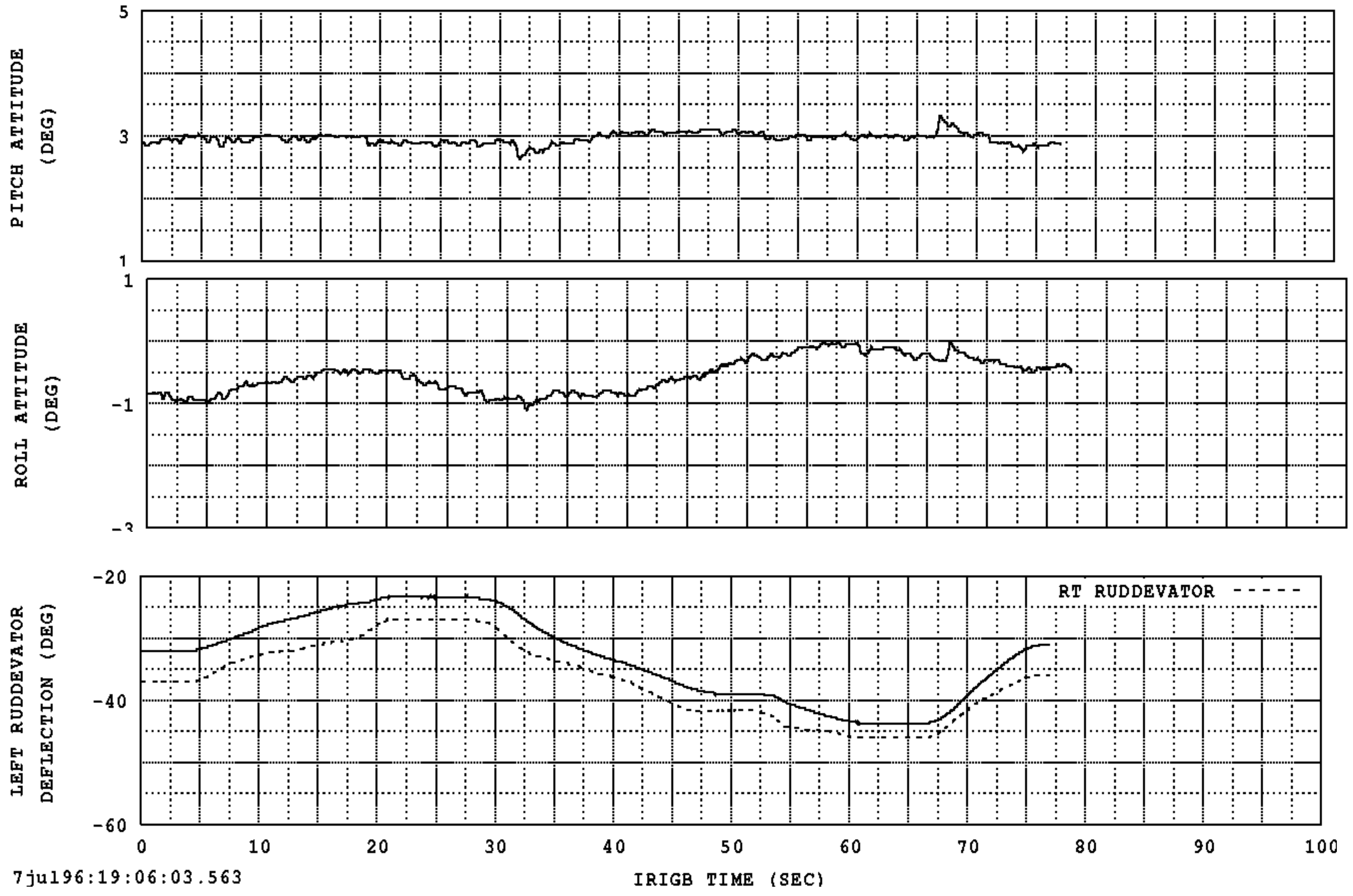
PITCH ATTITUDE (DEG)
5
3
1
ROLL ATTITUDE (DEG)
1
-1
-3
LEFT RUDDEVATOR DEFLECTION (DEG)
-20
-40
-60
RT RUDDEVATOR - - - - -
0
10
20
30
40
50
60
70
80
90
100
IRIGB TIME (SEC)
7jul96:19:06:03.563

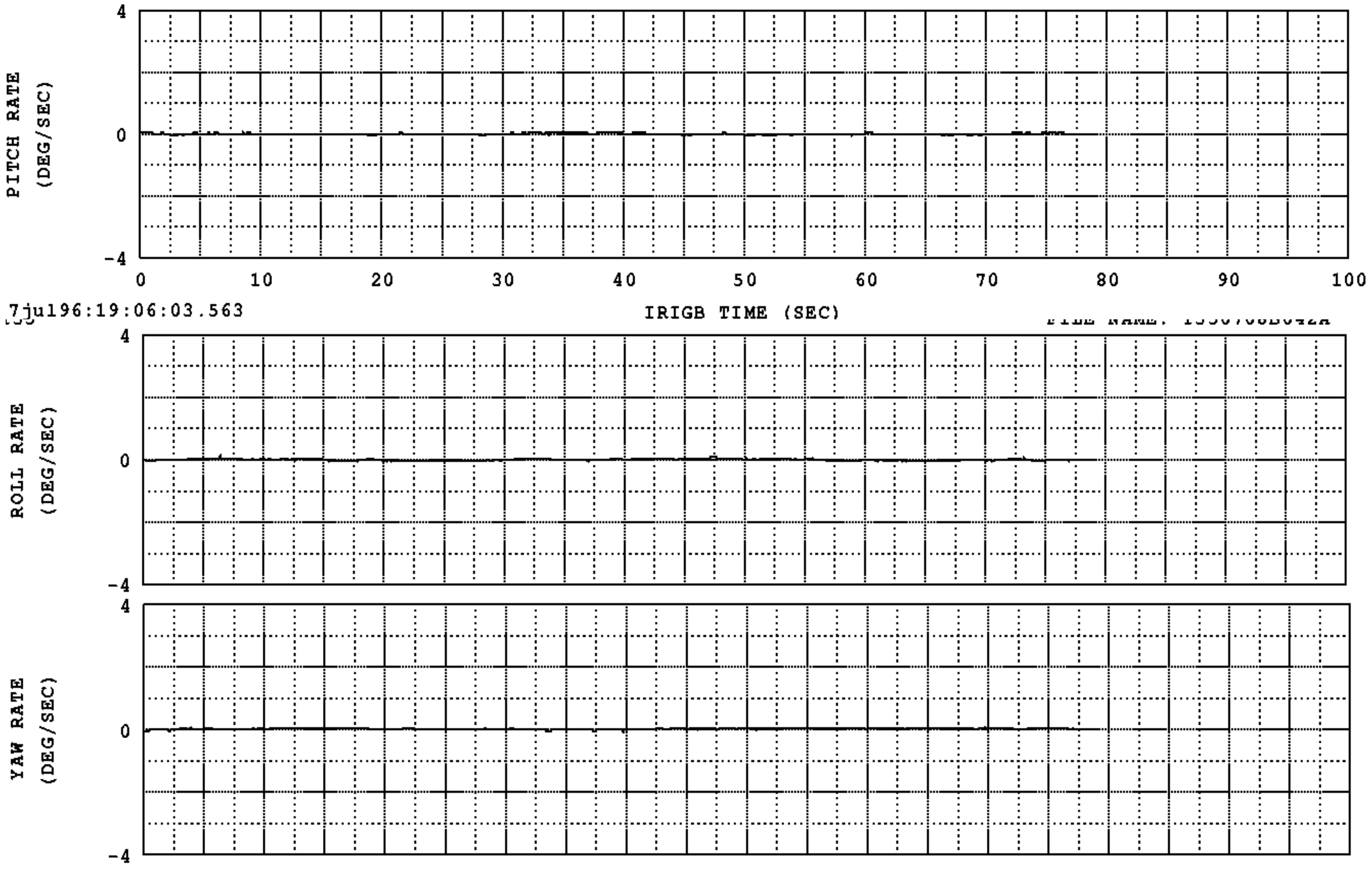

PITCH RATE (DEG/SEC)
4
0
-4
0
10
20
30
40
50
60
70
80
90
100
7jul96:19:06:03.563
IRIGB TIME (SEC)
ROLL RATE (DEG/SEC)
4
0
-4
YAW RATE (DEG/SEC)
4
0
-4

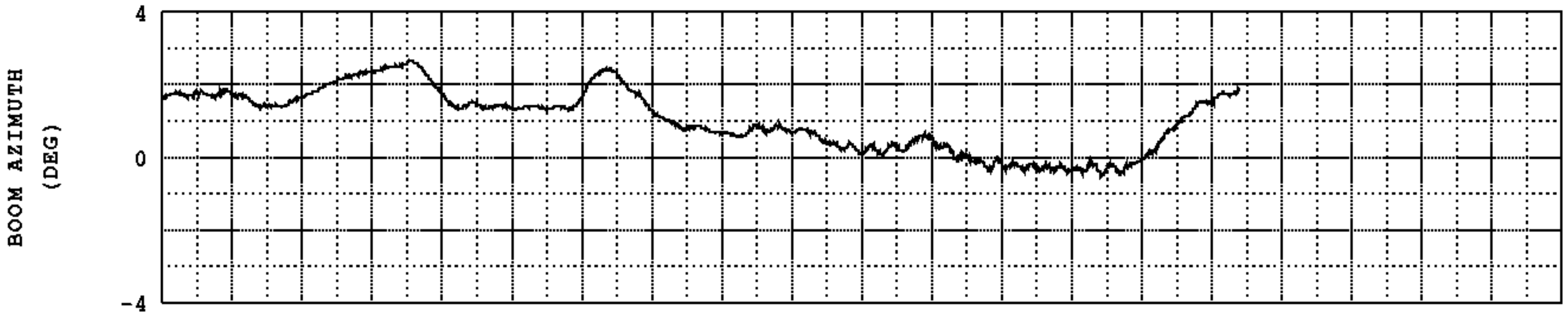
BOOM AZIMUTH
(DEG)
4
0
-4

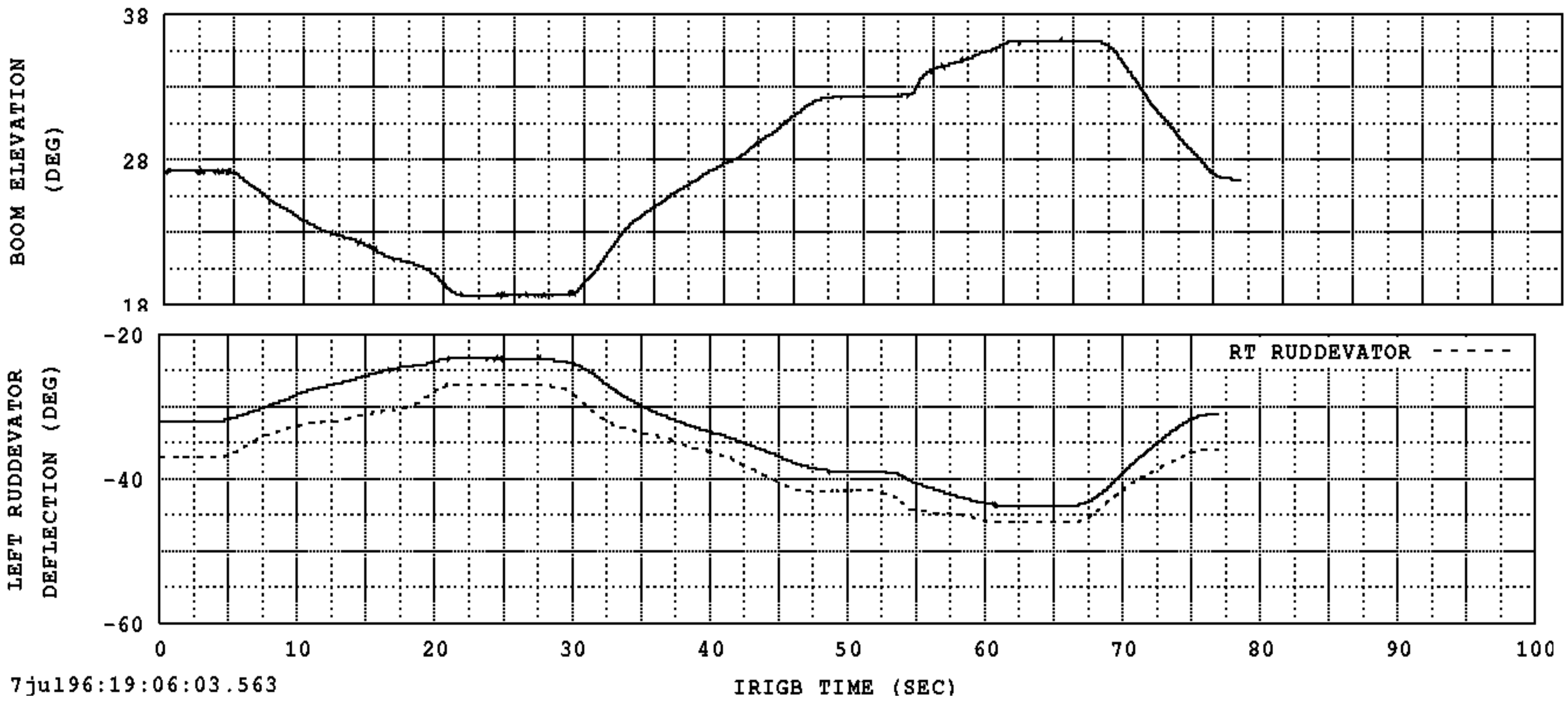

38
28
18
BOOM ELEVATION (DEG)
-20
-40
-60
LEFT RUDDEVATOR DEFLECTION (DEG)
RT RUDDEVATOR - - - - -
0
10
20
30
40
50
60
70
80
90
100
7jul96:19:06:03.563
IRIGB TIME (SEC)

T35

BOOM OPERATOR CONTROL CHARACTERISTICS
AZIMUTH
TNKR (070038) MID

KSR R98-271 KC-135R VOL II

EVENT NUMBER:	8.A.1.b.t	PROJECT NAME:	KC-135 AR Data Collection
ICP WINDOW:	0.00 -> 1.50 SEC	AIRCRAFT NAME:	Boeing KC-135R
TEST:	070	SERIAL NUMBER:	61-0320
RUN:	038		

Configuration and Trim

CALIBRATED ALT (FT)	= 20900.	KCAS (KT)	= 269.3	TRUE ALPHA (DEG)	= 2.9
AMBIENT AIR TEMP (C)	= -10.4	MACH NUMBER	= 0.598	TRUE BETA (DEG)	= -0.4
GEAR POSITION	= UP	YAW DAMPER	= ON	RUDDER BOOST	= ON
FLAP DEF (DEG)	= 0.0	EFAS	= OFF		
AX CORRECTED (G)	= 0.056	PITCH RATE (DEG/SEC)	= 0.0	PITCH ATTITUDE (DEG)	= 2.9
AY CORRECTED (G)	= 0.009	ROLL RATE (DEG/SEC)	= 0.1	ROLL ATTITUDE (DEG)	= -0.3
AZ CORRECTED (G)	= -0.986	YAW RATE (DEG/SEC)	= 0.0	HEADING (DEG)	= 290.5
STABILIZER DEF (DEG)	= -2.6			ELEVATOR TAB (DEG)	= 1.1
LT AILERON TAB (DEG)	= -0.9	RT AILERON TAB (DEG)	= -1.1	RUDDER TAB (DEG)	= 0.7
LT OTBD AIL (DEG)	= 0.0	LT OTBD SPLR (DEG)	= 0.4	ELEVATOR (DEG)	= -0.2
LT INBD AIL (DEG)	= -0.2	LT INBD SPLR (DEG)	= 0.2	RUDDER DEF (DEG)	= -0.4
RT INBD AIL (DEG)	= 1.0	RT INBD SPLR (DEG)	= 0.4	AUTOPILOT	= OFF
RT OTBD AIL (DEG)	= 0.0	RT OTBD SPLR (DEG)	= 0.3		

Weight And Balance

AIRCRAFT WEIGHT (LB)	= 246288.	CG LONG (%MAC)	= 30.98	IXX (SLUG-SQ FT)	= 3797438.
		CG LONG (FT)	= -71.76	IYY (SLUG-SQ FT)	= 3584778.
FUEL WEIGHT (LB)	= 123499.	CG LATERAL (FT)	= 0.16	IZZ (SLUG-SQ FT)	= 7218431.
FUEL TEMP (DEG C)	= 14.5	CG VERTICAL (FT)	= -16.25	IXZ (SLUG-SQ FT)	= 234073.

Engine Parameters

Engine 1		Engine 2		Engine 3		Engine 4	
N1 (%)	= 77.5	N1 (%)	= 76.3	N1 (%)	= 77.3	N1 (%)	= 76.9
EGT (DEG C)	= 612.	EGT (DEG C)	= 626.	EGT (DEG C)	= 605.	EGT (DEG C)	= 616.
N2 (%)	= 91.4	N2 (%)	= 90.6	N2 (%)	= 91.3	N2 (%)	= 91.1
FF (LB/HR)	= 2736.	FF (LB/HR)	= 2730.	FF (LB/HR)	= 2708.	FF (LB/HR)	= 2679.
THRUST POS (IN)	= 3.1	THRUST POS (IN)	= 3.2	THRUST POS (IN)	= 3.1	THRUST POS (IN)	= 3.1

Boom Parameters

AR CONNECT	= NO	AR DISCONNECT	= NO	AR READY	= YES
BOOM TELESCOPE (FT)	= 11.0	BOOM AZIMUTH (DEG)	= 0.4	BOOM ELEVATION (DEG)	= 28.6

DRAWN 22:51:23 03sep98
POST 20aug98 CONV 20aug98
KOHLMAN SYSTEMS RESEARCH
CHG 1 T8.A.1.019
PREPARED BY KSR

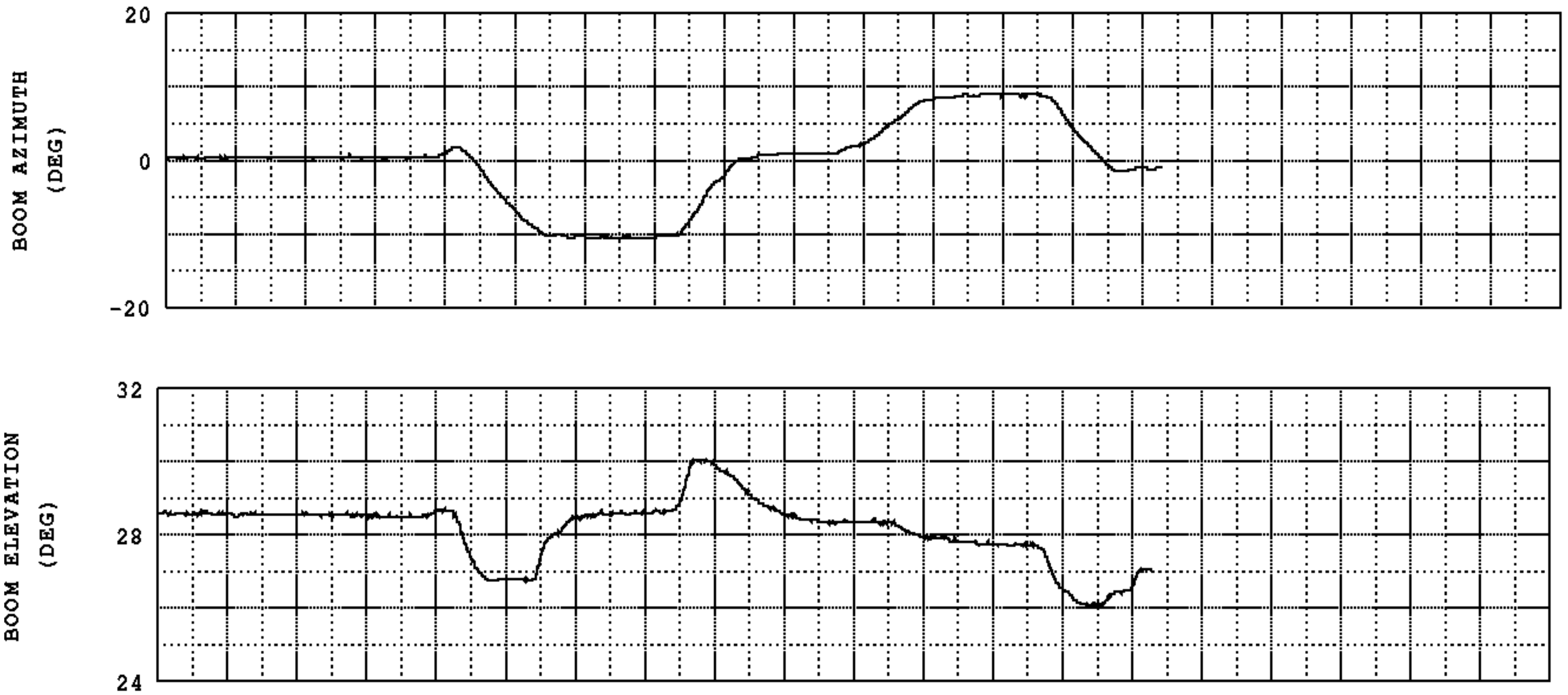
BOOM AZIMUTH (DEG)
20
0
-20
BOOM ELEVATION (DEG)
32
28
24

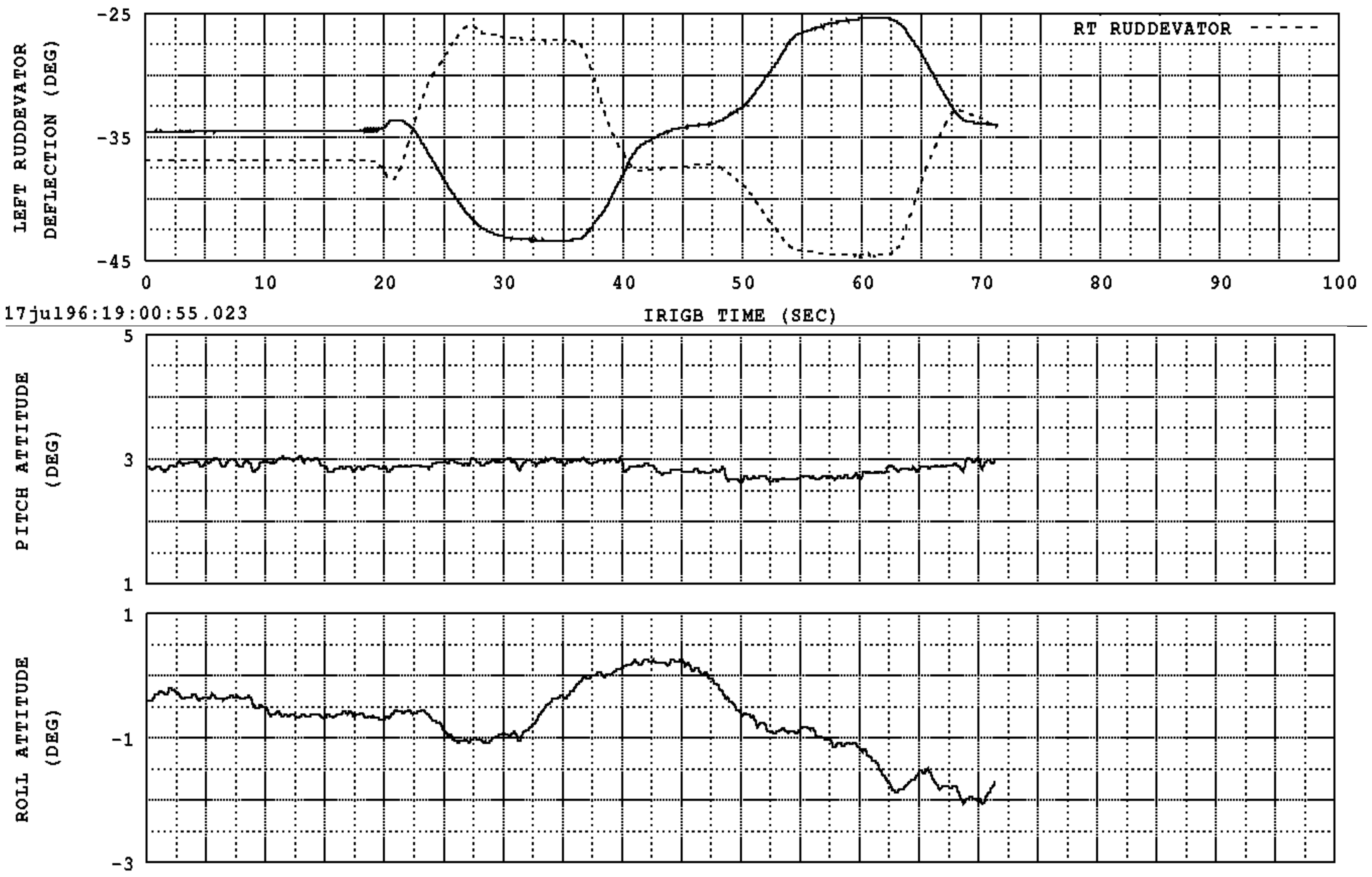
-25
-35
-45
LEFT RUDDEVATOR DEFLECTION (DEG)
RT RUDDEVATOR - - - - -
0
10
20
30
40
50
60
70
80
90
100
17jul96:19:00:55.023
IRIGB TIME (SEC)
5
3
1
PITCH ATTITUDE (DEG)
1
-1
-3
ROLL ATTITUDE (DEG)

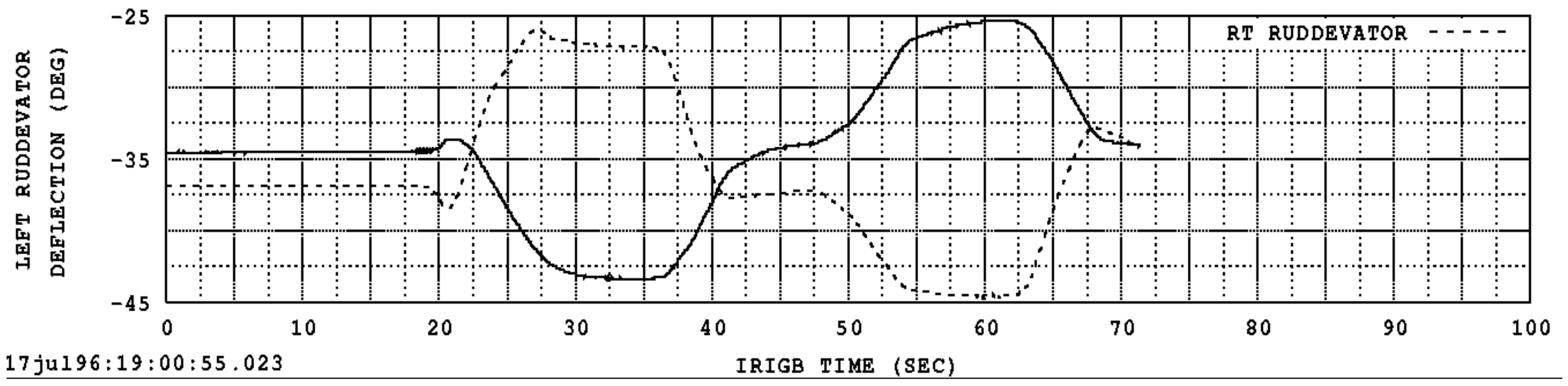

LEFT RUDDEVATOR DEFLECTION (DEG)
RT RUDDEVATOR - - - - -
-25
-35
-45
0
10
20
30
40
50
60
70
80
90
100
17jul96:19:00:55.023
IRIGB TIME (SEC)

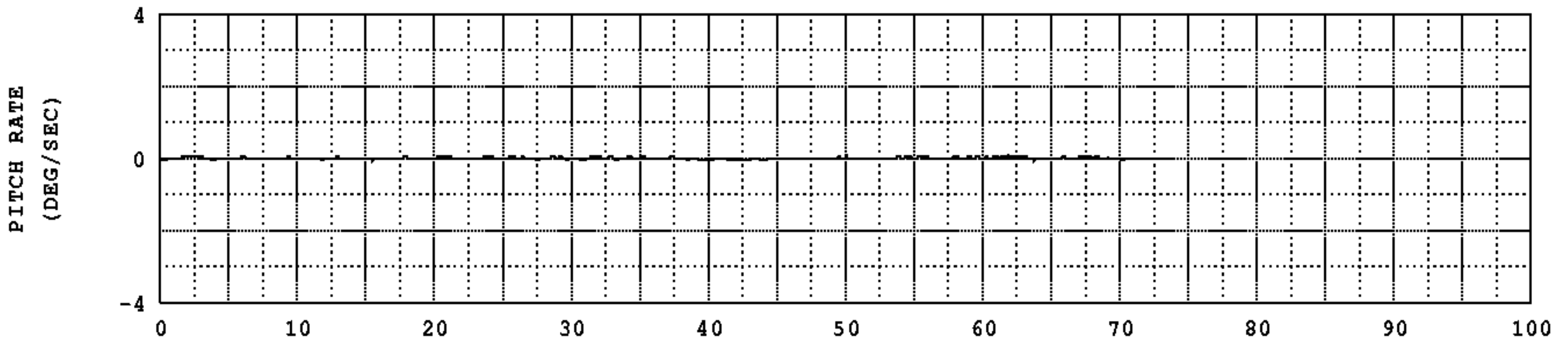

PITCH RATE (DEG/SEC)
4
0
-4
0
10
20
30
40
50
60
70
80
90
100

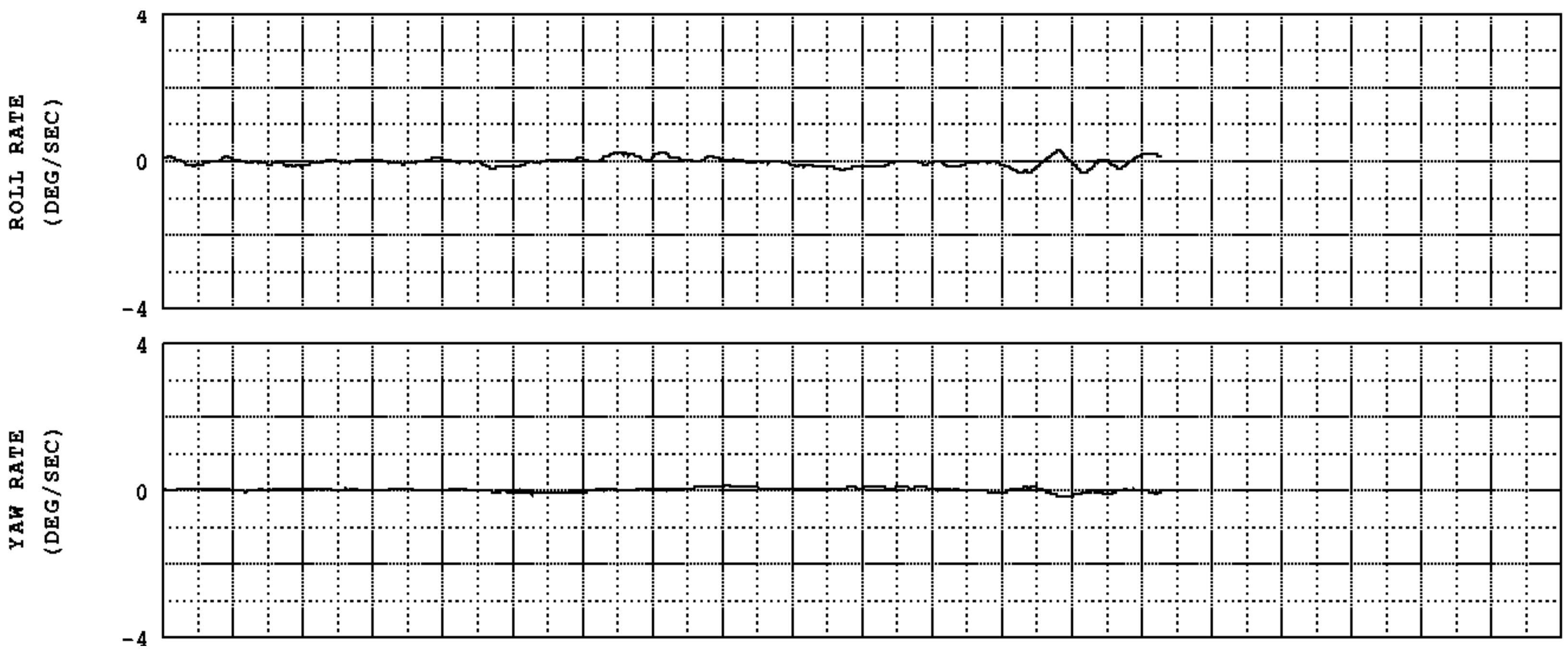
4
ROLL RATE (DEG/SEC)
0
-4
4
YAW RATE (DEG/SEC)
0
-4

Appendix C

```
          function [MMtx_B, RHSIvec_B] = TankerMass(Imat, mass)

Zmx = zeros(3,3);
MMtx = mass*eye(3);
IMtx = [Imat(1), Imat(4), Imat(5);...
        Imat(4), Imat(2), Imat(6);...
        Imat(5), Imat(6), Imat(3)];
MMtx_B = [[MMtx], [Zmx]; [Zmx], [IMtx]];

% Extract values from the state vector
omegaBI_B = zeros(3,1);
omegaBI_B(1,1) = vals(4);
omegaBI_B(2,1) = vals(5);
omegaBI_B(3,1) = vals(6);


% Right-hand side inertia vector
Mvec = zeros( 3, 1 );
tildeB = [     0, -omegaBI_B(3),  omegaBI_B(2); ...
            omegaBI_B(3),     0, -omegaBI_B(1); ...
           -omegaBI_B(2),  omegaBI_B(1),     0];
Ivec = tildeB*IMtx*omegaBI_B;
RHSIvec_B = [ [Mvec]; ...
            [Ivec]; ];
```

```
function [MMtx_F, RHSIvec_F] = FixedBoom(vals)


ENVg_I = [0; 0; 32.174];  % Gravitational acceleration vector (ft/sec^2)

% Fixed boom parameters
FBOOML = 332/12;  % fixed boom length (ft)
FBOOMM = 756.5/norm( ENVg_I );  % slugs
FBOOMrCG = [-228.88; 0; 0]/12;  % fixed boom center of mass (ft)
FBOOMIXX = 0.0;  % slug-ft^2
FBOOMIYY = 3.294e5/norm( ENVg_I );  % slug-ft^2
FBOOMIZZ = 3.294e5/norm( ENVg_I );  % slug-ft^2
FBOOMIXY = 0.0;  % slug-ft^2
FBOOMIXZ = 0.0;  % slug-ft^2
FBOOMIYZ = 0.0;  % slug-ft^2
FBOOMrFB_B = [583.325; 0; -12.5]/12;  % fixed boom pivot location (ft)
FBOOMnYaw_B = [0; 0; 1];  % Boom yaw axis (in the B basis)
FBOOMnPitch_F = [0; 1; 0];  % Boom pitch axis (in the F basis)
FBOOMDiam_in = [ 0.0, 240.0, 240.1, 332.0; ...
                 11.0,  11.0,  21.6,  21.6];
FBOOMrRF_F = [-294; 0; 0]/12;  % ruddevator pivot location (ft)
FBOOMRVc = 31/12;  % ruddevator chord (ft)
FBOOMRVL = 61/12;  % ruddevator length (ft)
FBOOMRVdihedral = 42*pi/180;  % ruddevator dihedral angle (rad)

Mmtx = FBOOMM*eye( 3 );
Rmtx = [0 0 0;0 0 0;0 0 0];
tildef = [     0, -FBOOMrCG(3),  FBOOMrCG(2); ...
            FBOOMrCG(3),     0, -FBOOMrCG(1); ...
           -FBOOMrCG(2),  FBOOMrCG(1),     0];
Rmtx = FBOOMM*tildef;
Imtx = [ FBOOMIXX, FBOOMIXY, FBOOMIXZ;
         FBOOMIXY, FBOOMIYY, FBOOMIYZ;
         FBOOMIXZ, FBOOMIYZ, FBOOMIZZ ];
MMtx_F = [ [Mmtx], [-Rmtx]; ...
         [Rmtx], [Imtx] ];
%MMtx_F = zeros(6,6);
% Extract values from the state vector
omegaBI_B = zeros(3,1);
omegaBI_B(1,1) = vals(4);
omegaBI_B(2,1) = vals(5);
omegaBI_B(3,1) = vals(6);



YawFdot = vals(7);
PitchFdot = vals(8);
yawF = vals(9);
pitchF = vals(10);
roll = 0;

% Define the direction cosine matrices

dca = zeros( 3, 3 );
dca(1,1) = cos( yawF )*cos( pitchF );
dca(1,2) = sin( yawF )*cos( pitchF );
dca(1,3) = -sin( pitchF );
dca(2,1) = cos( yawF )*sin( pitchF )*sin( roll ) - sin( yawF )*cos( roll
);
dca(2,2) = sin( yawF )*sin( pitchF )*sin( roll ) + cos( yawF )*cos( roll
);
dca(2,3) = cos( pitchF )*sin( roll );
dca(3,1) = cos( yawF )*sin( pitchF )*cos( roll ) + sin( yawF )*sin( roll
);
dca(3,2) = sin( yawF )*sin( pitchF )*cos( roll ) - cos( yawF )*sin( roll
);
dca(3,3) = cos( pitchF )*cos( roll );

C_FB = dca;  %  Direction Cosine mx

% Calculate the angular velocity
omegaFB_F = C_FB*FBOOMnYaw_B*YawFdot + FBOOMnPitch_F*PitchFdot;
omegaFI_F = omegaFB_F + C_FB*omegaBI_B;

tildewFI_F = [     0,         -omegaFI_F(3),  omegaFI_F(2); ...
                omegaFI_F(3),     0,          -omegaFI_F(1); ...
               -omegaFI_F(2),  omegaFI_F(1),     0];


% Right-hand side inertia vector
Mvec = FBOOMM*tildewFI_F*tildewFI_F*FBOOMrCG;
Ivec = tildewFI_F*Imtx*omegaFI_F;
RHSIvec_F = [ [Mvec]; ...
              [Ivec]; ];
%RHSIvec_F = zeros(6,1);
```

```
function [MMtx_E, RHSIvec_E] = BoomExt(vals)
%
% Construct the mass/inertia matrix and the right-hand side inertia
vector for the boom extension
%----------------------------------------

% Extract values from state vector
uE = vals(19); % Extension is controlled

% Boom extension parameters
EBOOML = 330/12;  % boom extension length (ft)
EBOOMM = 460.35/32.2;  % slugs
EBOOMrCG = [-178.84; 0; 0]/12;  % boom extension center of mass (ft)
EBOOMIXX = 0.0;  % slug-ft^2
EBOOMIYY = 1.414e5/32.2;  % slug-ft^2
EBOOMIZZ = 1.414e5/32.2;  % [slug-ft^2
EBOOMIXY = 0.0;  % slug-ft^2
EBOOMIXZ = 0.0;  % slug-ft^2
EBOOMIYZ = 0.0;  % slug-ft^2
EBOOMnExt_E = [1; 0; 0];  % Boom extension axis (in the E basis)
EBOOMrEF_F = [-2; 0; 0]/12;  % Stowed extension position (in the F
basis)
EBOOMD = 3.1*2/12;  % boom extension diameter (ft)

FBOOMrFB_B = [583.325; 0; -12.5]/12;  % fixed boom pivot location (ft)
FBOOMnYaw_B = [0; 0; 1];  % Boom yaw axis (in the B basis)
FBOOMnPitch_F = [0; 1; 0];  % Boom pitch axis (in the F basis)


% Contributions from fuel during extension
fuel = 0.14546;  % fuel distributed mass (slug/ft)
fmass = fuel*uE;

% Combined boom extension mass
mass = EBOOMM + fmass;

% Combined boom extension center of mass
rCG = (EBOOMM*EBOOMrCG + fmass*[uE/2; 0; 0])/mass;

% Combined boom extension moments of inertia
IYY = EBOOMIYY + (fmass*(uE/2)^2)/3;
IZZ = EBOOMIZZ + (fmass*(uE/2)^2)/3;

% Construct the mass/inertia matrix in the stowed position
Mmtx = mass*eye( 3 );
Rmtx = [0 0 0;0 0 0;0 0 0];
tildee = [     0,   -rCG(3),  rCG(2); ...
           rCG(3),     0,   -rCG(1); ...
          -rCG(2),  rCG(1),     0];
Rmtx = EBOOMM*tildee;

Imtx = [ EBOOMIXX, EBOOMIXY, EBOOMIXZ;
         EBOOMIXY,       IYY, EBOOMIYZ;
         EBOOMIXZ, EBOOMIYZ,       IZZ ];
MMtx_E = [ [Mmtx], [-Rmtx]; ...
           [Rmtx], [Imtx] ];
```

```
%MMtx_E = zeros(6,6);

% Extract values from the state vector
omegaBI_B = zeros(3,1);
omegaBI_B(1,1) = vals(4);
omegaBI_B(2,1) = vals(5);
omegaBI_B(3,1) = vals(6);

YawFdot = vals(7);
PitchFdot = vals(8);
yawF = vals(9);
pitchF = vals(10);
roll = 0;

% Define the direction cosine matrices

dca = zeros( 3, 3 );
dca(1,1) = cos( yawF )*cos( pitchF );
dca(1,2) = sin( yawF )*cos( pitchF );
dca(1,3) = -sin( pitchF );
dca(2,1) = cos( yawF )*sin( pitchF )*sin( roll ) - sin( yawF )*cos( roll
);
dca(2,2) = sin( yawF )*sin( pitchF )*sin( roll ) + cos( yawF )*cos( roll
);
dca(2,3) = cos( pitchF )*sin( roll );
dca(3,1) = cos( yawF )*sin( pitchF )*cos( roll ) + sin( yawF )*sin( roll
);
dca(3,2) = sin( yawF )*sin( pitchF )*cos( roll ) - cos( yawF )*sin( roll
);
dca(3,3) = cos( pitchF )*cos( roll );

C_FB = dca;  %  Direction Cosine mx
C_EF = eye( 3 );
C_EB = C_EF*C_FB;

% Calculate the angular velocity
omegaEF_E = zeros( 3, 1 );
omegaFB_F = C_FB*FBOOMnYaw_B*YawFdot + FBOOMnPitch_F*PitchFdot;
omegaEI_E = omegaEF_E + C_EF*omegaFB_F + C_EB*omegaBI_B;

tildewEI_E = [     0,         -omegaEI_E(3),  omegaEI_E(2); ...
                omegaEI_E(3),     0,          -omegaEI_E(1); ...
               -omegaEI_E(2),  omegaEI_E(1),     0];


% Right-hand side inertia vector
Mvec = mass*tildewEI_E*tildewEI_E*rCG;
Ivec = tildewEI_E*Imtx*omegaEI_E;
RHSIvec_E = [ [Mvec]; ...
             [Ivec]; ];
%RHSIvec_E = zeros(6,1);
```

```
function [fdragF_F, mdragF_F, fgravF_F, mgravF_F ] =
FixedBoomDrag_Gravity(vals)
%
% Calculate the drag/gravity forces/moments on the fixed boom.
%
%----------------------------------------
 % Extract values from the state vector
%Tanker Velocity in the I frame
vBI_I = zeros(3,1);
vBI_I(1,1) = vals(1);
vBI_I(2,1) = vals(2);
vBI_I(3,1) = vals(3);
%Tanker angular velocity in the B frame
omegaBI_B = zeros(3,1);
omegaBI_B(1,1) = vals(4);
omegaBI_B(2,1) = vals(5);
omegaBI_B(3,1) = vals(6);
%  Tanker Euler Angles
yawB = vals(13);
pitchB = vals(12);
rollB = vals(11);
%  Fixed Boom angular Rates
YawFdot = vals(7);
PitchFdot = vals(8);
%  Fixed Boom Attitude
yawF = vals(9);
pitchF = vals(10);
rollF = 0;

%  Atmosperic data
ENVrho = vals(14); % density;  % Air density at sea level (slug/ft^3)
ENVa = vals(15); %vsound;  % Speed of sound (ft/sec)
% visc from the original AFRL program does not update (comes in as 0)
ENVvisc = 3.21596084e-7; % vals(16);  %visc;  % Viscosity (lbf-sec/ft^2)
ENVg_I = [0; 0; 32.174];  % Gravitational acceleration vector (ft/sec^2)

FBOOMnYaw_B = [0; 0; 1];  % Boom yaw axis (in the B basis)
FBOOMnPitch_F = [0; 1; 0];  % Boom pitch axis (in the F basis)
FBOOMrFB_B = [583.325; 0; -12.5]/12;  % fixed boom pivot location (ft)
FBOOML = 332/12;  % fixed boom length (ft)
FBOOMM = 756.5/32.2;  % slugs
FBOOMrCG = [-228.88; 0; 0]/12;  % fixed boom center of mass (ft)
FBOOMDiam_in = [ 0.0, 240.0, 240.1, 332.0; ...
                 11.0,  11.0,  21.6,  21.6];
% Define the direction cosine matrices

dca = zeros( 3, 3 );
dca(1,1) = cos( yawB )*cos( pitchB );
dca(1,2) = sin( yawB )*cos( pitchB );
dca(1,3) = -sin( pitchB );
dca(2,1) = cos( yawB )*sin( pitchB )*sin( rollB ) - sin( yawB )*cos(
rollB );
dca(2,2) = sin( yawB )*sin( pitchB )*sin( rollB ) + cos( yawB )*cos(
rollB );
dca(2,3) = cos( pitchB )*sin( rollB );
dca(3,1) = cos( yawB )*sin( pitchB )*cos( rollB ) + sin( yawB )*sin(
rollB );
```

```
dca(3,2) = sin( yawB )*sin( pitchB )*cos( rollB ) - cos( yawB )*sin(
rollB );
dca(3,3) = cos( pitchB )*cos( rollB );
C_BI = dca;

dca = zeros( 3, 3 );
dca(1,1) = cos( yawF )*cos( pitchF );
dca(1,2) = sin( yawF )*cos( pitchF );
dca(1,3) = -sin( pitchF );
dca(2,1) = cos( yawF )*sin( pitchF )*sin( rollF ) - sin( yawF )*cos(
rollF );
dca(2,2) = sin( yawF )*sin( pitchF )*sin( rollF ) + cos( yawF )*cos(
rollF );
dca(2,3) = cos( pitchF )*sin( rollF );
dca(3,1) = cos( yawF )*sin( pitchF )*cos( rollF ) + sin( yawF )*sin(
rollF );
dca(3,2) = sin( yawF )*sin( pitchF )*cos( rollF ) - cos( yawF )*sin(
rollF );
dca(3,3) = cos( pitchF )*cos( rollF );
C_FB = dca;

C_FI = C_FB*C_BI;

% Define the velocities and angular velocities
vBI_B = C_BI*vBI_I;
omegaFB_F = C_FB*FBOOMnYaw_B*YawFdot + FBOOMnPitch_F*PitchFdot;
omegaFI_F = omegaFB_F + C_FB*omegaBI_B;

x0 = FBOOML;
x1 = 0;
x = linspace(-x0, x1);
vpI_F = [0;0;0];


tildeFBOOMrFB_B = [     0,          -FBOOMrFB_B(3),  FBOOMrFB_B(2); ...
                   FBOOMrFB_B(3),      0,            -FBOOMrFB_B(1); ...
                   -FBOOMrFB_B(2),  FBOOMrFB_B(1),      0];

dragY = zeros(1,length(x));
dragZ = zeros(1,length(x));
momentY = zeros(1,length(x));
momentZ = zeros(1,length(x));
for j = 1:1:length(x)
    tilderpF_F = [ 0,      -0,     0; ...
                   0,       0,   -x(j); ...
                  -0,      x(j),   0];
    vpI_F = C_FB*(vBI_B - tildeFBOOMrFB_B*omegaBI_B) ...
        - tilderpF_F*omegaFI_F;
    Vy = vpI_F(2);
    Vz = vpI_F(3);
    V = sqrt( Vy^2 + Vz^2);
    % Calculate the cross section drag coefficient
    if( V > 1.0e-5 )
      diam = interp1( FBOOMDiam_in(1,:)/12, FBOOMDiam_in(2,:)/12, -x(j)
);
      Re = ENVrho*V*diam/ENVvisc;
      if( Re <= 1 )
```

```
        Cd = 8*pi/(Re*(0.5 - 0.577216 + log(8/Re)));
      elseif( Re <= 1.0e5 )
        Cd = 1 + 10/Re^(2/3);
      elseif( Re <= 2.5e5 )
        Cd = 1 - 0.82*((Re - 1.0e5)/(2.5e5 - 1.0e5))^2;
      elseif( Re <= 6.0e5 )
        Cd = 0.18;
      elseif( Re <= 4.0e6 )
        Cd = 0.18*(Re/6.0e5)^0.63;
      else
        Cd = 0.6;
      end
    %  Calculate the total drag force per unit length
    drag = (ENVrho/2)*diam*Cd*(V^2);
    %  Calculate the components of the drag vector for integration
    dragY(1,j) = -drag*Vy/V;
    dragZ(1,j) = -drag*Vz/V;
    else
      dragY(1,j) = 0;
      dragZ(1,j) = 0;
    end
    totalmom = cross([x(j);0;0], [0; dragY(1,j); dragZ(1,j)]);
    momentY(1,j) = totalmom(2);
    momentZ(1,j) = totalmom(3);

end

%  Trapezoidal Rule for numerical integrattion
areaDy = 0;
areaDz = 0;
areaMy = 0;
areaMz = 0;
for j = 1:1:length(x)-1
    x1 = x(j);
    x2 = x(j+1);
    y1 = dragY(j);
    y2 = dragY(j+1);
    z1 = dragZ(j);
    z2 = dragZ(j+1);
    My1 = momentY(j);
    My2 = momentY(j+1);
    Mz1 = momentZ(j);
    Mz2 = momentZ(j+1);
    areaDy = areaDy + (y2+y1)*(x2-x1)/2;
    areaDz = areaDz + (z2+z1)*(x2-x1)/2;
    areaMy = areaMy + (My2+My1)*(x2-x1)/2;
    areaMz = areaMz + (Mz2+Mz1)*(x2-x1)/2;
end

fdragF_F = [0; areaDy; areaDz];  %  Vector of drag force on the boom (no
ruddervator contribution)
mdragF_F = [0; areaMy; areaMz];  %  Vector of moments on the boom due to
drag (no ruddervator contribution)

%%%%%%%%%%%%%%%%%%%%%%%%%%%%%%%%%%%%%%%%%%%%%%%%%%%%%%%%%%%%%%%%%%%%%%%%%%
%%%
```

```
%            GRAVITY VECTOR CALCULATIONS FOR THE FIXED BOOM
%
%%%%%%%%%%%%%%%%%%%%%%%%%%%%%%%%%%%%%%%%%%%%%%%%%%%%%%%%%%%%%%%%%%%%%%%%
%%%


% Define the gravitational vector
gVec_F = C_FI*ENVg_I;

% Calculate the force acting at the boom pivot (F)
fgravF_F = FBOOMM*gVec_F;

% Calculate the moment acting about the boom pivot (F)
rCF_F = FBOOMrCG;
mgravF_F = cross( rCF_F, fgravF_F );
```

```
function  [frvL_F,  mrvL_F  ]  =  LeftRuddervator(vals,  TabCL,  TabCD,

timecount)


%Tanker Velocity in the I frame
vBI_I = zeros(3,1);
vBI_I(1,1) = vals(1);
vBI_I(2,1) = vals(2);
vBI_I(3,1) = vals(3);
%Tanker angular velocity in the B frame
omegaBI_B = zeros(3,1);
omegaBI_B(1,1) = vals(4);
omegaBI_B(2,1) = vals(5);
omegaBI_B(3,1) = vals(6);
%  Tanker Euler Angles
yawB = vals(13);
pitchB = vals(12);
rollB = vals(11);
%  Fixed Boom angular Rates
YawFdot = vals(7);
PitchFdot = vals(8);
%  Fixed Boom Attitude
yawF = vals(9);
pitchF = vals(10);
rollF = 0;
%%%%%%%%%%%%%%%%%%%%%%%%%%%%%%%%%%%%%%%%%%%%%%%%%%%%%%%%%%%%%%%%%%%%%%%%%%
%%
%  Ruddervator Angle Setup;
%%%%%%%%%%%%%%%%%%%%%%%%%%%%%%%%%%%%%%%%%%%%%%%%%%%%%%%%%%%%%%%%%%%%%%%%%%
%

theta = vals(17);  %Use this to use a Simulink input such as step


%This block is the ruddevator control pattern for the 'elevation' test.
%{
rvang = [-32, -32, -24, -24, -39, -39, -44, -44, -31];  % vector of LRV
position based off test data
shiftrvang = (rvang+9.32)*pi/180;  %  Force deflections to start at the
sim trim condition
xvec = [0, 5, 20, 30, 45, 52, 60, 67, 80];  %  Vector showing the time
of each position from the above vector
theta = interp1(xvec, shiftrvang, timecount);  %  linearly interpolates
to find the LRV position at a certain time
%}
%%%%%%%%%%%%%%

%This block is the ruddevator control pattern for the 'azimuth' test
data for the same ruddevator deflections
%{
%  Use this block to define a control position schedule (rvang)
according to time (xvec)
rvang = [-22.68, -22.68, -21.68, -31.68, -31.68, -23.18, -21.18, -15.18,
-13.18, -21.93, -22.18, -22.18]*pi/180; % vector of RRV position based
off test data
xvec = [0, 20, 21.25, 28, 37, 42.5, 49, 54, 62.5, 68, 75, 80 ];  %
Vector showing the time of each position from the above vector
theta = interp1(xvec, rvang, timecount);  %  linearly interpolates to
find the LRV position at a certain time
%%%%%%%%%%%%%%%
%}
%%%%%%%%%%%%%%%%%%%%%%%%%%%%%%%%%%%%%%%%%%%%%%%%%%%%%%%%%%%%%%%%%%%%%%%%
%%%%

%  Atmosperic data
ENVrho = vals(14); % density;  % Air density at sea level (slug/ft^3)
ENVa = vals(15); %vsound;  % Speed of sound (ft/sec)
ENVvisc = vals(16);  %visc;  % Viscosity (lbf-sec/ft^2)
ENVg_I = [0; 0; 32.174];  % Gravitational acceleration vector (ft/sec^2)

FBOOMnYaw_B = [0; 0; 1];  % Boom yaw axis (in the B basis)
FBOOMnPitch_F = [0; 1; 0];  % Boom pitch axis (in the F basis)
FBOOMrFB_B = [583.325; 0; -12.5]/12;  % fixed boom pivot location (ft)
FBOOML = 332/12;  % fixed boom length (ft)
FBOOMM = 756.5/32.2;  % slugs
FBOOMrCG = [-228.88; 0; 0]/12;  % fixed boom center of mass (ft)
FBOOMDiam_in = [ 0.0, 240.0, 240.1, 332.0; ...
                 11.0,  11.0,  21.6,  21.6];
FBOOMrRF_F = [-294; 0; 0]/12;  % ruddevator pivot location (ft)
FBOOMRVc = 31/12;  % ruddevator chord (ft)
FBOOMRVL = 61/12;  % ruddevator length (ft)
FBOOMRVdihedral = 42*pi/180;  % ruddevator dihedral angle (rad)
FBOOMRVTabCL = TabCL;
FBOOMRVTabCD = TabCD;
FBOOMRVCtrl = 0;  %boomCtrl(:,1:3);  % ruddevator control angles (deg)


% Define the direction cosine matrices

dca = zeros( 3, 3 );
dca(1,1) = cos( yawB )*cos( pitchB );
dca(1,2) = sin( yawB )*cos( pitchB );
dca(1,3) = -sin( pitchB );
dca(2,1) = cos( yawB )*sin( pitchB )*sin( rollB ) - sin( yawB )*cos(
rollB );
dca(2,2) = sin( yawB )*sin( pitchB )*sin( rollB ) + cos( yawB )*cos(
rollB );
dca(2,3) = cos( pitchB )*sin( rollB );
dca(3,1) = cos( yawB )*sin( pitchB )*cos( rollB ) + sin( yawB )*sin(
rollB );
dca(3,2) = sin( yawB )*sin( pitchB )*cos( rollB ) - cos( yawB )*sin(
rollB );
dca(3,3) = cos( pitchB )*cos( rollB );
C_BI = dca;

dca = zeros( 3, 3 );
dca(1,1) = cos( yawF )*cos( pitchF );
dca(1,2) = sin( yawF )*cos( pitchF );
dca(1,3) = -sin( pitchF );
dca(2,1) = cos( yawF )*sin( pitchF )*sin( rollF ) - sin( yawF )*cos(
rollF );
```

```
dca(2,2) = sin( yawF )*sin( pitchF )*sin( rollF ) + cos( yawF )*cos(
rollF );
dca(2,3) = cos( pitchF )*sin( rollF );
dca(3,1) = cos( yawF )*sin( pitchF )*cos( rollF ) + sin( yawF )*sin(
rollF );
dca(3,2) = sin( yawF )*sin( pitchF )*cos( rollF ) - cos( yawF )*sin(
rollF );
dca(3,3) = cos( pitchF )*cos( rollF );
C_FB = dca;

C_FI = C_FB*C_BI;

% Define the velocities and angular velocities
vBI_B = C_BI*vBI_I;
omegaFB_F = C_FB*FBOOMnYaw_B*YawFdot + FBOOMnPitch_F*PitchFdot;
omegaFI_F = omegaFB_F + C_FB*omegaBI_B;


%%%%%%%%%%%%%%%%%%%%%%%%%%%%%%%%%%%%%%%%%%%%%%%%%%%%%%%%%%%%%%%%%%%%%%%%
%%%
%            FORCE VECTOR CALCULATIONS FOR THE RUDDERVATORS
%
%%%%%%%%%%%%%%%%%%%%%%%%%%%%%%%%%%%%%%%%%%%%%%%%%%%%%%%%%%%%%%%%%%%%%%%%
%%%

%%%%%%%%%%%%%%%%%%%%%%%%%%%%%%%%%%%%%%%%%%%%%%%%%%%%%%%%%%%%%%%%
%                  Left Ruddervator                            %
%%%%%%%%%%%%%%%%%%%%%%%%%%%%%%%%%%%%%%%%%%%%%%%%%%%%%%%%%%%%%%%%
yaw = 0; pitch = 0;
roll = FBOOMRVdihedral;
dca = zeros( 3, 3 );
dca(1,1) = cos( yaw )*cos( pitch );
dca(1,2) = sin( yaw )*cos( pitch );
dca(1,3) = -sin( pitch );
dca(2,1) = cos( yaw )*sin( pitch )*sin( roll ) - sin( yaw )*cos( roll );
dca(2,2) = sin( yaw )*sin( pitch )*sin( roll ) + cos( yaw )*cos( roll );
dca(2,3) = cos( pitch )*sin( roll );
dca(3,1) = cos( yaw )*sin( pitch )*cos( roll ) + sin( yaw )*sin( roll );
dca(3,2) = sin( yaw )*sin( pitch )*cos( roll ) - cos( yaw )*sin( roll );
dca(3,3) = cos( pitch )*cos( roll );

C_WF = dca;
C_WB = C_WF*C_FB;
C_FW = C_WF';

y0 = -FBOOMRVL;
y1 = -interp1( FBOOMDiam_in(1,:)/12, FBOOMDiam_in(2,:)/12, ...
                 -FBOOMrRF_F(1) )/2;
y = linspace(y0, y1);   %  Integration limits
tildeFBOOMrFB_B = [     0,         -FBOOMrFB_B(3),  FBOOMrFB_B(2); ...
                   FBOOMrFB_B(3),     0,          -FBOOMrFB_B(1); ...
                   -FBOOMrFB_B(2),  FBOOMrFB_B(1),     0];

C_WZ = zeros(3,3);
df_W = zeros(3,1);
df_Wx = zeros(1, length(y));
df_Wz = zeros(1, length(y));
```

```
dm_Wx = zeros(1, length(y));
dm_Wz = zeros(1, length(y));
AoAvecCL = [TabCL(2:40, 1)];
AoAvecCD = [TabCD(2:56, 1)];
for j = 1:1:length(y)
    rpF_F = FBOOMrRF_F + C_FW*[0;y(j);0    tilderpF_F = [     0,        -
rpF_F(3),    rpF_F(2); ...
                   rpF_F(3),     0,          -rpF_F(1); ...
                   -rpF_F(2),   rpF_F(1),      0];
    vpI_W = C_WB*(vBI_B - tildeFBOOMrFB_B*omegaBI_B) ...
            - C_WF*tilderpF_F*omegaFI_F;
    V = vpI_W;
    VxVy = sign( V(1) )*sqrt( V(1)^2 + V(2)^2 );
    SweepFactor = abs( V(1)/VxVy );
    phi = atan2( V(3), VxVy );
    AoA = atan2( SweepFactor*sin( theta ), cos( theta ) ) + phi;
    shiftAoA = (abs( AoA ) > pi)*sign( AoA )*(2*pi);
    AoA = AoA - shiftAoA;
    AoAdeg = AoA*180/pi;
    % Calculate the section Mach number
    Vnorm = norm( V );
    Mach = abs( Vnorm/ENVa );
        %  Interpolate from the C81 tables (this is where the 2D
interpolation fn was  moved to one.  Can’t use interp2 in an embedded fn
    CLvec = zeros(39,1);
    CDvec = zeros(55,1);
    if Mach >0 & Mach <= .1
        CLvec = [TabCL(2:40, 2)];
        CDvec = [TabCD(2:56, 2)];
    elseif Mach >.1 && Mach <= .25
        CLvec = [TabCL(2:40, 3)];
        CDvec = [TabCD(2:56, 3)];

    elseif Mach >.25 && Mach <= .35
        CLvec = [TabCL(2:40, 4)];
        CDvec = [TabCD(2:56, 4)];

    elseif Mach >.35 && Mach <= .45
        CLvec = [TabCL(2:40, 5)];
        CDvec = [TabCD(2:56, 5)];

    elseif Mach >.45 && Mach <= .55
        CLvec = [TabCL(2:40, 6)];
        CDvec = [TabCD(2:56, 6)];

    elseif Mach >.55 && Mach <= .8
        CLvec = [TabCL(2:40, 7)];
        CDvec = [TabCD(2:56, 7)];

    elseif Mach >.8 && Mach <= 1
        CLvec = [TabCL(2:40, 8)];
        CDvec = [TabCD(2:56, 8)];
    end
    k0 = CLvec;
    g0 = CDvec;
    CL = interp1(AoAvecCL, k0, AoAdeg);
    CD = interp1(AoAvecCD, g0, AoAdeg);
    % Calculate the section forces

    df_Zx = (ENVrho/2)*(Vnorm^2)*FBOOMRVc*CD;
    df_Zz = (ENVrho/2)*(Vnorm^2)*FBOOMRVc*CL;
    yaw = 0; roll = 0;
    pitch = pi - phi;
    dca = zeros( 3, 3 );
    dca(1,1) = cos( yaw )*cos( pitch );
    dca(1,2) = sin( yaw )*cos( pitch );
    dca(1,3) = -sin( pitch );
    dca(2,1) = cos( yaw )*sin( pitch )*sin( roll ) - sin( yaw )*cos(
roll );
    dca(2,2) = sin( yaw )*sin( pitch )*sin( roll ) + cos( yaw )*cos(
roll );
    dca(2,3) = cos( pitch )*sin( roll );
    dca(3,1) = cos( yaw )*sin( pitch )*cos( roll ) + sin( yaw )*sin(
roll );
    dca(3,2) = sin( yaw )*sin( pitch )*cos( roll ) - cos( yaw )*sin(
roll );
    dca(3,3) = cos( pitch )*cos( roll );
    C_WZ = dca;
    df_W = C_WZ*[df_Zx;0;df_Zz];
    df_Wx(1,j) = df_W(1);   %  vector of differential forces to
integrate
    df_Wz(1,j) = df_W(3);   %  vector of differential forces to
integrate

    totalmom = cross([0; y(j); 0], [df_Wx(1,j); 0; df_Wz(1,j)]);
    dm_Wx(1,j) = totalmom(1);   %  vector of differential moments to
integrate
    dm_Wz(1,j) = totalmom(3);  %  vector of differential moments to
integrate
end

%  Trapezoidal Rule for numerical integrattion
areaDx = 0;
areaDz = 0;
areaMx = 0;
areaMz = 0;
for j = 1:1:length(y)-1
    x1 = y(j);
    x2 = y(j+1);
    y1 = df_Wx(j);
    y2 = df_Wx(j+1);
    z1 = df_Wz(j);
    z2 = df_Wz(j+1);
    Mx1 = dm_Wx(j);
    Mx2 = dm_Wx(j+1);
    Mz1 = dm_Wz(j);
    Mz2 = dm_Wz(j+1);
    areaDx = areaDx + (y2+y1)*(x2-x1)/2;
    areaDz = areaDz + (z2+z1)*(x2-x1)/2;
    areaMx = areaMx + (Mx2+Mx1)*(x2-x1)/2;
    areaMz = areaMz + (Mz2+Mz1)*(x2-x1)/2;
end
```

```
frvW_W = [areaDx; 0; areaDz];  %  Vector of force on the LEFT
ruddervator (in the W basis)
mrvW_W = [areaMx; 0; areaMz];  %  Vector of moments on the LEFT
ruddervator (in the W basis)

frvL_F = C_FW*frvW_W;   %  Vector of force on the LEFT ruddervator (in
the F basis)
mrvL_F = C_FW*mrvW_W;   %  Vector of moments on the LEFT ruddervator (in
the F basis)
```

```
function [frvR_F, mrvR_F ] = RightRuddervator( vals, TabCL, TabCD,
timecount)
%
% Calculate the force/moment contribution of the right RV
%
%-----------------------------------------
%Tanker Velocity in the I frame

vBI_I = zeros(3,1);
vBI_I(1,1) = vals(1);
vBI_I(2,1) = vals(2);
vBI_I(3,1) = vals(3);

%Tanker angular velocity in the B frame
omegaBI_B = zeros(3,1);
omegaBI_B(1,1) = vals(4);
omegaBI_B(2,1) = vals(5);
omegaBI_B(3,1) = vals(6);
%  Tanker Euler Angles
yawB = vals(13);
pitchB = vals(12);
rollB = vals(11);
%  Fixed Boom angular Rates
YawFdot = vals(7);
PitchFdot = vals(8);
%  Fixed Boom Attitude
yawF = vals(9);
pitchF = vals(10);
rollF = 0;
%  Ruddervator Angle;
theta = vals(18);  % Use this if you want to use a step or ramp input
%%%%%%%%%

%  Ruddervator Angle;  Use this for the flight test data

%  This block is the ruddevator control pattern for the 'elevation' test
data for the same ruddevator deflections
%{
rvang = [-32, -32, -24, -24, -39, -39, -44, -44, -31];  % vector of RRV
position based off test data
shiftrvang = (rvang+9.32)*pi/180;  %  Force deflections to start at the
trim condition
xvec = [0, 5, 20, 30, 45, 52, 60, 67, 80];  %  Vector showing the time
of each position from the above vector
theta = interp1(xvec, shiftrvang, timecount);  %  linearly interpolates
to find the RRV position at a certain time
%%%%%%%%%%%%%%%%
%}

%This block is the ruddevator control pattern for the 'azimuth' test
data for the same ruddevator deflections
%{
rvang = [-22.68, -22.68, -23.68, -14.68, -14.68, -22.68, -24.18, -29.18,
-31.43, -22.43, -22.18, -22.18]*pi/180; % vector of RRV position based
off test data
xvec = [0, 20, 21.25, 28, 37, 42.5, 49, 54, 62.5, 68, 75, 80, ];  %
Vector showing the time of each position from the above vector
theta = interp1(xvec, rvang, timecount);  %  linearly interpolates to
find the RRV position at a certain time
%}
%%%%%%%%%%%%%%%%%%%

%  Atmosperic data
ENVrho = vals(14); % density;  % Air density at sea level (slug/ft^3)
ENVa = vals(15); %vsound;  % Speed of sound (ft/sec)
ENVvisc = vals(16);  %visc;  % Viscosity (lbf-sec/ft^2)
ENVg_I = [0; 0; 32.174];  % Gravitational acceleration vector (ft/sec^2)

FBOOMnYaw_B = [0; 0; 1];  % Boom yaw axis (in the B basis)
FBOOMnPitch_F = [0; 1; 0];  % Boom pitch axis (in the F basis)
FBOOMrFB_B = [583.325; 0; -12.5]/12;  % fixed boom pivot location (ft)
FBOOML = 332/12;  % fixed boom length (ft)
FBOOMM = 756.5/32.2;  % slugs
FBOOMrCG = [-228.88; 0; 0]/12;  % fixed boom center of mass (ft)
FBOOMDiam_in = [ 0.0, 240.0, 240.1, 332.0; ...
                 11.0,  11.0,  21.6,  21.6];
FBOOMrRF_F = [-294; 0; 0]/12;  % ruddevator pivot location (ft)
FBOOMRVc = 31/12;  % ruddevator chord (ft)
FBOOMRVL = 61/12;  % ruddevator length (ft)
FBOOMRVdihedral = 42*pi/180;  % ruddevator dihedral angle (rad)
FBOOMRVTabCL = TabCL;
FBOOMRVTabCD = TabCD;
FBOOMRVCtrl = 0;  %boomCtrl(:,1:3);  % ruddevator control angles (deg)


% Define the direction cosine matrices

dca = zeros( 3, 3 );
dca(1,1) = cos( yawB )*cos( pitchB );
dca(1,2) = sin( yawB )*cos( pitchB );
dca(1,3) = -sin( pitchB );
dca(2,1) = cos( yawB )*sin( pitchB )*sin( rollB ) - sin( yawB )*cos(
rollB );
dca(2,2) = sin( yawB )*sin( pitchB )*sin( rollB ) + cos( yawB )*cos(
rollB );
dca(2,3) = cos( pitchB )*sin( rollB );
dca(3,1) = cos( yawB )*sin( pitchB )*cos( rollB ) + sin( yawB )*sin(
rollB );
dca(3,2) = sin( yawB )*sin( pitchB )*cos( rollB ) - cos( yawB )*sin(
rollB );
dca(3,3) = cos( pitchB )*cos( rollB );
C_BI = dca;

dca = zeros( 3, 3 );
dca(1,1) = cos( yawF )*cos( pitchF );
dca(1,2) = sin( yawF )*cos( pitchF );
dca(1,3) = -sin( pitchF );
dca(2,1) = cos( yawF )*sin( pitchF )*sin( rollF ) - sin( yawF )*cos(
rollF );
dca(2,2) = sin( yawF )*sin( pitchF )*sin( rollF ) + cos( yawF )*cos(
rollF );
dca(2,3) = cos( pitchF )*sin( rollF );
dca(3,1) = cos( yawF )*sin( pitchF )*cos( rollF ) + sin( yawF )*sin(
rollF );
```

```
dca(3,2) = sin( yawF )*sin( pitchF )*cos( rollF ) - cos( yawF )*sin(
rollF );
dca(3,3) = cos( pitchF )*cos( rollF );
C_FB = dca;

C_FI = C_FB*C_BI;

% Define the velocities and angular velocities
vBI_B = C_BI*vBI_I;
omegaFB_F = C_FB*FBOOMnYaw_B*YawFdot + FBOOMnPitch_F*PitchFdot;
omegaFI_F = omegaFB_F + C_FB*omegaBI_B;


%%%%%%%%%%%%%%%%%%%%%%%%%%%%%%%%%%%%%%%%%%%%%%%%%%%%%%%%%%%%%%%%%%%%%%%%
%%%
%            FORCE VECTOR CALCULATIONS FOR THE RUDDERVATORS
%
%%%%%%%%%%%%%%%%%%%%%%%%%%%%%%%%%%%%%%%%%%%%%%%%%%%%%%%%%%%%%%%%%%%%%%%%
%%%

%%%%%%%%%%%%%%%%%%%%%%%%%%%%%%%%%%%%%%%%%%%%%%%%%%%%%%%%%%%%%%%%%
%                  Right Ruddervator                            %
%%%%%%%%%%%%%%%%%%%%%%%%%%%%%%%%%%%%%%%%%%%%%%%%%%%%%%%%%%%%%%%%%
yaw = 0; pitch = 0;
roll = -FBOOMRVdihedral;
dca = zeros( 3, 3 );
dca(1,1) = cos( yaw )*cos( pitch );
dca(1,2) = sin( yaw )*cos( pitch );
dca(1,3) = -sin( pitch );
dca(2,1) = cos( yaw )*sin( pitch )*sin( roll ) - sin( yaw )*cos( roll );
dca(2,2) = sin( yaw )*sin( pitch )*sin( roll ) + cos( yaw )*cos( roll );
dca(2,3) = cos( pitch )*sin( roll );
dca(3,1) = cos( yaw )*sin( pitch )*cos( roll ) + sin( yaw )*sin( roll );
dca(3,2) = sin( yaw )*sin( pitch )*cos( roll ) - cos( yaw )*sin( roll );
dca(3,3) = cos( pitch )*cos( roll );

C_WF = dca;
C_WB = C_WF*C_FB;
C_FW = C_WF';

y1 = FBOOMRVL;
y0 = interp1( FBOOMDiam_in(1,:)/12, FBOOMDiam_in(2,:)/12, ...
                 -FBOOMrRF_F(1) )/2;
y = linspace(y0, y1);   %  Integration limits
tildeFBOOMrFB_B = [     0,         -FBOOMrFB_B(3),  FBOOMrFB_B(2); ...
                   FBOOMrFB_B(3),     0,           -FBOOMrFB_B(1); ...
                   -FBOOMrFB_B(2),  FBOOMrFB_B(1),     0];

C_WZ = zeros(3,3);
df_W = zeros(3,1);
df_Wx = zeros(1, length(y));
df_Wz = zeros(1, length(y));
dm_Wx = zeros(1, length(y));
dm_Wz = zeros(1, length(y));
AoAvecCL = [TabCL(2:40, 1)];
AoAvecCD = [TabCD(2:56, 1)];
for j = 1:1:length(y)
```

```
    rpF_F = FBOOMrRF_F + C_FW*[0;y(j);
    tilderpF_F = [     0,       -rpF_F(3),    rpF_F(2); ...
                   rpF_F(3),     0,           -rpF_F(1); ...
                   -rpF_F(2),   rpF_F(1),      0];
    vpI_W = C_WB*(vBI_B - tildeFBOOMrFB_B*omegaBI_B) ...
            - C_WF*tilderpF_F*omegaFI_F;
    V = vpI_W;
    VxVy = sign( V(1) )*sqrt( V(1)^2 + V(2)^2 );
    SweepFactor = abs( V(1)/VxVy );
    phi = atan2( V(3), VxVy );
    AoA = atan2( SweepFactor*sin( theta ), cos( theta ) ) + phi;
    shiftAoA = (abs( AoA ) > pi)*sign( AoA )*(2*pi);
    AoA = AoA - shiftAoA;
    AoAdeg = AoA*180/pi;
    % Calculate the section Mach number
    Vnorm = norm( V );
    Mach = abs( Vnorm/ENVa );
        %  Interpolate from the C81 tables (again, can’t use interp2 in
%an embedded fn
    CLvec = zeros(39,1);
    CDvec = zeros(55,1);
    if Mach >0 & Mach <= .1
        CLvec = [TabCL(2:40, 2)];
        CDvec = [TabCD(2:56, 2)];
    elseif Mach >.1 && Mach <= .25
        CLvec = [TabCL(2:40, 3)];
        CDvec = [TabCD(2:56, 3)];

    elseif Mach >.25 && Mach <= .35
        CLvec = [TabCL(2:40, 4)];
        CDvec = [TabCD(2:56, 4)];

    elseif Mach >.35 && Mach <= .45
        CLvec = [TabCL(2:40, 5)];
        CDvec = [TabCD(2:56, 5)];

    elseif Mach >.45 && Mach <= .55
        CLvec = [TabCL(2:40, 6)];
        CDvec = [TabCD(2:56, 6)];

    elseif Mach >.55 && Mach <= .8
        CLvec = [TabCL(2:40, 7)];
        CDvec = [TabCD(2:56, 7)];

    elseif Mach >.8 && Mach <= 1
        CLvec = [TabCL(2:40, 8)];
        CDvec = [TabCD(2:56, 8)];
    end
    k0 = CLvec;
    g0 = CDvec;
    CL = interp1(AoAvecCL, k0, AoAdeg);
    CD = interp1(AoAvecCD, g0, AoAdeg);
    % Calculate the section forces

    df_Zx = (ENVrho/2)*(Vnorm^2)*FBOOMRVc*CD;
    df_Zz = (ENVrho/2)*(Vnorm^2)*FBOOMRVc*CL;
    yaw = 0; roll = 0;
    pitch = pi - phi;
    dca = zeros( 3, 3 );
    dca(1,1) = cos( yaw )*cos( pitch );
    dca(1,2) = sin( yaw )*cos( pitch );
    dca(1,3) = -sin( pitch );
    dca(2,1) = cos( yaw )*sin( pitch )*sin( roll ) - sin( yaw )*cos(
roll );
    dca(2,2) = sin( yaw )*sin( pitch )*sin( roll ) + cos( yaw )*cos(
roll );
    dca(2,3) = cos( pitch )*sin( roll );
    dca(3,1) = cos( yaw )*sin( pitch )*cos( roll ) + sin( yaw )*sin(
roll );
    dca(3,2) = sin( yaw )*sin( pitch )*cos( roll ) - cos( yaw )*sin(
roll );
    dca(3,3) = cos( pitch )*cos( roll );
    C_WZ = dca;
    df_W = C_WZ*[df_Zx;0;df_Zz];
    df_Wx(1,j) = df_W(1);   %  vector of differential forces to
integrate
    df_Wz(1,j) = df_W(3);   %  vector of differential forces to
integrate

    totalmom = cross([0; y(j); 0], [df_Wx(1,j); 0; df_Wz(1,j)]);
    dm_Wx(1,j) = totalmom(1);   %  vector of differential moments to
integrate
    dm_Wz(1,j) = totalmom(3);  %  vector of differential moments to
integrate
end

%  Trapezoidal Rule for numerical integrattion
areaDx = 0;
areaDz = 0;
areaMx = 0;
areaMz = 0;
for j = 1:1:length(y)-1
    x1 = y(j);
    x2 = y(j+1);
    y1 = df_Wx(j);
    y2 = df_Wx(j+1);
    z1 = df_Wz(j);
    z2 = df_Wz(j+1);
    Mx1 = dm_Wx(j);
    Mx2 = dm_Wx(j+1);
    Mz1 = dm_Wz(j);
    Mz2 = dm_Wz(j+1);
    areaDx = areaDx + (y2+y1)*(x2-x1)/2;
    areaDz = areaDz + (z2+z1)*(x2-x1)/2;
    areaMx = areaMx + (Mx2+Mx1)*(x2-x1)/2;
    areaMz = areaMz + (Mz2+Mz1)*(x2-x1)/2;
end

frvW_W = [areaDx; 0; areaDz];  %  Vector of force on the LEFT
ruddervator (in the W basis)
mrvW_W = [areaMx; 0; areaMz];  %  Vector of moments on the LEFT
ruddervator (in the W basis)

frvR_F = C_FW*frvW_W;   %  Vector of force on the LEFT ruddervator (in
the F basis)
```

```
mrvR_F = C_FW*mrvW_W;   %  Vector of moments on the LEFT ruddervator (in
the F basis)
```

```
function [faeroE_E, maeroE_E, fgravE_E, mgravE_E] =
BoomEXTENSION_Drag_Gravity( vals )
%
% Calculate the aero/gravity force/moment for the boom ext
%
%----------------------------------------
%Tanker Velocity in the I frame
vBI_I = zeros(3,1);
vBI_I(1,1) = vals(1);
vBI_I(2,1) = vals(2);
vBI_I(3,1) = vals(3);
%Tanker angular velocity in the B frame
omegaBI_B = zeros(3,1);
omegaBI_B(1,1) = vals(4);
omegaBI_B(2,1) = vals(5);
omegaBI_B(3,1) = vals(6);
%  Tanker Euler Angles
yawB = vals(13);
pitchB = vals(12);
rollB = vals(11);
%  Fixed Boom angular Rates
YawFdot = vals(7);
PitchFdot = vals(8);
%  Fixed Boom Attitude
yawF = vals(9);
pitchF = vals(10);
rollF = 0;
%  Atmosperic data
ENVrho = vals(14); % density;  % Air density at sea level (slug/ft^3)
ENVa = vals(15); %vsound;  % Speed of sound (ft/sec)
ENVvisc = 3.21596084e-7;  %vals(16);  %visc;  % Viscosity (lbf-sec/ft^2)
ENVg_I = [0; 0; 32.174];  % Gravitational acceleration vector (ft/sec^2)

%  Boom Exntesion parameters
EBOOML = 330/12;  % boom extension length (ft)
EBOOMM = 460.35/norm( ENVg_I );  % slugs
EBOOMrCG = [-178.84; 0; 0]/12;  % boom extension center of mass (ft)
EBOOMnExt_E = [1; 0; 0];  % Boom extension axis (in the E basis)
EBOOMrEF_F = [-2; 0; 0]/12;  % Stowed extension position (in the F
basis)
EBOOMD = 3.1*2/12;  % boom extension diameter (ft)
%EBOOM.Ctrl = ExtControl( boomCtrl(:,[1,4]) );
VE = vals(20);   %  Boom extension velocity
uE = vals(19);   %  Boom Extension Position

%  Fixed Boom Parameters
FBOOMnYaw_B = [0; 0; 1];  % Boom yaw axis (in the B basis)
FBOOMnPitch_F = [0; 1; 0];  % Boom pitch axis (in the F basis)
FBOOMrFB_B = [583.325; 0; -12.5]/12;  % fixed boom pivot location (ft)
FBOOML = 332/12;  % fixed boom length (ft)
FBOOMM = 756.5/32.2;  % slugs
FBOOMrCG = [-228.88; 0; 0]/12;  % fixed boom center of mass (ft)
FBOOMDiam_in = [ 0.0, 240.0, 240.1, 332.0; ...
                 11.0,  11.0,  21.6,  21.6];

% Define the direction cosine matrices
```

```
dca = zeros( 3, 3 );
dca(1,1) = cos( yawB )*cos( pitchB );
dca(1,2) = sin( yawB )*cos( pitchB );
dca(1,3) = -sin( pitchB );
dca(2,1) = cos( yawB )*sin( pitchB )*sin( rollB ) - sin( yawB )*cos(
rollB );
dca(2,2) = sin( yawB )*sin( pitchB )*sin( rollB ) + cos( yawB )*cos(
rollB );
dca(2,3) = cos( pitchB )*sin( rollB );
dca(3,1) = cos( yawB )*sin( pitchB )*cos( rollB ) + sin( yawB )*sin(
rollB );
dca(3,2) = sin( yawB )*sin( pitchB )*cos( rollB ) - cos( yawB )*sin(
rollB );
dca(3,3) = cos( pitchB )*cos( rollB );
C_BI = dca;

dca = zeros( 3, 3 );
dca(1,1) = cos( yawF )*cos( pitchF );
dca(1,2) = sin( yawF )*cos( pitchF );
dca(1,3) = -sin( pitchF );
dca(2,1) = cos( yawF )*sin( pitchF )*sin( rollF ) - sin( yawF )*cos(
rollF );
dca(2,2) = sin( yawF )*sin( pitchF )*sin( rollF ) + cos( yawF )*cos(
rollF );
dca(2,3) = cos( pitchF )*sin( rollF );
dca(3,1) = cos( yawF )*sin( pitchF )*cos( rollF ) + sin( yawF )*sin(
rollF );
dca(3,2) = sin( yawF )*sin( pitchF )*cos( rollF ) - cos( yawF )*sin(
rollF );
dca(3,3) = cos( pitchF )*cos( rollF );
C_FB = dca;

C_FI = C_FB*C_BI;
C_EF = eye(3);
C_EB = C_EF*C_FB;
C_EI = C_EF*C_FB*C_BI;
% Define the velocities and angular velocities
vBI_B = C_BI*vBI_I;
vEF_E = C_EF*[-VE;0;0];
omegaFB_F = C_FB*FBOOMnYaw_B*YawFdot + FBOOMnPitch_F*PitchFdot;
omegaFI_F = omegaFB_F + C_FB*omegaBI_B;
omegaEI_E = C_EF*omegaFI_F;

%  integration limits
x1 = -FBOOML;
x0 = x1-uE;

if x1-x0 <.1
    faeroE_E = [0;0;0];
    maeroE_E = [0;0;0];
else
    x = linspace(x0, x1);
    vpI_F = [0;0;0];
    rEF_F = EBOOMrEF_F + [-uE;0;0];
    tildeEBOOMrEF_F = [     0,       -rEF_F(3),    rEF_F(2); ...
                       rEF_F(3),       0,        -rEF_F(1); ...
                       -rEF_F(2),    rEF_F(1),      0];
    tildeFBOOMrFB_B = [     0,         -FBOOMrFB_B(3),  FBOOMrFB_B(2);
...
                       FBOOMrFB_B(3),     0,           -FBOOMrFB_B(1);
...
                       -FBOOMrFB_B(2),  FBOOMrFB_B(1),     0];



    dragY = zeros(1, length(x));
    dragZ = zeros(1, length(x));
    momentY = zeros(1, length(x));
    momentZ = zeros(1, length(x));
    for j = 1:1:length(x)
      rpE_E = [x(j);0;0] + C_EF*rEF_F;
      tilderpE_E = [ 0,     -0,    0; ...
                     0,      0,   -x(j); ...
                    -0,     x(j),  0];
      vpI_E = C_EB*(vBI_B-tildeFBOOMrFB_B*omegaBI_B)...
          -C_EF*tildeEBOOMrEF_F*omegaFI_F - tilderpE_E*omegaEI_E +
vEF_E;
      Vy = vpI_E(2);
      Vz = vpI_E(3);
      V = sqrt( Vy^2 + Vz^2);
      % Calculate the cross section drag coefficient
      if( V > 1.0e-5 )
        Re = ENVrho*V*EBOOMD/ENVvisc;
        if( Re <= 1 )
          Cd = 8*pi/(Re*(0.5 - 0.577216 + log(8/Re)));
        elseif( Re <= 1.0e5 )
          Cd = 1 + 10/Re^(2/3);
        elseif( Re <= 2.5e5 )
          Cd = 1 - 0.82*((Re - 1.0e5)/(2.5e5 - 1.0e5))^2;
        elseif( Re <= 6.0e5 )
          Cd = 0.18;
        elseif( Re <= 4.0e6 )
          Cd = 0.18*(Re/6.0e5)^0.63;
        else
          Cd = 0.6;
        end
      % Calculate the total drag force per unit length
      drag = (ENVrho/2)*EBOOMD*Cd*(V^2);
      %Calculate the components of the drag vector
      dragY(1, j) = -drag*Vy/V;
      dragZ(1, j) = -drag*Vz/V;

      else
        dragY(1, j) = 0;
        dragZ(1, j) = 0;
      end

    totalmom = cross([x(j);0;0], [0; dragY(1,j); dragZ(1,j)]);
    momentY(1,j) = totalmom(2);
    momentZ(1,j) = totalmom(3);

    end
    %  Trapezoidal Rule for numerical integrattion
    areaDy = 0;
    areaDz = 0;
    areaMy = 0;
    areaMz = 0;
    for j = 1:1:length(x)-1
      x1 = x(j);
      x2 = x(j+1);
      y1 = dragY(j);
      y2 = dragY(j+1);
      z1 = dragZ(j);
      z2 = dragZ(j+1);
      My1 = momentY(j);
      My2 = momentY(j+1);
      Mz1 = momentZ(j);
      Mz2 = momentZ(j+1);
      areaDy = areaDy + (y2+y1)*(x2-x1)/2;
      areaDz = areaDz + (z2+z1)*(x2-x1)/2;
      areaMy = areaMy + (My2+My1)*(x2-x1)/2;
      areaMz = areaMz + (Mz2+Mz1)*(x2-x1)/2;
    end
    faeroE_E = [0; areaDy; areaDz];  %  Vector of drag force on the boom
extension
    maeroE_E = [0; areaMy; areaMz];  %  Vector of moments on the boom
extension due to drag
end


%%%%%%%%%%%%%%%%%%%%%%%%%%%%%%%%%%%%%%%%%%%%%%%%%%%%%%%%%%%%%%%%%%%%%%%%%%%
%%%
%           GRAVITY VECTOR CALCULATIONS FOR THE BOOM EXTENSION
%
%%%%%%%%%%%%%%%%%%%%%%%%%%%%%%%%%%%%%%%%%%%%%%%%%%%%%%%%%%%%%%%%%%%%%%%%%%%
%%%


% Define the gravitational vector
gVec_E = C_EI*ENVg_I;

% Contributions from fuel during extension
fuel = 0.14546;  % fuel distributed mass (slug/ft)
fmass = fuel*uE;

% Combined boom extension mass and fuel mass
mass = EBOOMM + fmass;

% Combined boom extension center of mass
rCG_E = (EBOOMM*EBOOMrCG + fmass*[uE/2; 0; 0])/mass;

% Calculate the force acting at the inboard end of the boom extension
(E)
fgravE_E = mass*gVec_E;

% Calculate the moment acting about the inboard end of the boom
extension (E)
mgravE_E = cross( rCG_E, fgravE_E );
```

```
function bmtx  = VelocityTransformation(vals)
%
% Construct the velocity transformation matrix for the system


%  Tanker Euler Angles
yawB = vals(13);
pitchB = vals(12);
rollB = vals(11);

%  Fixed Boom Attitude
yawF = vals(9);
pitchF = vals(10);
rollF = 0;

uE = vals(19);  %

FBOOMrFB_B = [583.325; 0; -12.5]/12;  % fixed boom pivot location (ft)
FBOOMnYaw_B = [0; 0; 1];  % Boom yaw axis (in the B basis)
FBOOMnPitch_F = [0; 1; 0];  % Boom pitch axis (in the F basis)
EBOOMrEF_F = [-2; 0; 0]/12;  % Stowed extension position (in the F
basis)
EBOOMnExt_E = [1; 0; 0];  % Boom extension axis (in the E basis)


% Define the direction cosine matrices

dca = zeros( 3, 3 );
dca(1,1) = cos( yawB )*cos( pitchB );
dca(1,2) = sin( yawB )*cos( pitchB );
dca(1,3) = -sin( pitchB );
dca(2,1) = cos( yawB )*sin( pitchB )*sin( rollB ) - sin( yawB )*cos(
rollB );
dca(2,2) = sin( yawB )*sin( pitchB )*sin( rollB ) + cos( yawB )*cos(
rollB );
dca(2,3) = cos( pitchB )*sin( rollB );
dca(3,1) = cos( yawB )*sin( pitchB )*cos( rollB ) + sin( yawB )*sin(
rollB );
dca(3,2) = sin( yawB )*sin( pitchB )*cos( rollB ) - cos( yawB )*sin(
rollB );
dca(3,3) = cos( pitchB )*cos( rollB );
C_BI = dca;

dca(1,1) = cos( yawF )*cos( pitchF );
dca(1,2) = sin( yawF )*cos( pitchF );
dca(1,3) = -sin( pitchF );
dca(2,1) = cos( yawF )*sin( pitchF )*sin( rollF ) - sin( yawF )*cos(
rollF );
dca(2,2) = sin( yawF )*sin( pitchF )*sin( rollF ) + cos( yawF )*cos(
rollF );
dca(2,3) = cos( pitchF )*sin( rollF );
dca(3,1) = cos( yawF )*sin( pitchF )*cos( rollF ) + sin( yawF )*sin(
rollF );
dca(3,2) = sin( yawF )*sin( pitchF )*cos( rollF ) - cos( yawF )*sin(
rollF );
dca(3,3) = cos( pitchF )*cos( rollF );
```

```
C_FB = dca;

C_BF = C_FB';
C_EF = eye( 3 );
C_FI = C_FB*C_BI;
C_EI = C_EF*C_FI;
C_EB = C_EF*C_FB;

% Define the position vectors
rEF_F = EBOOMrEF_F + [ -uE; 0; 0 ];
rEB_B = C_BF*rEF_F + FBOOMrFB_B;

% Define the zero blocks
zmtx = zeros( 3, 3 );
zvec = zeros( 3, 1 );

% Build the floating joint block for the tanker rows
bmtx_BB = [ [C_BI], [zmtx]; ...
            [zmtx], [eye( 3 )] ];

% Build the floating joint block for the refueling boom rows

tildeFBOOMrFB_B =  [     0,            -FBOOMrFB_B(3),   FBOOMrFB_B(2);
...
                       FBOOMrFB_B(3),        0,          -FBOOMrFB_B(1);
...
                      -FBOOMrFB_B(2),     FBOOMrFB_B(1),     0];
bmtx_BF = [ [C_FI], [-C_FB*tildeFBOOMrFB_B]; ...
            [zmtx], [C_FB] ];

% Build the floating joint block for the boom extension rows

tilderEB_B = [     0,   -rEB_B(3),  rEB_B(2); ...
              rEB_B(3),     0,     -rEB_B(1); ...
             -rEB_B(2),  rEB_B(1),     0];

bmtx_BE = [ [C_EI], [-C_EB*tilderEB_B]; ...
            [zmtx], [C_EB] ];

% Build the universal joint block for the refueling boom
bmtx_FF = [ [zvec],              [zvec]; ...
            [C_FB*FBOOMnYaw_B], [FBOOMnPitch_F] ];

% Build the universal joint block for the boom extension
bmtx_FE = [ [zvec],              [zvec]; ...
            [C_EB*FBOOMnYaw_B], [C_EF*FBOOMnPitch_F] ];

% Build the prismatic joint block for the boom extension
bmtx_EE = [ [EBOOMnExt_E]; ...
            [zvec] ];

% Assemble the velocity transformation matrix
zmtx_61 = zeros( 6, 1 );
zmtx_62 = zeros( 6, 2 );
bmtx = [ [bmtx_BB], [zmtx_62], [zmtx_61]; ...
         [bmtx_BF], [bmtx_FF], [zmtx_61]; ...
```

```
    [bmtx_BE], [bmtx_FE], [bmtx_EE] ];
```

```
function bdotmtx = AccelerationTransformation( vals )
%
% Construct the acceleration transformation matrix for the system
%
% Separate the required joint states


%  Tanker Euler Angles
yawB = vals(13);
pitchB = vals(12);
rollB = vals(11);

%  Fixed Boom Attitude
yawF = vals(9);
pitchF = vals(10);
rollF = 0;

%  Fixed Boom angular Rates
YawFdot = vals(7);
PitchFdot = vals(8);

FBOOMnYaw_B = [0; 0; 1];  % Boom yaw axis (in the B basis)
FBOOMnPitch_F = [0; 1; 0];  % Boom pitch axis (in the F basis)
FBOOMrFB_B = [583.325; 0; -12.5]/12;  % fixed boom pivot location (ft)
EBOOMnExt_E = [1; 0; 0];  % Boom extension axis (in the E basis)

% Define the direction cosine matrices

dca = zeros( 3, 3 );
dca(1,1) = cos( yawB )*cos( pitchB );
dca(1,2) = sin( yawB )*cos( pitchB );
dca(1,3) = -sin( pitchB );
dca(2,1) = cos( yawB )*sin( pitchB )*sin( rollB ) - sin( yawB )*cos(
rollB );
dca(2,2) = sin( yawB )*sin( pitchB )*sin( rollB ) + cos( yawB )*cos(
rollB );
dca(2,3) = cos( pitchB )*sin( rollB );
dca(3,1) = cos( yawB )*sin( pitchB )*cos( rollB ) + sin( yawB )*sin(
rollB );
dca(3,2) = sin( yawB )*sin( pitchB )*cos( rollB ) - cos( yawB )*sin(
rollB );
dca(3,3) = cos( pitchB )*cos( rollB );
C_BI = dca;

dca(1,1) = cos( yawF )*cos( pitchF );
dca(1,2) = sin( yawF )*cos( pitchF );
dca(1,3) = -sin( pitchF );
dca(2,1) = cos( yawF )*sin( pitchF )*sin( rollF ) - sin( yawF )*cos(
rollF );
dca(2,2) = sin( yawF )*sin( pitchF )*sin( rollF ) + cos( yawF )*cos(
rollF );
dca(2,3) = cos( pitchF )*sin( rollF );
dca(3,1) = cos( yawF )*sin( pitchF )*cos( rollF ) + sin( yawF )*sin(
rollF );
dca(3,2) = sin( yawF )*sin( pitchF )*cos( rollF ) - cos( yawF )*sin(
rollF );
dca(3,3) = cos( pitchF )*cos( rollF );
```

```
C_FB = dca;

C_EF = eye( 3 );
C_EB = C_EF*C_FB;

% Define the angular velocities
%Tanker angular velocity in the B frame
omegaBI_B = zeros(3,1);
omegaBI_B(1,1) = vals(4);
omegaBI_B(2,1) = vals(5);
omegaBI_B(3,1) = vals(6);
omegaFB_F = C_FB*FBOOMnYaw_B*YawFdot + FBOOMnPitch_F*PitchFdot;
omegaFI_F = omegaFB_F + C_FB*omegaBI_B;
omegaFI_E = C_EF*omegaFI_F;

% Build the floating joint block for the tanker
bdotmtx_BB = zeros( 6, 6 );

% Build the floating joint block for the refueling boom
bdotmtx_BF = zeros( 6, 6 );
tilde_wBI = [     0,      -omegaBI_B(3),  omegaBI_B(2); ...
              omegaBI_B(3),     0,       -omegaBI_B(1); ...
             -omegaBI_B(2),  omegaBI_B(1),     0];
tilde_omegaBI_B = [     0,       -tilde_wBI(3),  tilde_wBI(2); ...
                    tilde_wBI(3),      0,       -tilde_wBI(1); ...
                   -tilde_wBI(2),  tilde_wBI(1),     0];


BF_vec =  -C_FB*tilde_omegaBI_B*FBOOMrFB_B;
bdotmtx_BF(1,4) = BF_vec(1);
bdotmtx_BF(2,5) = BF_vec(2);
bdotmtx_BF(3,6) = BF_vec(3);

% Build the floating joint block for the boom extension
bdotmtx_BE = zeros( 6, 6 );

BE_vec =  -C_EB*tilde_omegaBI_B*FBOOMrFB_B;
bdotmtx_BE(1,4) = BE_vec(1);
bdotmtx_BE(2,5) = BE_vec(2);
bdotmtx_BE(3,6) = BE_vec(3);

% Build the universal joint block for the refueling boom
bdotmtx_FF = zeros( 6, 2 );
FF_vec1 =  C_FB*tilde_wBI*FBOOMnYaw_B;
bdotmtx_FF(4,1) = FF_vec1(1);
bdotmtx_FF(5,1) = FF_vec1(2);
bdotmtx_FF(6,1) = FF_vec1(3);


tilde_omegaFI_F = [     0,       -omegaFI_F(3),  omegaFI_F(2); ...
                    omegaFI_F(3),      0,        -omegaFI_F(1); ...
                   -omegaFI_F(2),  omegaFI_F(1),     0];

FF_vec2 = tilde_omegaFI_F*FBOOMnPitch_F;
bdotmtx_FF(4,2) = FF_vec2(1);
bdotmtx_FF(5,2) = FF_vec2(2);
bdotmtx_FF(6,2) = FF_vec2(3);
% Build the universal joint block for the boom extension
bdotmtx_FE = zeros( 6, 2 );

FE_vec1 =  C_EB*tilde_wBI*FBOOMnYaw_B;
bdotmtx_FE(4,1) = FE_vec1(1);
bdotmtx_FE(5,1) = FE_vec1(2);
bdotmtx_FE(6,1) = FE_vec1(3);


FE_vec2 = C_EF*tilde_omegaFI_F*FBOOMnPitch_F;
bdotmtx_FE(4,2) = FE_vec2(1);
bdotmtx_FE(5,2) = FE_vec2(2);
bdotmtx_FE(6,2) = FE_vec2(3);

% Build the prismatic joint block for the boom extension
bdotmtx_EE = zeros( 6, 1 );
tilde_omegaFI_E = [     0,       -omegaFI_E(3),  omegaFI_E(2); ...
                    omegaFI_E(3),      0,        -omegaFI_E(1); ...
                   -omegaFI_E(2),  omegaFI_E(1),     0];


EE_vec =  tilde_omegaFI_E*EBOOMnExt_E;
bdotmtx_EE(1,1) = EE_vec(1);
bdotmtx_EE(2,1) = EE_vec(2);
bdotmtx_EE(3,1) = EE_vec(3);


% Assemble the acceleration transformation matrix
zeromtx_61 = zeros( 6, 1 );
zeromtx_62 = zeros( 6, 2 );
bdotmtx = [ [bdotmtx_BB], [zeromtx_62], [zeromtx_61]; ...
            [bdotmtx_BF], [bdotmtx_FF], [zeromtx_61]; ...
            [bdotmtx_BE], [bdotmtx_FE], [bdotmtx_EE] ];
```

```
function MMtx_BFE = uncoupled18x18(MMtx_B, MMtx_F, MMtx_E)

Zmx = zeros(6,6);
MMtx_BFE = [[MMtx_B], [Zmx], [Zmx];...
           [Zmx], [MMtx_F], [Zmx];...
           [Zmx],  [Zmx],  [MMtx_E]];
```

```
function ForceVector  = combined(faeroB_B, maeroB_B, allforces)

%{
allforces(1:3) = Fixed Drag Force
allforces(4:6) = Fixed drag moments
allforces(7:9) = Fixed gravity forces
allforces(10:12) = Fixed gravity moments
allforces(13:15) = Left ruddervator force
allforces(16:18) = Left ruddervator moment
allforces(19:21) = Right ruddervator force
allforces(22:24) = Right ruddervator moment
allforces(25:27) = Ext Drag Force
allforces(28:30) = Ext drag momoents
allforces(31:33) = Ext gravity forces
allforces(34:36) = Extgravity moments
%}

FBOOMrRF_F = [-294; 0; 0]/12;  % ruddevator pivot location (ft)
maeroF_F = allforces(4:6) + allforces(16:18) + cross( FBOOMrRF_F,
allforces(13:15))...
    + allforces(22:24) + cross( FBOOMrRF_F, allforces(19:21));

faeroF_F = allforces(1:3) + allforces(13:15) + allforces(19:21);


ForceVector = zeros(18,1);
ForceVector = [  faeroB_B;...
                 maeroB_B;...
                 faeroF_F + allforces(7:9);...
                 maeroF_F + allforces(10:12);...
                 allforces(25:27) + allforces(31:33);...
                 allforces(28:30) + allforces(34:36)];
```

```
function accelvec = RHS_I_Bdot_Eta(MMtx, BdotMtx, VB_I, velFB)
.

velFB(1) = VB_I(1);
velFB(2) = VB_I(2);
velFB(3) = VB_I(3);
accelvec = MMtx*BdotMtx*velFB;
```

```
function accelerations = eta_double_dot(MMtx, RHSvec, BMtx)
.

% Transform the uncoupled inertia matrix to the (9x9) joint inertia
matrix
BTMB = BMtx'*MMtx*BMtx;

% Combine and transform the complete right hand side
BTRHSVec = BMtx'*RHSvec;

accelerations = inv( BTMB )*BTRHSVec;
accelerations(9) = 0; % Control the boom ext
```

Bibliography

1. Aerial Refueling, http://www.arthistoryclub.com/art_history/Air_refueling, 4 Jan 07
2. Blake, William, Dogan, Atilla and Shinya Sato, "Flight control and Simulation for Aerial Refueling", AIAA Paper No. 2005-6264, AIAA Guidance, Navigation, and Control Conference and Exhibit, San Francisco, California, August 2005
3. Boeing Integrated Defense Systems, KC-135 Stratotanker, 2007, http://www.boeing.com/defense-space/military/kc135-strat/597-53.html
4. Burns, Scott R and Curtis S. Clark, "The Automated Aerial Refueling Simulation at the AVTAS Laboratory", AIAA Paper No. 2005-6008, AIAA Modeling and Simulation Technologies Conference and Exhibit, San Francisco, California, August 2005
5. Campa, G. et al, "Development of Modeling and Control Tools for Aerial Refueling", AIAA Paper No. 2003-5798, AIAA Guidance, Navigation, and Control Conference and Exhibit, Austin, Texas, August 2003
6. Campa, Giampiero et al, "Automated Aerial Refueling for UAVsUsing a Combined GPS-Machine Vision Guidance", AIAA Paper No. 2004-5350, AIAA Guidance, Navigation, and Control Conference and Exhibit San Francisco, California, August 2005
7. Campbell, T.G., et al "System Study of the KC-135 Aerial Refueling System, Vol. I and II", M.S. Thesis, Department of Aeronautics and Astronautics, Air Force Institute of Technology, Wright Patterson AFB, OH, 1989.
8. Feitshans, Greogry L., Rowe, Allen J. and Robert D. Williams, "A Prototype UAV Control Station Interface for Automated Aerial Refueling", AIAA Paper No. 2005-6009, AIAA Guidance, Navigation, and Control Conference and Exhibit San Francisco, California, August 2005
9. Kim, S.S. and Vanderploeg, M.L., "A General and Efficient Method for Dynamic Analysis of Mechanical Systems Using Velocity Transformation", *ASME Journal of Mechanisms, Transmissions, and Automation in Design*, Vol. 108, No. 2, 1986, pp. 176-182.
10. Kohlman Systems Research, Inc. Report R98-271-Volume II "Computer Software Product End Items for the AMC Simulator Aerodynamic Upgrade: Aerial Refueling Data Collection and Analysis for Two Tankers and Three Receivers. Volume II: Flight Test Time History Report for KC-135R/C-17A Aircraft Pair, Change 1", August 1998
11. Kunz, D.L. and Smith, A.L., "Dynamic Coupling of the KC-135 Tanker and Boom for Modeling and Simulation", AIAA Paper No. 2006-6480, AIAA Modeling and Simulation Technologies Conference and Exhibit, Keystone, Colorado, August 2006

12. Schulze, H.E., The Boeing Company, Seattle, Washington, U.S. Patent for "Simplified Aircraft Boom Control Mechanism", Patent Number 2,960,295, November 1960.

13. Speer, Thomas E, NACA 65-012 Airfoil, http://www.basiliscus.com/ProaSections/Paper/N65012alpha2.JPG

14. U.S. Cost, Aircraft Characteristics: KC-135 Stratotanker, http://www.uscost.net/AircraftCharacteristics/ackc135.htm

15. Wilson, Joe D., "Refueling Realism", *Technology Today*, The Southwestern Research Institute, Summer 2005

Vita

Captain Jeremy Smith is a 1997 graduate of Tucker County High School in Hambleton, West Virginia. After a year at the United States Coast Guard Academy, he transferred to the University of Tennessee where in 2002 he earned a Bachelor of Science in Aerospace Engineering and a commission from AFROTC Detachment 800.

His first assignment was at the 327th Contractor Logistics Support Group, 327th Aircraft Sustainment Wing, Oklahoma City Air Logistics Center, Tinker AFB, Oklahoma. While at Tinker AFB, he served in a variety of engineering and support positions including the VC-25 modification engineer, Air Force Academy aircraft and C-20 Lead Engineer, and Executive Officer to the Commander of the 327th Contractor Logistocs Support Group. He also deployed to Diego Garcia, British Indian Ocean Territory as the project manager for construction of the B-2 deployable shelter system.

Following the assignment at Tinker, he moved to Dayton, Ohio to attend the Air Force Institute of Technology in order to pursue graduate studies in Aeronautical Engineering.

REPORT DOCUMENTATION PAGE			*Form Approved* *OMB No. 074-0188*

1. REPORT DATE *(DD-MM-YYYY)* 23 March 2007	**2. REPORT TYPE** Master's Thesis	**3. DATES COVERED** *(From – To)* August 2005 – March 2007

4. TITLE AND SUBTITLE **Simulation of the Dynamically Coupled KC-135 Tanker and Refueling Boom**	**5a. CONTRACT NUMBER**
	5b. GRANT NUMBER
	5c. PROGRAM ELEMENT NUMBER
6. AUTHOR(S) Smith, Jeremy J., Captain, USAF	**5d. PROJECT NUMBER**
	5e. TASK NUMBER
	5f. WORK UNIT NUMBER
7. PERFORMING ORGANIZATION NAMES(S) AND ADDRESS(S) Air Force Institute of Technology, Graduate School of Engineering and Management (AFIT/EN), 2950 Hobson Way, Building 640, WPAFB OH 45433-8865	**8. PERFORMING ORGANIZATION REPORT NUMBER** AFIT/GAE/ENY/07-M21
9. SPONSORING/MONITORING AGENCY NAME(S) AND ADDRESS(ES) Curtis Clark, US Air Force Research Laboratory, Air Vehicles Directorate (AFRL/VACD), 2130 Eighth Street, Wright-Patterson AFB, OH 45433	**10. SPONSOR/MONITOR'S ACRONYM(S)**
	11. SPONSOR/MONITOR'S REPORT NUMBER(S)

12. DISTRIBUTION/AVAILABILITY STATEMENT

APPROVED FOR PUBLIC RELEASE; DISTRIBUTION UNLIMITED.

13. SUPPLEMENTARY NOTES

14. ABSTRACT

Future Air Force requirements for the use of unmanned aircraft will require Automated Aerial Refueling (AAR). Current AAR research requires a precision model to simulate the refueling process of a KC-135 tanker and a UAV. There are existing high fidelity models of the tanker aircraft, refueling boom and proposed receiver aircraft. However, none of the models are coupled. Since boom orientation and motion is known to change the trim of the tanker aircraft, which in turn influences all other aspects of the refueling process, a new model is needed.

The new model was created by integrating an existing KC-135 tanker and refueling boom model. The tanker boom equations of motion were coupled using joint coordinates and the velocity transformation. Assessment of the new model investigated boom and tanker motion in comparison with other established models. Ultimately, behavior of the new model was validated by a comparison of simulation results to flight test data.

15. SUBJECT TERMS

Tanker, Boom, Coupled, Automated Aerial Refueling, KC-135, Flying Boom

16. SECURITY CLASSIFICATION OF:			**17. LIMITATION OF ABSTRACT**	**18. NUMBER OF PAGES**	**19a. NAME OF RESPONSIBLE PERSON** Kunz, Donald K., PhD
a. REPORT	**b. ABSTRACT**	**c. THIS PAGE**			**19b. TELEPHONE NUMBER** *(Include area code)*
U	U	U	UU	109	(937) 255-3636, ext 4548 (dkunz@afit.edu)